STUDIES ON CORRELATION - INDUCED SPECTRAL CHANGES

by

Ajay Wasan

DEPARTMENT OF PHYSICS

Indian Institute of Technology Kanpur

DECEMBER, 1997

STUDIES ON CORRELATION-INDUCED SPECTRAL CHANGES

A Thesis Submitted
in Partial Fulfillment of the Requirements
for the Degree of
Doctor of Philosophy

by

Ajay Wasan

to the
DEPARTMENT OF PHYSICS
INDIAN INSTITUTE OF TECHNOLOGY KANPUR
December, 1997

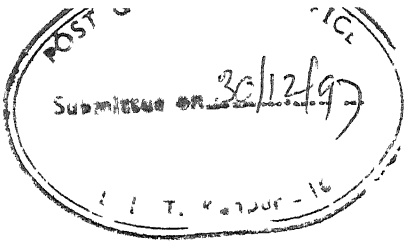

CERTIFICATE

It is certified that the work contained in the thesis entitled "*Studies on Correlation-Induced Spectral Changes*" by Ajay Wasan has been carried out under our supervision and that this work has not been submitted elsewhere for a degree.

Dr. H.C. Kandpal
Optical Radiation Standards
National Physical Laboratory
New Delhi, India

Dr. J Rai
Department of Physics
Indian Institute of Technology
Kanpur, India

Synopsis

Most of us know that the lines observed in the spectra of radiation that reaches earth from astronomical objects are shifted relative to those observed in the spectra from the same elements on earth. Generally, the lines are shifted towards the longer wavelengths which is called redshift. In some cases, they are shifted towards shorter wavelength called blueshift. From these observed shifts, the understanding of the structure of the universe is studied by astronomer which has far reaching consequence. There are three well known causes of these shifts, i.e., shift due to relative motion of the source and the observer known as Doppler's shift, due to the expansion of the whole universe known as the cosmological shift and the shift due to gravitation. The gravitational redshift is observed when the light passes through a strong gravitational field, e.g., when light passes in the neighbourhood of a dense star such as a neutron star. The discovery of quasi-stellar objects known as quasars and their links with galaxies but the amount of redshift shown by the galaxies and quasars being different posed problems in astronomy. These problems could not be explained on the basis of existing theories. Although the majority of the astronomers do not consider that there can be other mechanisms of redshifts except the existing mechanisms, but a few well-known astronomers, on the other hand, consider the possibility that there could be some other explanation to these puzzles. About a decade ago, Wolf showed that there is a mechanism which is deeply rooted in present day physics which has nothing to do with the Doppler effect, the expanding universe or gravitation and which can nevertheless generate redshift of spectral lines. The mechanism is correlation-induced spectral shift.

We are familiar with light sources that belong to one of two well-defined categories, namely, incoherent and coherent sources. Emission from a thermal source is a highly disordered process. Such a source is said to be an incoherent or a chaotic source. A well-stabilised laser, on the other hand, generates light in a highly ordered manner and is said to be a coherent source. In the statistical sense incoherent and

coherent sources represents two extreme cases. However, in the two extremes; they are termed partially coherent sources. The degree of coherence (correlation) that exists within a source or in an optical field can be described in terms of various correlation functions. Within the framework of classical scalar theory, the correlation functions that characterise the statistical properties of the sources and of the partially coherent fields they generate may be described in the space-time or in the space-frequency domain. The space-frequency description has been developed only recently. It has led to the elucidations of a number of coherence phenomena as well as to the predictions of new effects.

It was assumed until recently that the spectrum is an intrinsic property of radiation that does not change on propagation of radiation in free space. That this assumption may not always hold was suggested in an early investigation by Mandel who analyzed the spectral distribution of light in the region of superposition of two light beams having the same spectral distribution. Not long ago, Wolf discovered on rather general grounds that the spectrum of light, which originates in an extended source whether a primary source (a set of radiating atoms or molecules) or a secondary source obtained by allowing the radiation from a primary source to pass through an aperture, i.e., an opening in an opaque screen in an optical system, depends not only on the source spectrum but also on the degree of spatial coherence of the source. Wolf also predicted that the spectrum of the light will, in general, be different at different points in space. This is one of the most significant discoveries in modern optics in recent times.

In this thesis the following experimental studied have been made to verify certain theoretical prediction and to show the applications of correlation-induced spectral changes.

In *chapter 1* some of the basic concepts of optical coherence theory in space-time domain and space-frequency domain are briefly described to understand the nature of partially coherent light fields. To formulate these basic concepts of the theory of partially coherent light, the polarization properties of the electromagnetic field were

ignored and it was treated as scalar field. Radiation from model sources, scaling law and theoretical and experimental studies on spectral changes due to source correlation are described.

In *chapter 2* an experimental study on spectral changes produced on passing partially coherent light through an annular aperture is made for on-axis and off-axis measurements. The dependence of the observed spectral shift on the ratio of the radius of central obstruction to that of the outer radius of opening of annular aperture is investigated.

In *chapter 3* using the spectral interference law, the degree of spectral coherence $|\mu_{12}(\omega)|$ between the two sources formed over the planes of the light collecting mirrors of a laboratory version of Michelson's stellar interferometer is determined from the measurement of the spectral changes produced on superimposition of radiation from these two sources. The theoretically expected values of $|\mu_{12}(\omega)|$ using the experimental parameters in the van Cittert-Zernike theorem agree well with the experimentally calculated values of $|\mu_{12}(\omega)|$ within experimental errors. A new-interferometric equivalence principle is used to determine the angular size of the source from the zeros of $|\mu_{12}(\omega)|$ in the frequency scale. This new technique makes the determination of the angular size of a source less time consuming and simpler than the conventional methods.

In *chapter 4* the effect of single and double grating monochromator on the coherence properties of light fields is studied experimentally in detail by measuring the degree of coherence of the field at the entrance and exit slits of a monochromator. It is found that the state of spatial (spectral) coherence of the light field incident at the entrance slit of a monochromator is modified considerably at the exit slits of single and double monochromator. The spectral degree of coherence (SDC) at the exit slit of double monochromator is found to be more than the SDC at the exit slit of single monochromator. It is therefore, necessary that while synthesizing a secondary source at

the exit slit of a monochromator the coherence properties of the secondary source must be carefully studied to analyze properly the far-field spectrum of such a source.

In *chapter 5* the spectral degree of coherence, produced by a quasi-homogeneous source masked with an amplitude grating, over the plane of a Young's double slit of fixed based line length is determined from the spectral measurements using spectral interference law. The experimental results are compared with the theoretically expected spectral degree of coherence obtained for the experimental parameters in the accessible optical frequencies. The highest accessible temporal frequency is mapped onto zero spatial frequency and the other temporal frequencies to the corresponding low spatial frequencies. The Fourier inversion of the spectral degree of coherence over the mapped spatial frequencies is used to determine the source intensity-profile. Our findings indicate that this technique can be utilised for reconstructing the source intensity-profile of a large class of sources.

In *chapter 6* an experimental study of the spectra of partially coherent field, propagating beyond an optical system (a lens), reveals that no spectral shift takes place on the geometrical-image plane, while large blue shift occurs at the back focal plane of the optical system for on-axis points of observation. Different light sources taken for the study are (1) partially coherent fields produced by a multimode laser and (2) A quasi-homogeneous source with different degrees of spatial coherence. These results are consistent with the theory and might find applications in metrology.

Acknowledgments

I express my sincere gratitude to Dr. J. Rai for introducing me to the fields of partial coherence and nonlinear optics, and for sharing his wide experience in optical science and constant encouragement.

I express deep sense of indebtedness to Dr. H.C. Kandpal for his skillful guidance and constant inspiration during the course of my studies at NPL, New Delhi. I also thank him for providing me excellent working conditions and laboratory facilities throughout the work. It has been a great privilege to work with him.

I am grateful to Dr. K.K. Sharma for his valuable suggestions and encouragement. I very sincerely acknowledge the support and invaluable help of Dr A.K. Majumdar, Dr. R.K. Thareja, Dr. R. Parsad, Dr. H.D. Bisht, Dr. (Mrs.) Pradhan. I express my thanks to all the staff members of the Physics Department IIT, Kanpur for their assistance.

The freedom to work, which I enjoyed at the Optical Radiation Standards Division of NPL, was really appreciating. I also express my sincere thanks to Dr. K.C. Joshi, Dr. J.S. Vaishya, Mrs. S. Manrai and Dr. Titus for their help and encouragement. I am also thankful to Mr. Bahuguna, Mr. Sudama and Mr. Satish for providing me excellent technical support in NPL, New Delhi.

Furthermore, I wish to thank every one who has helped me especially my friends Alok, Gautam, Rajan, Divakar, Swapan, Shanti, Sandeep, Sushil, Sarangi, Sethji, Tuhin, Nimal, Ramanan, and Abir for memorables support and help during my struggling days.

Finally, my parents, my brothers Manoj and Neeraj and family friends deserve heartiest acknowledgments for their constant encouragement, support and patience.

Ajay Wasan

List of Publications

[1] "Correlation-induced spectral changes on passing partially coherent light through an annular aperture", Ajay Wasan, H.C. Kandpal, D.S. Mehta, J.S. Vaishya and K.C. Joshi, *Opt. Commun.* **121** (1995) 89-94.

[2] "Space-frequency equivalence principle in a laboratory version of Michelson's stellar interferometer", H.C. Kandpal, Ajay Wasan, J.S. Vaishya and K.C. Joshi, *Opt. Commun.* **132** (1996) 503-510.

[3] "Study on coherence properties of light fields as influenced by a monochromator", H.C. Kandpal, Ajay Wasan, J.S. Vaishya and K.C. Joshi, *J. Opt. (Paris)* **28** (1997) 199-206.

[4] "Spectroscopy of partially coherent fields at geometrical-image plane and Fourier transform plane of a lens", H.C. Kandpal, Ajay Wasan and J.S. Vaishya, *Opt. Commun.* (in press).

[5] Reconstruction of optical source-profile from spectral measurements in Young's interference experiment", Ajay Wasan, H.C. Kandpal and J.S. Vaishya, submitted to *Appl. Opt.*.

[6] "A new approach to stellar interferometry based on spatial-coherence spectroscopy", H.C. Kandpal, J.S. Vaishya, S.S.K. Titus, Ajay Wasan and E.S.R. Gopal, *Ind. J. Pure and Appl. Phys.* **37** (1997) 000 (in press).

Table of Contents

List of Figures

Chapter 1

Introduction

Light fields generated from real physical sources fluctuate randomly to some extent. On microscopic level quantum mechanical fluctuations produce randomness and on macroscopic level the randomness occurs as a consequence of these microscopic fluctuations, even in free space. In real physical sources spontaneous emission causes random fluctuations and even in the case of lasers, spontaneous emission can not be suppressed completely. In addition to spontaneous emission, random fluctuations are caused in the case of lasers by the vibration of the mirrors at the end of the laser cavities. There are many other processes which can give rise to random fluctuations of light fields. For example interaction of light with matter such as the scattering of light by a medium whose physical properties vary in space and in time in a random manner due to fluctuations in the density, the temperature or the pressure, or propagation of light through a medium of random inhomogeneities. These processes produce randomness in the light field. In any realizable experiment the randomness can not be suppressed completely. Optical coherence theory was developed to describe the random nature of light.

There are two well defined categories of light sources. These are, the traditional thermal sources such as incandescent matter or gas discharge and a laser. Emission from a thermal source is a highly disordered process and is said to be an incoherent source. A well stabilized laser source, on the other hand, generates light

in a highly ordered manner and is said to be a highly coherent source. Statistically, incoherent and coherent sources represents two extreme cases. While describing the phenomena of physical optics and diffraction theory, light is assumed to be perfectly coherent in both spatial as well as temporal senses whereas in radiometry it is generally assumed to be in the incoherent limit. However, in most cases of practical interest we generally deal with light sources and fields that are in between the two extremes; they are termed as partially coherent sources and fields. The degree of order that exists in an optical field produced by a source of any kind may be described in terms of various correlations functions. These correlation functions are the basic theoretical tools for the analyses of statistical properties of partially coherent light fields.

Coherence theory deals with the statistical similarity between light fluctuations at two (or more) space-time points. It is said to be *spatial coherence* when such similarity exists between the fluctuations at two space points, but with time taken to be fixed. On the other hand, it is said to be *temporal* coherence, when statistical similarity exists at two instants of time, but at the same spatial point. In order to describe statistical properties of the light fields generated by any kind of sources optical coherence theory must be employed.

As light propagates, the statistical nature of random light field, in general, changes even in vacuum so it will affect both its spatial and its temporal coherence properties. Historically the first investigation concerning the subject of partial coherence (spatial coherence) was made by Verdet [1] who studied the size of coherence area of light from an extended primary source. Later researches by Michelson established the connection between the visibility of interference fringes and the intensity distribution on the surface of an extended source [2], and between

the visibility and the energy distribution in a spectral line [3]. He used the variant of Young's double slit interference experiment [4] in his stellar interferometer for measuring the stellar radii and angular separation of double stars. Michelson's results, although were not explicitly concerned with the subject of partial coherence, but his investigations contributed a great deal to the clarification and development of this subject. It was von Laue [5] who first measured the correlation of light fluctuation quantitatively. Further contributions were made by Berek [6] who used the concept of correlation in investigating image formation in a microscope.

The foundation of the subject was, in fact, laid by van Cittert [7] who determined the joint probability distribution for the light disturbance at any two points on a screen illuminated by an extended primary source. He also determined the probability distribution for the light disturbances at any one point, but at two different instants of time [8] and the distributions were found to be Gaussian. Appropriate correlation coefficients were calculated within the accuracy of these studies. Later, a different and a simpler approach to subject of partial coherence was introduced by Zernike [9] with the concept of degree of coherence. Zernike's degree of coherence is found to be equivalent to the correlation coefficients formulated by van Cittert in many practical situations. In conclusion, spatial coherence properties of light fields were described quantitatively by van Cittert and Zernike in different manners. These ideas were further simplified and applied by Hopkins [10] in solving coherence problems of instrumental optics, e.g., in image formation and resolving power.

All these investigations mentioned so far contributed a lot to the development of the subject of partial coherence and bridged the gap between the two extreme cases, namely, complete coherence and complete incoherence. But

these results were restricted to the quasi-monochromatic light and to situations where the path difference between the interfering beams being sufficiently small, i.e. less than the correlation length of the incident beams. The subject of partial coherence was further generalized and simplified by a number of researcher, viz. Wolf [11,12] and Blanc-Lapierre and Dumontet [13] to deal with more complex situations and to formulate the theory rigorously. The attractive feature of their work was the introduction of more general correlation functions and precise measurement of the correlation properties of the field variables at two space-time points. Such second order correlation functions were adequate for the analysis of the usual optical experiments involving interference and diffraction of light from steady sources. Consequently, the optical coherence theory, also known as second order coherence theory in space-time domain, came to existence.

Shortly after the second order coherence theory was formulated, Hanbury Brown and Twiss [14,15] demonstrated experimentally the correlation of intensity fluctuations in light beams. This correlation was a contracted form of the forth-order amplitude correlations. Once they established the existence of correlated intensity fluctuations using laboratory light sources, the technique was applied to stellar interferometry. This observation led to the study of higher order correlation effects in optical fields.

Initially, the coherence theory was formulated theoretically in space-time domain based on either classical or quantum description of the optical fields. Although the traditional characterization of field is adequate for the analysis of all elementary phenomenan of interference and diffraction with light of any state of coherence and many more practical situations in different branches of physical sciences, but in many physical situations which involve the interaction of light with

matter, use of space-frequency representation is found to be more appropriate than the space-time representation. This is so because the response of matter, such as the dielectric constant, the refractive index or the magnetic susceptibility, to an incident field is not described by time-dependent but rather by frequency-dependent response functions. The theoretical study of optical coherence effect on the spectrum of light was first introduced in space-frequency domain by Mandel and Wolf [16]. Later, Wolf [17-20] formulated coherence theory in space-frequency domain, which has greatly simplified the theoretical analysis of many problems and has led to the discovery of non-invariance of spectrum on propagation of radiation even in free space [21-23] also known as *'the Wolf effect'* In this thesis, some of the phenomena concerning the Wolf effect and some of its implications are discussed.

Some of the basic concepts of optical coherence theory in space-time domain and space-frequency domain are briefly described in the following sections which are important to understand the nature of partially coherent light fields. To formulate these basic concepts of the theory of partially coherent light, the polarization properties of the electromagnetic field were ignored, for simplicity, and it was treated as scalar field. In the subsequent sections, radiation from model sources, scaling law and spectral changes due to source correlation are described. (These subjects have been treated in detail in many books and reviews [24-33].)

§1.1 Coherence theory of optical fields in space-time domain

The concept of optical coherence has long been associated with two-beam interference, presumably because interference is the simplest phenomenon that reveals a precise measure of correlations between the fluctuating field variables at two space-time points. The simplest correlation function in the space-time domain

formulation of coherence theory is the mutual coherence function and is defined by the expression [24,30]

$$\Gamma(\mathbf{r}_1,\mathbf{r}_2,t_1,t_2)=\langle V^*(\mathbf{r}_1,t_1)V(\mathbf{r}_2,t_2)\rangle, \tag{1.1}$$

where $V(\mathbf{r},t)$ is the complex analytical signal representing the fluctuating field at a point specified by a position vector $\mathbf{r}$ and at time t, angular brackets denote a statistical average taken over the realization of the field ensemble and the asterisk denotes the complex conjugate.

Usually it is assumed that the field fluctuations are statistically stationary, at least in the wide sense, which means that all the ensemble averages are independent of the origin of time [34]. Consequently the mutual coherence function is dependent on the time argument through the difference of time $(\tau = t_1 - t_2)$. Hence in the expression (1.1), $\Gamma(\mathbf{r}_1,\mathbf{r}_2,t_1,t_2)$ may be replaced by $\Gamma(\mathbf{r}_1,\mathbf{r}_2,\tau)$, so

$$\Gamma(\mathbf{r}_1,\mathbf{r}_2,\tau)=\langle V^*(\mathbf{r}_1,t_1)V(\mathbf{r}_2,t_2+\tau)\rangle. \tag{1.2}$$

This function $\Gamma(\mathbf{r}_1,\mathbf{r}_2,\tau)$ was first introduced by Wolf [11] in elementary coherence theory and is known as the mutual coherence function of the field vibrations at point $\mathbf{r}_1$ and $\mathbf{r}_2$. The vibrations at point $\mathbf{r}_2$ are considered at time τ later than at $\mathbf{r}_1$. In the general theory of random processes, the function $\Gamma(\mathbf{r}_1,\mathbf{r}_2,\tau)$ is the simplest two point cross-correlation function of the fluctuating field that characterizes the statistical similarity of the field fluctuations at two space-time points and time delay τ.

In free space, the field satisfies the inhomogeneous wave equation [30] which is given by

$$\left(\nabla^2 - \frac{1}{c^2}\frac{\partial^2}{\partial t^2}\right)V(\mathbf{r},t) = -4\pi Q(\mathbf{r},t), \tag{1.3}$$

where c is the velocity of light in vacuum. $Q(\mathbf{r},t)$ is a fluctuating source variable (which is also assumed zero mean stationary random analytic signal) and $V(\mathbf{r},t)$ is the field which the source generates. It can be shown that when the source is stationary, at least in the wide sense, the second order correlation functions of the field and of the source are related by the fourth-order differential equation [30]

$$\left(\nabla_1^2 - \frac{1}{c^2}\frac{\partial^2}{\partial \tau^2}\right)\left(\nabla_2^2 - \frac{1}{c^2}\frac{\partial^2}{\partial \tau^2}\right)\Gamma_V(\mathbf{r}_1,\mathbf{r}_2,\tau) = (4\pi)^2\Gamma_Q(\mathbf{r}_1,\mathbf{r}_2,\tau), \tag{1.4}$$

where $\Gamma_V(\mathbf{r}_1,\mathbf{r}_2,\tau)$ and $\Gamma_Q(\mathbf{r}_1,\mathbf{r}_2,\tau)$ are the correlation functions of the field distribution and source distribution respectively. ∇_1^2 is the Laplacian with respect to the coordinate $\mathbf{r}_1$ and ∇_2^2 is the Laplacian with respect to the coordinate $\mathbf{r}_2$.

There are two cases of mutual coherence function. (*a*) When the two points coincide (i.e. $\mathbf{r}_1 = \mathbf{r}_2 = \mathbf{r}$), one obtains

$$\Gamma_V(\mathbf{r},\mathbf{r},\tau) = \langle V^*(\mathbf{r},t)V(\mathbf{r},t+\tau)\rangle. \tag{1.5}$$

Eq. (1.5) is called the self coherence or the autocorrelation function of $V(\mathbf{r},t)$. The autocorrelation function implies the statistical similarity of the field function at different instants of time but at the same point $\mathbf{r}$. (*b*) The average field intensity $I_V(\mathbf{r})$ of the fluctuating field at any point is a special case of self coherence when $\tau = 0$ so

$$I_V(\mathbf{r}) = \Gamma_V(\mathbf{r},\mathbf{r},0) \tag{1.6a}$$

$$= \langle V^*(\mathbf{r},t)V(\mathbf{r},t)\rangle. \tag{1.6b}$$

In many practical cases, the field is assumed to be ergodic. Ergodicity means that an ensemble average or the statistical average is equal to the corresponding time average [30,34]

$$\left\langle V^*(\mathbf{r}_1,t)V(\mathbf{r}_2,t+\tau)\right\rangle = \overline{V^*(\mathbf{r}_1,t)V(\mathbf{r}_2,t+\tau)} \tag{1.7a}$$

$$= \lim_{T\to\infty}\frac{1}{2T}\int_{-T}^{T} V^*(\mathbf{r}_1,t)V(\mathbf{r}_2,t+\tau)dt\,. \tag{1.7b}$$

Eq. (1.7) represents the mutual coherence function of an ergodic field.

In problems of practical interest it is convenient to normalize the mutual coherence function. The normalised mutual coherence function is called the complex degree of coherence of the field, which is directly related to the fringe visibility, and is defined by the expression [24,30]

$$\gamma_V(\mathbf{r}_1,\mathbf{r}_2,\tau) = \frac{\Gamma_V(\mathbf{r}_1,\mathbf{r}_2,\tau)}{\sqrt{\Gamma_V(\mathbf{r}_1,\mathbf{r}_1,0)}\sqrt{\Gamma_V(\mathbf{r}_2,\mathbf{r}_2,0)}} \tag{1.8}$$

and satisfies the Schwarz inequality [27]

$$\sqrt{\Gamma_V(\mathbf{r}_1,\mathbf{r}_1,0)}\sqrt{\Gamma_V(\mathbf{r}_2,\mathbf{r}_2,0)} \geq \left|\Gamma_V(\mathbf{r}_1,\mathbf{r}_2,\tau)\right|. \tag{1.9}$$

This inequality holds for any random field which is stationary in wide sense. Using the inequality (1.9), it can be shown that

$$0 \leq \left|\gamma_V(\mathbf{r}_1,\mathbf{r}_2,\tau)\right| \leq 1 \tag{1.10}$$

for all values of the arguments $\mathbf{r}_1$, $\mathbf{r}_2$ and τ of γ. More often the specified notation for $\gamma_V(\mathbf{r}_1,\mathbf{r}_2,\tau)$ is $\gamma_{12}(\tau)$. The extreme case $\left|\gamma_{12}(\tau)\right| = 0$ represents the complete incoherence of the field at two points and the other extreme case $\left|\gamma_{12}(\tau)\right| = 1$ represents the complete coherence. In between these two extreme cases $0 < \left|\gamma_{12}(\tau)\right| < 1$, the fluctuating field at two points is said to be partially coherent.

The complex degree of coherence $\gamma_V(\mathbf{r}_1,\mathbf{r}_2,\tau)$, with τ fixed, is a quantitative measure of spatial coherence of the field at the points $\mathbf{r}_1$ and $\mathbf{r}_2$ whereas $\gamma_V(\mathbf{r},\mathbf{r},\tau)$ is a quantitative measure of the temporal coherence of the field at a point $\mathbf{r}$ ($\mathbf{r}_1=\mathbf{r}_2$), at time t and $t+\tau$.

§1.2 Coherence theory of optical fields in space-frequency domain

In many optical experiments, particularly for the analysis of spectral properties of sources and of fields, it may be more appropriate to employ functions which characterise correlations of partially coherent light in the space-frequency domain. These correlation functions between fluctuatings fields are represented by the cross-spectral density function [16] which is related to mutual coherence function by the expression

$$W_V(\mathbf{r}_1,\mathbf{r}_2,\omega)=\frac{1}{2\pi}\int_{-\infty}^{\infty}\Gamma_V(\mathbf{r}_1,\mathbf{r}_2,\tau)e^{i\omega\tau}d\tau. \tag{1.11}$$

$W_V(\mathbf{r}_1,\mathbf{r}_2,\omega)$ characterizes the correlation at points $\mathbf{r}_1$ and $\mathbf{r}_2$ of the optical field at frequency ω in space-frequency domain. Similar expression can be written for cross-spectral density of a source. It is clear that the cross-spectral density and mutual coherence function form a Fourier transform pair which is the optical analogue of the Wiener-Khintchine theorem [35] in the theory of stationary random processes. Because of the unique relationship between the function and it's Fourier transform, this theorem implies that every member of the ensemble has the same power spectral density irrespective of its waveform. Therefore, on dealing with stationary random processes it is appropriate to work with cross-correlation functions and the power spectral density.

Later on, Wolf [17,18,20] and Agarwal and Wolf [36] explained explicitly more about cross-spectral densities and showed that the formula (1.11) does not

actually show that the cross-spectral density is a correlation function. However, it has been shown that under very general circumstances, one may construct ensembles of random, frequency-dependent realizations of the source variables $\{U_Q(\mathbf{r},\omega)\}$ and the field variables $\{U_V(\mathbf{r},\omega)\}$ such that the cross-spectral densities of the source and of the field can be given by

$$W_Q(\mathbf{r}_1,\mathbf{r}_2,\omega)=\langle U_Q^*(\mathbf{r}_1,\omega)U_Q(\mathbf{r}_2,\omega)\rangle_\omega \tag{1.12}$$

and

$$W_V(\mathbf{r}_1,\mathbf{r}_2,\omega)=\langle U_V^*(\mathbf{r}_1,\omega)U_V(\mathbf{r}_2,\omega)\rangle_\omega . \tag{1.13}$$

In these two formulae the subscript ω on the angular brackets indicates averaging over these ensembles of frequency-dependent functions. The functions $U_Q(\mathbf{r},\omega)$ and $U_V(\mathbf{r},\omega)$, which are coupled by the inhomogeneous Helmholtz equation in free space, are not the Fourier transform of the variable $Q(\mathbf{r},t)$ and $V(\mathbf{r},t)$. In fact, as is well known, the sample functions of stationary random process do not possess Fourier representation within the framework of ordinary function theory [18,30]. The functions $U_Q(\mathbf{r},\omega)$ and $U_V(\mathbf{r},\omega)$ have to be introduced in terms of eigenfunctions and eigenvalues of Fredholm integral equations, whose kernels are the cross-spectral densities.

The spectral densities $S_Q(\mathbf{r},\omega)$ and $S_V(\mathbf{r},\omega)$ (power spectrum or simply the spectrum) of the source variables and of field variables at point $\mathbf{r}$ are the special cases of cross-spectral density when two points $\mathbf{r}_1$ and $\mathbf{r}_2$ coincide to the point $\mathbf{r}$ therefore

$$S_Q(\mathbf{r},\omega)=W_Q(\mathbf{r},\mathbf{r},\omega)=\langle U_Q^*(\mathbf{r},\omega)U_Q(\mathbf{r},\omega)\rangle_\omega \tag{1.14a}$$

and

$$S_V(\mathbf{r},\omega)=W_V(\mathbf{r},\mathbf{r},\omega)=\langle U_V^*(\mathbf{r},\omega)U_V(\mathbf{r},\omega)\rangle_\omega . \tag{1.14b}$$

In other words, spectral density is just the 'diagonal elements' of the cross-spectral density.

Since, the field propagates in free space and satisfies the inhomogeneous wave equation, therefore it can be shown that the cross-spectral densities of the field and of the source are related by the fourth-order differential equation [30]

$$\left(\nabla_1^2 + k^2\right)\left(\nabla_2^2 + k^2\right) W_V(\mathbf{r}_1, \mathbf{r}_2, \omega) = (4\pi)^2 W_Q(\mathbf{r}_1, \mathbf{r}_2, \omega), \tag{1.15}$$

where ∇_j^2 (j = 1,2) is the Laplacian operator acting with respect to the coordinates of the point $\mathbf{r}_j$, and $k = \omega/c$ is the free-space wave number associated with the frequency ω and c being the velocity of light. The equation (1.15) shows that there is a linear transform relationship between the cross-spectral density W_Q of the source and the cross-spectral density W_V of the field. However, there is no such relationship between the spectrum of the field and the spectrum of the source. The spectrum of the field can be determined by determing with the cross-spectral density of the field, starting from the cross-spectral density of the source and following the sequence

$$W_Q(\mathbf{r}_1, \mathbf{r}_2, \omega) \rightarrow W_V(\mathbf{r}_1, \mathbf{r}_2, \omega) \rightarrow W_V(\mathbf{r}, \mathbf{r}, \omega) \equiv S_V(\mathbf{r}, \omega), \tag{1.16}$$

where in the first step (1.15) has to be used. In fact, in general, the spectrum $S_V(\mathbf{r}, \omega)$ of radiated field is determined from the source correlations characterised by the cross-spectral density $W_Q(\mathbf{r}_1, \mathbf{r}_2, \omega)$ of the source and not from the source spectrum.

In most cases of practical interest it is useful to define the normalized cross-spectral density function by the formula [16,30]

$$\mu_A(\mathbf{r}_1,\mathbf{r}_2,\omega)=\frac{W_A(\mathbf{r}_1,\mathbf{r}_2,\omega)}{\sqrt{W_A(\mathbf{r}_1,\mathbf{r}_1,\omega)}\sqrt{W_A(\mathbf{r}_2,\mathbf{r}_2,\omega)}} \tag{1.17}$$

$$=\frac{W_A(\mathbf{r}_1,\mathbf{r}_2,\omega)}{\sqrt{S_A(\mathbf{r}_1,\omega)}\sqrt{S_A(\mathbf{r}_2,\omega)}}, \tag{1.18}$$

where the subscript A stands for the source variables or for the field variables. $\mu_A(\mathbf{r}_1,\mathbf{r}_2,\omega)$ is known as the spectral degree of coherence (sometimes also called the degree of spatial coherence or the degree of spectral coherence) at frequency ω of the optical field at point $\mathbf{r}_1$ and $\mathbf{r}_2$. In the experiments which are described in the subsequent chapters the spectral degree of coherence $\mu_A(\mathbf{r}_1,\mathbf{r}_2,\omega)$ of the field variables is denoted by a notation $\mu_{12}(\omega)$.

It has been shown that cross-spectral density is a non-negative definite, continuous matrix [18] and follows the inequality

$$S_A(\mathbf{r},\omega)=W_A(\mathbf{r},\mathbf{r},\omega)\geq 0 \tag{1.19}$$

and

$$\sqrt{W_A(\mathbf{r}_1,\mathbf{r}_1,\omega)}\sqrt{W_A(\mathbf{r}_2,\mathbf{r}_2,\omega)}\geq\left|W_A(\mathbf{r}_1,\mathbf{r}_2,\omega)\right|. \tag{1.20}$$

Using the inequality (1.19) it is clear that

$$0\leq\left|\mu_A(\mathbf{r}_1,\mathbf{r}_2,\omega)\right|\leq 1, \tag{1.21}$$

for all the values of the arguments $\mathbf{r}_1$, $\mathbf{r}_2$ and ω. The extreme case when $\left|\mu_A(\mathbf{r}_1,\mathbf{r}_2,\omega)\right|=1$ may be said to represent complete coherence at frequency ω of the (source or field) fluctuations at the point $\mathbf{r}_1$ and $\mathbf{r}_2$, whilest $\left|\mu_A(\mathbf{r}_1,\mathbf{r}_2,\omega)\right|=0$ may be said to represent complete incoherence (complete absence of correlations) at frequency ω, at the two points. In between these two extremes the field at the two points is said to be partial coherent. The complex degree of coherence $\gamma_{12}(\omega)$ and spectral degree of coherence $\mu_{12}(\omega)$ measure different physical informations. The

relationship between the two degrees of coherence is discussed by Friberg and Wolf [37].

§1.3 Radiation from model sources

In coherence theory, one generally talks about primary sources (i.e. spatial distributions of charges and currents, etc.) and secondary sources (e.g., illuminated apertures). There are strong similarities between primary and secondary sources. In the case of a primary source the randomness comes from the true source fluctuations (fluctuating atoms and molecules), while in the case of a secondary source it comes from fluctuating boundary conditions of the field in the secondary source plane. These sources are defined by various models. In practice one deals with typical class of sources defined as Schell-model sources and quasi-homogeneous sources. In this section the expressions for the cross-spectral density of the field generated by Schell-model sources and quasi homogeneous sources are described.

1.3.1 Schell-model sources

In the framework of coherence theory in space-time domain, two dimensional planar model sources of this kind were first explained by A.C. Schell [38,39]. Later the model was adopted for formulation of coherence theory in space-frequency domain.

Schell-model sources are the sources whose degree of spectral coherence $\mu_A(\mathbf{r}_1,\mathbf{r}_2,\omega)$ for either primary or secondary source is stationary in space. It means that $\mu_A(\mathbf{r}_1,\mathbf{r}_2,\omega)$ depends on $\mathbf{r}_1$ and $\mathbf{r}_2$ only through the difference $\mathbf{r}_2-\mathbf{r}_1$, i.e. of the form

$$\mu_A(\mathbf{r}_1,\mathbf{r}_2,\omega)\equiv\mu_A(\mathbf{r}_2-\mathbf{r}_1,\omega), \tag{1.22}$$

for each effective frequency ω present in the source spectrum. Here A stands for field variables V, in the case of a Schell-model secondary source and variables Q, in the case of a Schell-model primary source. The cross-spectral density function of a Schell-model source is of the form

$$W_A(\mathbf{r}_1,\mathbf{r}_2,\omega)=\left[S_A(\mathbf{r}_1,\omega)\right]^{1/2}\left[S_A(\mathbf{r}_2,\omega)\right]^{1/2}\mu_A(\mathbf{r}_2-\mathbf{r}_1,\omega). \qquad (1.23)$$

where $S_A(\mathbf{r},\omega)$ is the spectral density of the light at a typical point in the source or field (plane). The Schell model sources do not assume low coherence, and therefore, can be applied to spatially stationary light fields of any state of coherence. The Schell model of the form shown in Eq. (1.23) has been used to represent both three-dimensional primary sources [40,41] and two-dimensional secondary sources [38,42,43].

1.3.2 Quasi-homogeneous sources

A useful model of partially coherent sources that are frequently encountered in nature or in laboratory are the so called quasi-homogeneous sources [44,45]. This is an important sub-class of Schell-model sources. A Schell-model source is called a quasi-homogeneous if the intensity of a Schell model source is essentially constant over any coherence area. Under these approximations, the cross-spectral density function for a quasi-homogeneous source is given by [41,30]

$$W_A(\rho_1,\rho_2,\omega)=S_A\left[\frac{1}{2}(\rho_1+\rho_2),\omega\right]\mu_A(\rho_2-\rho_1,\omega). \qquad (1.24a)$$

The above equation can be written as

$$W_A(\rho_1,\rho_2,\omega)=S_A[\rho,\omega]\mu_A(\rho',\omega), \qquad (1.24b)$$

where $\rho=(\rho_1+\rho_2)/2$, and $\rho'=\rho_2-\rho_1$. The subscript A stands for either V or Q for

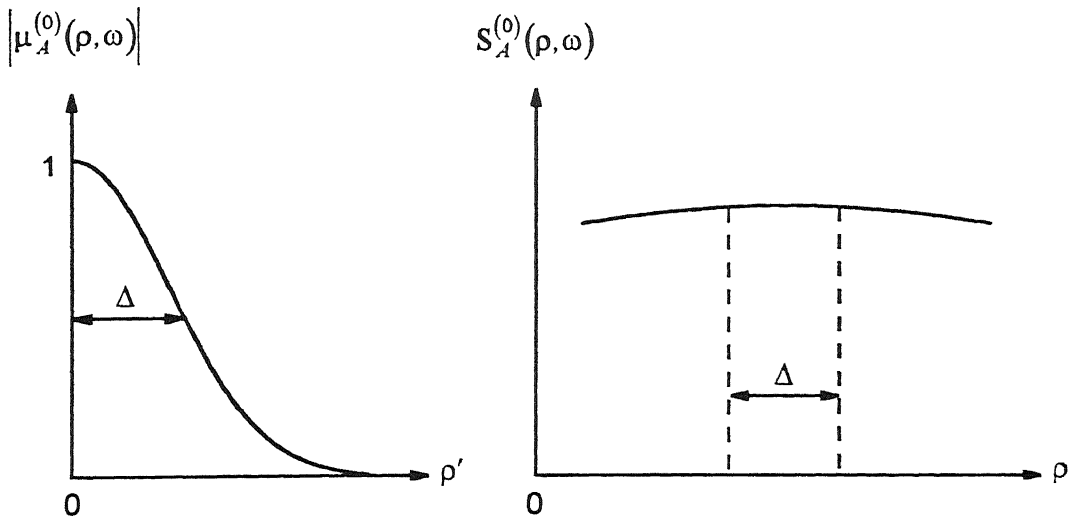

Fig. 1.1 A schematic, one-dimensional illustration of the variation of the absolute value of the spectral degree of coherence $|\mu^{(0)}(\rho',\omega)|$ (fast function of ρ') and of the spectral density $S^{(0)}(\rho,\omega)$ (slow function of ρ), with ω fixed, across a quasi-homogeneous source.

the field variable or a source variable respectively. It is clear that for a quasi-homogeneous source the spectral density $S_Q(\rho,\omega)$ varies so slowly with position that it is approximately constant over distances across the source that are of the order of the correlation length Δ (the effective width of $|\mu_Q(\rho',\omega)|$). Therefore $S_Q(\rho,\omega)$ is a slow function of ρ and $\mu_Q(\rho',\omega)$ is a fast function of ρ'. In addition, the linear dimensions of the source are large compared with the wavelength of light and with the correlation length Δ (Fig. 1.1).

Quasi-homogeneous sources are always spatially incoherent in the '*global*' sense, because their linear dimensions are large compared with the correlation length. This model is very good for representing two-dimensional secondary sources with sufficiently low coherence that the intensity does not vary over the

coherence area on the input plane [44,46]. It has also been applied to three-dimensional primary sources [41,40] and to two-dimensional primary and secondary sources [47,48].

The discovery that spatial coherence properties of a source affect the spectrum of emitted radiation grew out of the development of theoretical techniques for the study of coherence effects in space-frequency domain. The first theoretical prediction that the spectrum of light may differ from the spectrum of source was made by Wolf [21-23]. Since then a lot of theoretical and experimental studied have been made and several applications of these studies have been proposed. A brief account of the theoretical prediction about the spectral changes due to source correlation and that the changes may take place on propagation even in free space is given below.

§1.4 Spectral changes and scaling law

It was assumed until recently that spectrum is an intrinsic property of light that does not change as the radiation propagates in free-space. That this assumption may not always hold was first noted by Mandel [49,50]. He analyzed in his work on cross-spectral purity that the superposition of two beams of the same spectral density may lead to changes in the spectrum of light (at a fixed point) in the region of superposition. Not long ago, Wolf [21-23] discovered on rather general grounds that the spectrum of light, which originates in an extended source whether a primary source (a set of radiating atoms or molecules) or a secondary source obtained by allowing the radiation from a primary source to pass through an aperture, that is, an opening in an opaque screen in an optical system, depends not only on the source spectrum but also on the spatial coherence properties of the source. Wolf also predicted theoretically that the spectrum of light will, in general, be different from

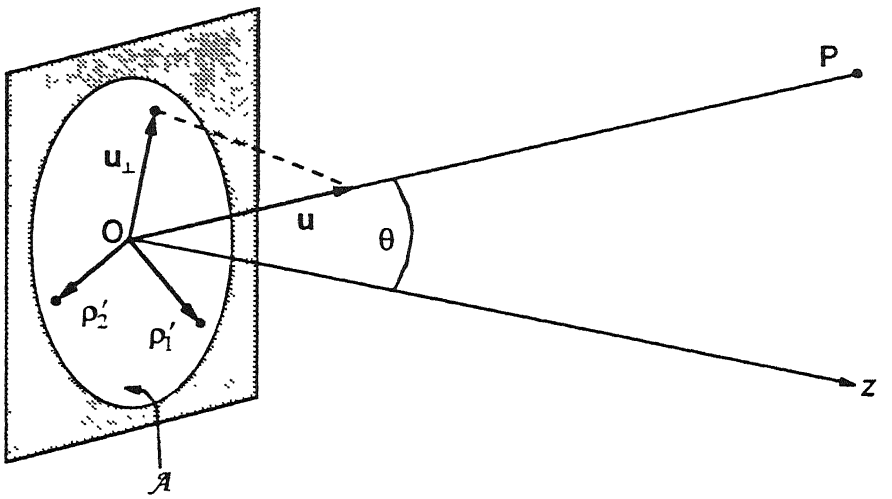

Fig. 1.2 Illustrating the notation relating to radiation from a planar secondary source. P is a point in the far-zone, specified by a position vector $\mathbf{r} = r\mathbf{u}$ ($\mathbf{u}^2 = 1$). The symbol $\mathbf{u}_\perp$ denotes a projection (considered as a two-dimensional vector) of the unit vector $\mathbf{u}$ onto the source plane.

the spectrum of the source and be different points in space on propagation in free space.

To show how correlations of the light across the source affect the spectrum of radiation field, we consider radiation from an extended source in the form of a planar secondary source such as an aperture in an opaque planar screen illuminated by radiation of any state of spatial coherence. Let the second-order coherence properties of the secondary be characterised by the cross-spectral density $W^{(0)}(\rho_1', \rho_2', \omega)$ where ρ_1' and ρ_2' are the two dimensional position vectors of any two points in the source plane (Fig. 1.2), the spectrum of the field at a point in the far-zone, generated by such a source is given by the formula [51]

$$S^{(\infty)}(r\mathbf{u}, \omega) = \frac{k^2 \cos^2\theta}{(2\pi)^2 r^2} \iint W^{(0)}(\rho_1', \rho_2', \omega) e^{[-ik\mathbf{u}_\perp \cdot (\rho_2' - \rho_1')]} d^2\rho_1 d^2\rho_2 . \qquad (1.25)$$

Here $\mathbf{r} \equiv r\mathbf{u}$ is the position vector of the point P, referred to an origin in source region, $\mathbf{u}$ is a real unit vector and $\mathbf{u}_\perp$ is the projection of $\mathbf{u}$, considered as a two dimensional vector on to the source plane. θ is the angle between $\mathbf{u}$ and normal to the source plane and $k = \omega/c$. Equation (1.25) shows that the spectrum of the field in the far-zone depends not only on the source spectrum $S^{(0)}(\rho,\omega) = W^{(0)}(\rho,\rho,\omega)$ of light distribution across the secondary source but also on the spectral degree of coherence.

As has been mentioned in the text that partially coherent sources that are frequently encountered in nature or in laboratory are the so-called quasi-homogeneous sources [30,44,45]. The cross-spectral density $W^{(0)}(\rho_1',\rho_2',\omega)$ of such a source as expressed in Eq. (1.24) can be given as

$$W^{(0)}(\rho_1',\rho_2',\omega) \approx S^{(0)}\left(\frac{\rho_1'+\rho_2'}{2},\omega\right)\mu^{(0)}(\rho_2'-\rho_1',\omega). \tag{1.26}$$

Let us introduced the normalised source spectrum $s^{(0)}(\rho,\omega)$ by the relation

$$s^{(0)}(\rho,\omega) = \frac{S^{(0)}(\rho,\omega)}{I^{(0)}(\rho)} \tag{1.27}$$

and $I^{(0)}(\rho)$ is the intensity across the source can be given by the formula

$$I^{(0)}(\rho) = \int_0^\infty S^{(0)}(\rho,\omega)d\omega. \tag{1.28}$$

It is also assumed that the normalised spectrum of the source is same throughout the source region such that $s^{(0)}(\rho,\omega) = s^{(0)}(\omega)$. Substituting from Eq. (1.27) and Eq. (1.28) in Eq. (1.26), we get

$$W^{(0)}(\rho_1',\rho_2',\omega) \approx s^{(0)}(\omega)I^{(0)}\left(\frac{\rho_1'+\rho_2'}{2}\right)\mu^{(0)}(\rho_2'-\rho_1',\omega). \tag{1.29}$$

On substituting Eq. (1.29) in Eq. (1.25), one obtains the expression for the far-field spectrum of the field generated by a planar, secondary, quasi-homogeneous source, whose normalised spectrum is same at each source point, therefore

$$S^{(\infty)}(r\mathbf{u},\omega)=\frac{(2\pi)^2 k^2 \cos^2\theta}{r^2}\tilde{I}^{(0)}(0)\tilde{\mu}^{(0)}(k\mathbf{u}_\perp,\omega)s^{(0)}(\omega), \qquad (1.30)$$

where $\tilde{I}^{(0)}(\mathbf{f})$ and $\tilde{\mu}^{(0)}(\mathbf{f},\omega)$ denote the two dimensional spatial Fourier transforms of the spatial distribution of this intensity and of the spectral degree of coherence. i.e.

$$\tilde{I}^{(0)}(\mathbf{f})=\frac{1}{(2\pi)^2}\int I^{(0)}(\rho)e^{(-i\mathbf{f}\cdot\rho)}d^2\rho \qquad (1.31a)$$

$$\tilde{\mu}^{(0)}(\mathbf{f},\omega)=\frac{1}{(2\pi)^2}\int \mu^{(0)}(\rho,\omega)e^{(-i\mathbf{f}\cdot\rho)}d^2\rho. \qquad (1.31b)$$

Equation (1.30) shows that the spectrum of the field in the far-zone depends on the coherence properties of the source through the spatial Fourier transform of its spectral degree of coherence. Thus one can immediately infer that the normalised spectrum of the field in the far-zone generated by a planar, secondary, quasi-homogeneous is not, in general, equal to the normalised spectrum of the light in the source plane and the normalised spectrum of the field in the far-zone $s^{(\infty)}(r\mathbf{u},\omega)$ is related to normalised $s^{(0)}(\omega)$ of the source by the formula

$$s^{(\infty)}(r\mathbf{u},\omega)\equiv\frac{S^{(\infty)}(r\mathbf{u},\omega)}{\int_0^\infty S^{(\infty)}(r\mathbf{u},\omega)d\omega}$$

$$=s^{(0)}(\omega)\frac{\left[\omega^2\tilde{\mu}^{(0)}(k\mathbf{u}_\perp,\omega)\right]}{\int_0^\infty\left[\omega'^2\tilde{\mu}^{(0)}(k'\mathbf{u}_\perp,\omega')\right]s^{(0)}(\omega')d\omega'}, \qquad (1.32)$$

where $k'=\omega'/c$.

To explain the reason why such coherence-induced spectral changes were not observed until recently, Wolf [21,30] showed that the usual thermal sources employed in laboratories or commonly encountered in nature have special coherence properties which ensure that the normalised spectrum of the radiation they emit in free space is the same throughout the far-zone and is equal to normalised source spectrum.

Let us consider a planar, secondary, quasi-homogeneous source, whose normalised spectrum is the same at every point on the source. It has been shown by Wolf [21,52] and Ohtsuka [53] that a necessary and sufficient condition for a field radiated by such a source to have the same normalised spectrum throughout the far-zone and across the source plane is that its spectral degree of coherence has the function form

$$\mu^{(0)}(\rho_2-\rho_1,\omega)=h\left[k(\rho_2-\rho_1)\right], \qquad \left(k=\frac{\omega}{c}=\frac{2\pi}{\lambda}\right). \tag{1.33}$$

This formula expresses the so-called *scaling law* and shows that if one changes the wavelength, one can compensate for the change in $\mu^{(0)}(\rho_2-\rho_1,\omega)$ by an appropriate change in $(\rho_2-\rho_1)$. More precisely the scaling law arises from the fact that for certain sources, the knowledge of the spectral degree of coherence $\mu^{(0)}(\rho_2-\rho_1,\omega)$ at one frequency gives information about the spectral degree of coherence at all frequencies; one only needs to scale appropriately the separation of the points represented by the vector $(\rho_2-\rho_1)$.

It turns out that the scaling law is satisfied by some of the most commonly occurring sources found in nature and in the laboratory. For example, the spectral degree of coherence of Lambertian sources and of a blackbody sources can be shown to be given by the formula [21,30]

$$\mu^{(0)}(\rho_2-\rho_1,\omega)=\frac{sin\left(k|\rho_2-\rho_1|\right)}{k|\rho_2-\rho_1|}. \qquad (1.34)$$

This expression evidently satisfies the scaling law, and consequently the normalised spectrum of the field generated by such sources is the same throughout the far-zone and is equal to the normalised spectrum of the field across the source. However, if the spectral degree of coherence does not satisfy the scaling law, the normalised far-field spectrum will, in general, be different in different direction in the far-zone and will differ from the source spectrum.

§1.5 Spectral Changes in Young's interference experiment

Spectral changes in Young's interference experiments with broad-band light are not as well understood as their quasi-monochromatic counterparts, probably because in such experiments no interference fringes formed. However, if one were to analyse the spectrum of the light in the region of superposition, one would observe a modulation of it. The fact that the superposition of two beams of the same spectral density may lead to change in the spectrum of light in the region of superposition was first noted by Mandel [49,50], in his work on cross-spectral purity.

One can readily derive an expression for the spectrum of light in the region of superposition. For this purpose consider partially coherent light incident from the left onto an opaque screen containing two small identical apertures at P_1 and P_2 (Fig. 1.3). The field at these points may be represented by ensembles of frequency-dependent realisation $\{U(P_1,\omega)\}$ and $\{U(P_2,\omega)\}$. We assume that the apertures are sufficiently small so that the amplitude of the field is effectively constant over each of them and also that the angles of incidence and diffraction are small. Then the

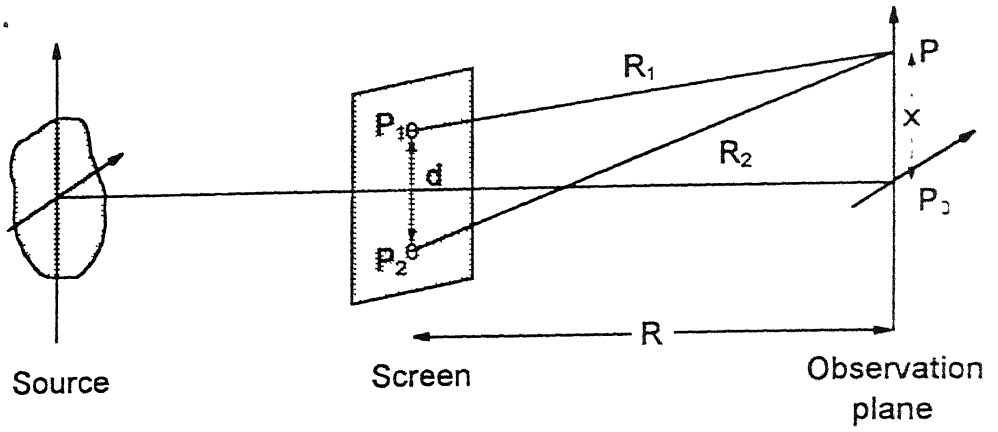

Fig. 1.3 Young's interference experiment with light of any state of coherence.

field at a point P beyond the screen is, to a good approximation, given by the following expression [54]

$$U(P,\omega)=ikA\left[U(P_1,\omega)\frac{e^{ikR_1}}{R_1}+U(P_2,\omega)\frac{e^{ikR_2}}{R_2}\right]. \qquad (1.35)$$

Here A is the area of each pinhole, R_1 and R_2 are the distances from each pinhole to the point P and, as before, $k=\omega/c$ is the wavenumber associated with frequency ω, c being the speed of light.

On substituting from (1.35) into (1.14b), we obtain for the spectrum of the light at the point P the expression [54]

$$S(P,\omega)=S^{(1)}(P,\omega)+S^{(2)}(P,\omega)+2\sqrt{S^{(1)}(P,\omega)}\sqrt{S^{(2)}(P,\omega)}$$
$$\times\left|\mu(P_1,P_2,\omega)\right|\cos\left[\beta(P_1,P_2,\omega)+\omega(R_2-R_1)/c\right]. \qquad (1.36)$$

Here $S^{(1)}(P,\omega)$ is the spectral density of the light at P which would be obtained if the small aperture at P_1 alone was open, $S^{(2)}(P,\omega)$ has a similar meaning if only the aperture at P_2 was open and $\beta(P_1,P_2,\omega)$ denotes the phase of the spectral degree of coherence [54]

$$\mu(P_1,P_2,\omega) \equiv |\mu(P_1,P_2,\omega)| e^{i\beta(P_1,P_2,\omega)}. \tag{1.37}$$

The formula (1.36) is the so-called spectral interference law relating to superposition of beams for any state of spatial coherence [16].

Let us assume. as is commonly the case, that $S^{(2)}(P,\omega) \approx S^{(1)}(P,\omega)$ and let d be the distance between the two pinholes. Consider the spectral density at the point P, at distance x from the axis of symmetry in an observation plane at distance R behind the plane containing the pinholes. Assuming that $x/R << 1$, one can make the approximation [54]

$$R_2 - R_1 \approx \frac{xd}{R} \tag{1.38}$$

and Eq. (1.36) then reduces to

$$S(P,\omega) \approx 2S^{(1)}(P,\omega)\{1+|\mu(P_1,P_2,\omega)|\cos[\beta(P_1,P_2,\omega)+\omega\, xd/cR]\}. \tag{1.39}$$

This formula implies the following two results: (i) at any fixed frequency ω, the spectral density varies sinusoidally with the distance x of the point from the axis, with the amplitude and the phase of the variation depending on the (generally complex) spectral degree of coherence $\mu(P_1,P_2,\omega)$; and (ii) at any fixed point P in the observation plane the spectrum $S(P,\omega)$ will, in general, differ from the spectrum $S^1(P,\omega)$, the change depending also on the spectral degree of coherence $\mu(P_1,P_2,\omega)$ of the light at the two pinholes [54,55].

§1.6 Experimental confirmations

Since the discovery of the phenomenon of spectral variance on propagation of radiation (due to coherence), many experiments have been performed to verify of these theoretical predictions. The first experimental tests of the theoretical prediction of spectral invariance and non-invariance due to correlation of fluctuations across the source were performed by Morris and Faklis [56,57]. They measured the far-field spectra produced by two different planar, secondary, quasi-homogeneous (PSQh) sources. The first system was an ordinary lens which obeyed the scaling law, and the normalized spectra were found to be invariant on propagation. The second system was a Fourier achromat which consisted of a combination of optical elements. It was shown that this system violated the scaling law. The spectral degree of coherence of light produced at focal plane of the Fourier achromat was effectively independent of frequency over the whole spectral range for which the lens has been achromatized. Hence spectra were found non-invariant on propagation.

An interesting experiment for showing the effects of source correlations on the spectra of emitted radiation was designed by Indebetouw [58]. In this optical system a secondary source was synthesized having varying degrees of coherence. It was shown that different pupil masks can generate different spectral degrees of coherence of the synthesized source at each frequency of the dispersed spectrum. In general, such a secondary source did not satisfy the scaling law and, consequently, the spectrum of light differed in the far-zone of the source.

It is well known that, generally in practice, diffracting and sometimes also dispersive elements are interposed between the source and the detector. This has been noted that a diffracting aperture will, in general, change the coherence

properties of the light which passes through it, even in the absence of dispersive medium. It is known if partially coherent light is diffracted by an aperture whose linear dimensions are of the order of or smaller than the width of the transverse correlations of the incident light, the light which emerges from the aperture will be essentially spatially coherent. However, if the size of the aperture is sufficiently large, the emerging light will be partially coherent. Consequently the spectrum of the light which is transmitted by the aperture to be, in general, affected by the size of the aperture. This effect was first noted by Kandpal, Vaishya and Joshi [59] with a simple optical experiment. Their experimental setup consisted of different filter-lens combinations, with apertures of varying sizes so that for small frequency sampling a properly achromatized secondary source with varying degree of coherence could be produced. The normalized spectrum observed in the far-zone was found to be different than the source spectrum. Further the systematic studies of the effect of aperture size on the spectrum of the light diffracted by an aperture was made by Foley [60,61]. This simple experiment has not only verified the theoretical predictions but also has shown direct implications in basic and applied research [62]. One of the important applications of these observations has been shown to explain the discrepancies in the maintenance of the spectroradiometric scales by national laboratories in different countries [59].

It has been shown that cross-spectrally pure light can be generated, for example, by linear filtering of light that emerges from the two pinholes in Young's interference experiments [63]. It has also been confirmed experimentally that the spectra in the region of superposition show spectral changes, i.e. shift in the peak of the wavelength for narrow bandwidth of light and spectral modulations with broad-band light in Young's interference experiment [64,65]. The experimental studies on correlation-induced spectral changes and spectral modulations produced in two

beam interference with broad-band light have potential application in determining experimentally the spectral degree of coherence of partially coherent fields [66] The knowledge of spectral degree of coherence is often important in remote sensing [67,68].

The connections between Young's interference experiment and the measurement of the complex degree of coherence of light in space-time domain is well-known. Michelson's well-known technique for determining angular diameters of stars by determining complex degree of coherence forms the basis for interferometric imaging which is one of the most powerful methods currently employed in radio astronomy. It makes use of multiple-element interferometers to determine the degree of coherence at several pairs of detectors in the radiation field reaching the Earth from distant radio sources. The detector system used in such instruments filters out the incoming radiation to make it quasi-monochromatic. Interference fringes are formed and the degree of coherence is determined from measurement of their visibility. The intensity distribution across the source, which is assumed to be essentially incoherent, is then obtained by the use of van Cittert-Zernike theorem. However, it has been shown theoretically [67,68] and experimentally [69] that spectroscopic method for observing coherence-introduced spectral changes is a novel method for determining spatial coherence properties of a incident light over broad frequency range. In many cases of interest, the field correlations in the far-zone of radiating sources obey the so called space-frequency equivalence principle. Some of the practical problems encountered in determining the intensity distribution across sources in traditional interferometric methods can be overcome by making use of determining spatial coherence properties over a large frequency range from the spectral changes produced due to interference. The essence of space-frequency principle is that measurement of spectral degree of

coherence over some frequency ω by doubling the vector separation of the detectors (radio antennas) is equivalent to making the measurements at the original vector separation but at frequency 2ω. Kandpal et.al [70] have shown by laboratory experiments that a trade-off of this kind could be potentially powerful technique for determining intensity distribution across sources and also the angular separation of a pair of sources [69]. These laboratory experiments might find applications in astronomy in synthetic aperture imaging and also determining angular separation of double stars by simple, quick and cost effective methods.

It has been shown both theoretically [71] and experimentally [72] that if two partially coherent beams are made incident at the entrance beam splitter of a Mach-Zehnder interferometer and spectrum of one of the beams at the output of the interferometer is probed, one observes spectral modulations. The spectral modulations depend on the degree of spectral coherence between the two beams and also on the optical path difference of the beams in the arms of the interferometer. It has been shown experimentally that from only two spectral measurements one can get information about the degree of spectral coherence and also the optical path difference. Since optical path difference of the order of the average wavelength of the radiation can be determined experimentally, this method could be a better technique for measuring small displacements and thickness of transparent films very accurately.

Wolf [23] showed also the effect of source correlation on the spectra of emitted fields by taking simple example of radiation from two small fluctuating sources and showed that the far-field spectrum shifts towards shorter wavelengths (i.e. blue shift) or towards longer wavelengths (red shift) depending on the correlation existing between the two fluctuating sources. The prediction that the

energy redistribution in the spectrum of radiated field due to source correlation may result in apparent shift of spectral line was demonstrated experimentally by Bocko, Douglass and Knox [73] using electronically generated acoustical sources. In the optical domain the prediction was verified by Gori, Guattari, Palma and Padovani [74] by producing partially correlated sources obtained by mixing two independent light beams with nearly the same spectra. A potential application of coherence-induced spectral changes with radiation from two small sources was proposed by Gamliel and Wolf [75] who showed that by controlling the spectral degree of coherence it is possible to modulate the spectrum, e.g. narrowing and broadening of a spectral line or generation of several lines from a single spectral line [76].

§1.6 Motivation and outline of the thesis

Induced by the developments which took place in the past few years after the discovery of correlation-induced spectral changes also known as the *'Wolf effect'*, the study on the effect of spatial coherence on the spectra of radiated fields has been extended further to verify experimentally certain theoretical predictions and to show a few applications of this phenomenon.

In *chapter 2*, an experimental study has been made to clearly demonstrate the spectral changes that take place due to source correlation and that due to diffraction.

In *chapter 3*, the space-frequency equivalence principle has been applied to determine the angular sizes of sources by determining the degree of spatial coherence from the spectral changes produced on interference in a laboratory version of Michelson's stellar interferometer. This is an important study which might find application in remote sensing. The study carried out in *chapter 4* is the

reconstruction of source intensity profile using the space-frequency equivalence principle in Young's double slit experiment. This may be utilised in automated inspection.

In *chapter 5*, it has been shown experimentally that the spectra of partially coherent fields, propagating beyond an optical system (a lens) reveal no spectral shift on the geometrical-image plane, while large blue shift occurs at the back focal plane of the optical system for on-axis points of observation. In many spectroscopic measurements a monochromator is used as a device to filter out the radiation. It has been shown in *chapter 6* that the optics in a monochromator affects the coherence properties of the radiation fields. The impact of these studies would be in metrology.

References

[1] E. Verdet, *Ann. Scientif. l'École Normale supérieure* **2** (1865) 291.

[2] A.A. Michelson, *Phil. Mag.* (5) **30** (1890) 1; **31** (1891) 256, *Astrophys. J.* **51** (1920) 257.

[3] A.A. Michelson, *Phil. Mag.* (5) **31** (1891) 338; **34** (1892) 280.

[4] T. Young, *Phil. Trans. Roy. Soc.* **xcii** 12 (1802) 387; *Young's Works*, Vol. 1, pp. 140, 170.

[5] M. von Laue, *Ann. d. Physik* (4) **23** (1907) 1, 795.

[6] M. Berek, *Z. Phys.* **36** (1926) 675, 824 ; **37** (1926) 387; **40** (1926) 420.

[7] P.H. van Cittert, *Physica* **1** (1934) 201.

[8] P.H. van Cittert, *Physica* **6** (1939) 1129.

[9] F. Zernike, *Physica* **5** (1938) 785.

[10] H.H. Hopkins, *Proc. Roy. Soc. A* **208** (1951) 263; ibid, A **217** (1953) 408.

[11] E. Wolf, *Proc. Roy Soc. A* **230** (1955) 246; ibid; A **225** (1954) 96.

[12] E. Wolf, *Nuovo Cimento* **12** (1954) 884.

[13] A. Blanc-Lapierre and P. Dumontet, *Rev. d' Optique* **34** (1955) 1.

[14] R. Hanbury Brown and R.Q. Twiss, *Proc. Roy. Soc. A* **242** (1957) 300.

[15] R. Hanbury-Brown and R.Q. Twiss, *Proc. Roy. Soc. A* **243** (1957) 291.

[16] L. Mandel and E. Wolf, *J. Opt. Soc. Am.* **66** (1976) 529.

[17] E. Wolf, *Opt. Commun.* **38** (1981) 3.

[18] E. Wolf, *J. Opt. Soc. Am.* **72** (1982) 343.

[19] E. Wolf, *Opt. Lett.* **8** (1983) 250.

[20] E. Wolf, *J. Opt. Soc. Am. A* **3** (1986) 76.

[21] E. Wolf, *Phys. Rev. Lett.* **56** (1986) 1370.

[22] E. Wolf, *Nature* **326** (1987) 363.

[23] E. Wolf, *Phys. Rev. Lett.* **68** (1987) 2646.

[24] M. Born and E. Wolf, *"Principles of Optics"* (Pergamon Press, Oxford, Sixth ed., 1980) chapter 10.

[25] J.W. Goodman, *"Statistical Optics"* (Wiley, Chichester, 1985).

[26] M.J. Beran and G.B. Parrent, *"Theory of Partial Coherence"* (Prentice-Hall, Englewood Cliffs, N.J., 1964).

[27] L. Mandel and E. Wolf, *Rev. Mod. Phys.* **37** (1965) 231.

[28] J. Parina, *"Coherence of Light"* (Reidel, Dordrecht, Second ed., 1985).

[29] A.S. Marathay, *"Elements of Optical Coherence Theory"* (John Wiley and Sons, 1982).

[30] L. Mandel and E. Wolf, *"Optical Coherence and Quantum Optics"* (Cambridge University Press, Cambridge, 1995).

[31] W.H. Carter, *"Hand Book on Optics"* (Ed. M Beas *etal.* McGraw Hill Publications 1996).

[32] H.C. Kandpal, J.S. Vaishya and K.C. Joshi, *Opt. Eng.* **33** (1994) 1996.

[33] E. Wolf and D.F.V. James, *Rep. Prog. Phys.* **59** (1996) 771.

[34] W.B. Davenport and W.L. Root, *"Random Signals and Noise"* (MeGraw-Hill, New York, 1958).

[35] C. Kittel, *"Elementary Statistical Physics"* (Wiley, New York 1958).

[36] G. S. Agarwal and E. Wolf, *J. Mod. Opt.* **40** (1993) 1489.

[37] A.T. Friberg and E. Wolf, *Opt. Lett.* **20** (1995) 623.

[38] A.C. Schell, *"The Multiple Plate Antenna"* (Doctoral Dissertation, Massachusetts Institute of Technology, 1961).

[39] A.C. Schell, *IEEE Trans.* Antennas Propag. AP-**15** (1967) 187.

[40] W.H. Carter and E. Wolf, *Optica Acta* **28** (1981) 227.

[41] W.H. Carter and E. Wolf, *Optica Acta* **28** (1981) 245.

[42] E. Collett and E. Wolf, *Opt. Lett.* **2** (1978) 27.

[43] W.H. Carter and M. Bertolotti, *J. Opt. Soc. Am.* **68** (1978) 329.

[44] W.H. Carter and E. Wolf, *J. Opt. Soc. Am. 67* (1977) 785.

[45] J.W. Goodman, *Proc. IEEE* **53** (1965) 1688.

[46] W.H. Carter and E. Wolf, *J. Opt. Soc. Am. A* **2** (1985) 1994.

[47] E. Wolf and W.H. Carter, *J. Opt. Soc. Am.* **68** (1978) 953.

[48] W.H. Carter, *J. Opt. Soc. Am. A* **1** (1984) 716.

[49] L. Mandel, *J. Opt. Soc. Am.* **51** (1961) 1342.

[50] L. Mandel, *J. Opt. Soc. Am.* **52** (1962) 1335.

[51] E.W. Marchand and E.Wolf, *J.Opt. Soc. Am.* **64** (1974) 1219.

[52] E. Wolf, *J. Mod. Opt.* **39** (1992) 9.

[53] Y. Ohtsuka, *Opt. Rev. Japan* **2** (1995) 347.

[54] D.F.V. James and E. Wolf, *Phys. Letts. A* **157** (1991) 6

[55] D.F.V. James and E. Wolf, *Opt. Commun.* **81** (1991) 150.

[56] G.M. Morris and D. Faklis, *Opt. Commun.* **62** (1987) 5.

[57] D. Faklis and G.M. Morris, *Opt. Lett.* **13** (1988) 4.

[58] G. Indebetouw, *J. Mod. Opt.* **36** (1989) 251.

[59] H.C. Kandpal, J.S. Vaishya and K.C. Joshi, *Opt. Commun.* **73** (1989) 169.

[60] J.T. Foley, *Opt. Commun.* **75** (1990) 347.

[61] J.T. Foley, *J. Opt. Soc. Am. A* **8** (1991) 1099.

[62] H.C. Kandpal, J.S. Vaishya and K.C. Joshi, *Phys. Rev. A* **41** (1990) 4541.

[63] H.C. Kandpal, K. Saxena, D.S. Mehta, J.S. Vaishya and K.C. Joshi, *Opt. Commun.* **99** (1993) 157.

[64] H.C. Kandpal, J.S. Vaishya, M. Chander, K. Saxena, D.S. Mehta and K.C. Joshi, *Phys. Letts. A* **167** (1992) 114.

[65] M. Santarsiero and F. Gori, *Phys. Letts. A* **167** (1992) 123.

[66] K. Saxena, D.S. Mehta, H.C. Kandpal, J.S. Vaishya and K.C. Joshi, *Opt. Commun.* **111** (1994) 423.

[67] D.F.V. James and E. Wolf, *Radio Science* **26** (1991) 1239.

[68] D.F.V. James, H.C. Kandpal and E. Wolf, *Astrophys. J.* **445** (1995) 406.

[69] H.C. Kandpal, K. Saxena, D.S. Mehta, J.S. Vaishya and K.C. Joshi, *J. Mod. Opt.* **42** (1995) 447.

[70] H.C. Kandpal, K. Saxena, D.S. Mehta, J.S. Vaishya and K.C. Joshi, *J. Mod. Opt.* **42** (1995) 455.

[71] G.S. Agarwal and D.F.V. James, *J. Mod. Opt.* **40** (1993) 1431.

[72] D.S. Mehta, H.C. Kandpal, K. Saxena, J.S. Vaishya and K.C. Joshi, *Opt. Commun.* **119** (1995) 352.

[73] M.F. Bocko, D.H. Douglass and R.S. Knox, *Phys. Rev. Lett.* **58** (1987) 2649.

[74] F. Gori, G. Guattari, C. Palma and C. Padovani, *Opt. Commun.* **67** (1988) 1.

[75] A. Gamliel and E. Wolf, *Opt. Commun.* **65** (1988) 91.

[76] H.C. Kandpal, J.S. Vaishya and K.C. Joshi, *Opt. Commun.* **77** (1990) 1 {erratum: ibid., **78** (1990) 444}.

Chapter 2

Correlation-induced spectral changes on passing partially coherent light through an annular aperture

It has already been explained in *chapter one* that when light propagates from planar, partially coherent, secondary source which has the same spectrum at all source points, the normalised spectrum of the light in the far-zone will, in general, be different at different observation points and be different from the normalised spectrum of the light in source plane. This change in the spectrum can be produced when (i) the correlation function of the emitted light does not satisfy the Wolf's scaling law [1], (ii) the secondary source does not satisfy the quasi-homogeneous condition [2,3]. It was also shown that if such a source is quasi-homogeneous and satisfies the scaling law, the normalised spectrum of the light will be the same at all observation points in the far-zone. It will be the same as the normalised spectrum of the light in the source plane [1]. These predictions have been verified experimentally by a number of researcher [4,5].

Recently, it was shown theoretically that spectral changes take place when partially coherent light is passed through an annular aperture [6]. The paper analysed change in the spectrum that are produced due to source-correlations at on-axis observation points in the far-zone of the annular aperture.

In this chapter, experimental results of the study of the spectral shifts are discussed at on-axis points and off-axis points in the far-zone of an annular aperture when partially coherent light is passed through the annular aperture. The changes in the spectra are found to depend on the ratio of the radius of central obstruction to the outer radius of the annular aperture and also on the degree of spectral coherence at the annular aperture.

§2.1 Theory

The schematic arrangement of the optical system is shown in Fig. 2.1. A circular, spatially incoherent, polychromatic, planar source σ of radius a_S is illuminated by light and is in the front focal plane of a thin achromatic lens L of focal length f. The source (σ) is assumed to be uniform, i.e. its spectrum $S^{(s)}(\omega)$ is assumed to be the same at all source points. Here ω denotes (angular) frequency. An opaque screen with an annular aperture A is placed at the back focal plane of the

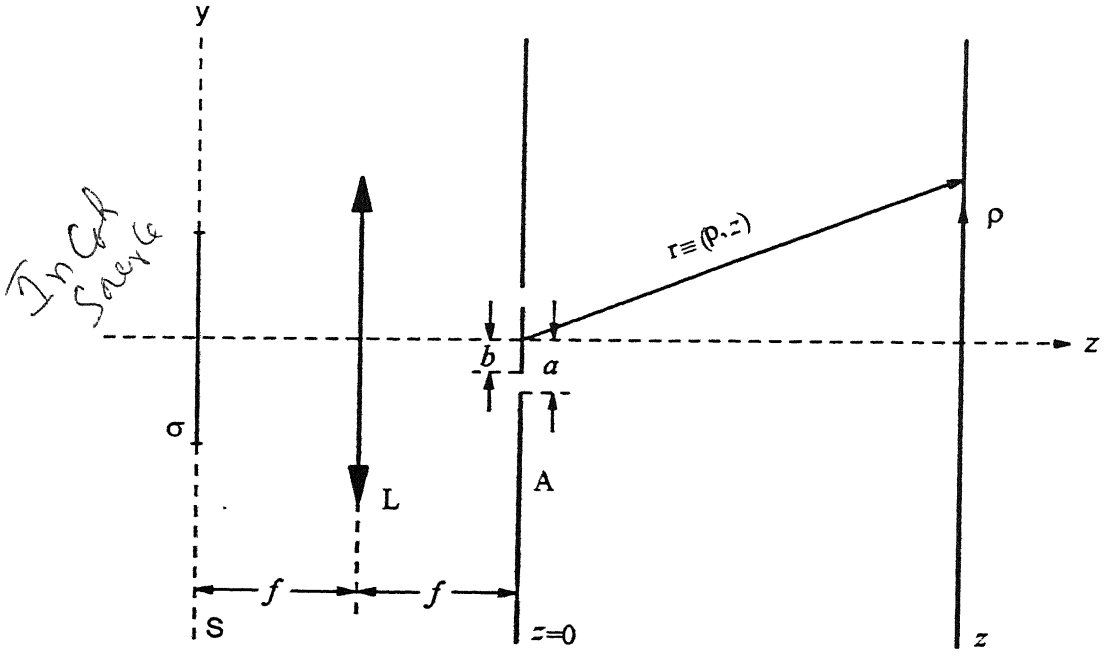

Fig. 2.1 The optical system.

Lens L. The outer radius of the annular aperture is a, the inner radius of the aperture is b, and the ratio b/a is called central obstruction ε. The plane of opaque screen is at z=0. The observation point P located by position vector $\mathbf{r} = (\rho, z)$ denotes an observation point in the far-zone of the aperture. Here investigation is limited to on-axis observation points, i.e. to the case $\rho = 0$.

To determine $S(z,\omega)$, we must know the cross spectral density of the light in the aperture A. Consider two points P_1 and P_2 in A which are located by position vectors ρ_1' and ρ_2'. If the radius of lens is large enough so that its finite size may be neglected the cross spectral density of the light at P_1 and P_2 is given by [7]

$$W^{(0)}(\rho_1', \rho_2', \omega) = S^{(0)}(\omega)\mu^{(0)}(\rho_1', \rho_2', \omega), \tag{2.1}$$

where

$$S^{(0)}(\omega) = \eta S^{(S)}(\omega), \tag{2.2}$$

$$\mu^{(0)}(\rho_1', \rho_2', \omega) = 2\frac{J_1\left(k|\rho_2' - \rho_1'|a_S/f\right)}{k|\rho_2' - \rho_1'|a_S/f}. \tag{2.3}$$

Here η is a constant, $k = \omega/c$, c is the speed of light in vacuo, and J_1 is the Bessel function of order 1. $S^{(0)}(\omega)$ and $\mu^{(0)}(\rho_1', \rho_2', \omega)$ are, respectively, the spectrum and the spectrum and the complex degree of spatial coherence at frequency ω of the light in the aperture A.

The spectrum of the light at on-axis point of observation in the far-zone of the aperture, as derived by Pu [6] is given by the expression

$$S(z,\omega) = \left(\frac{af}{a_S z}\right)S^{(0)}(\omega)\left[M_1(\omega) - \varepsilon^2 M_2(\omega)\right], \tag{2.4}$$

where

$$M_1(\omega) = 1 - J_0^2\left[3.832a/L(\omega)\right] - J_1^2\left[3.832a/L(\omega)\right], \tag{2.5}$$

$$M_2(\omega) = 1 - J_0^2\left[3.832\varepsilon a / L(\omega)\right] - J_1^2\left[3.832\varepsilon a / L(\omega)\right], \tag{2.6}$$

J_0 and J_1 are the Bessel functions of order zero and first degree, respectively

$$L(\omega) = 3.832 f / k a_S = 3.832 c f / \omega a_S \tag{2.7}$$

is called the effective correlation length of light on the annular aperture. Thus the spectrum $S(z,\omega)$ at the on-axis observation point in the far-zone is modified by geometrical factors and two frequency dependent factors $M_1(\omega)$ and $M_2(\omega)$ which depend on a/L(ω), and ε. If ε = 0, Eq. (2.4) shows that the spectrum of the light at on-axis point of observation in the far-zone of the aperture has the form

$$S(z,\omega) = \left(\frac{af}{a_S z}\right) M_1(\omega) S^{(0)}(\omega). \tag{2.8}$$

This expression is derived by Foley [2] for circular aperture.

§2.2 Experimental details and results

The experimental setup used is shown in Fig. 2. A 750 W tungsten-halogen lamp operated by a highly stabilized dc power supply was used as a source. To generate a planar secondary uniform illuminated incoherent source, the light from the primary source (tungsten-halogen lamp) was transmitted through a ground glass diffuser. The transmitted light was made incident on a circular aperture (σ) of radius a_S = 250 μm at front focal plane of an achromatic lens (focal length = 20 cm), which was placed about 15 cm away from the diffuser plate. The circular aperture is defined as plane I. It was assumed that, in this case, the spectrum is same at all points within the aperture at plane I. At the back focal plane of the achromatic lens defined as plane II, we introduced either a circular aperture or annular apertures of different sizes. Different interference filters with different peak wavelengths were placed just before secondary source plane II.

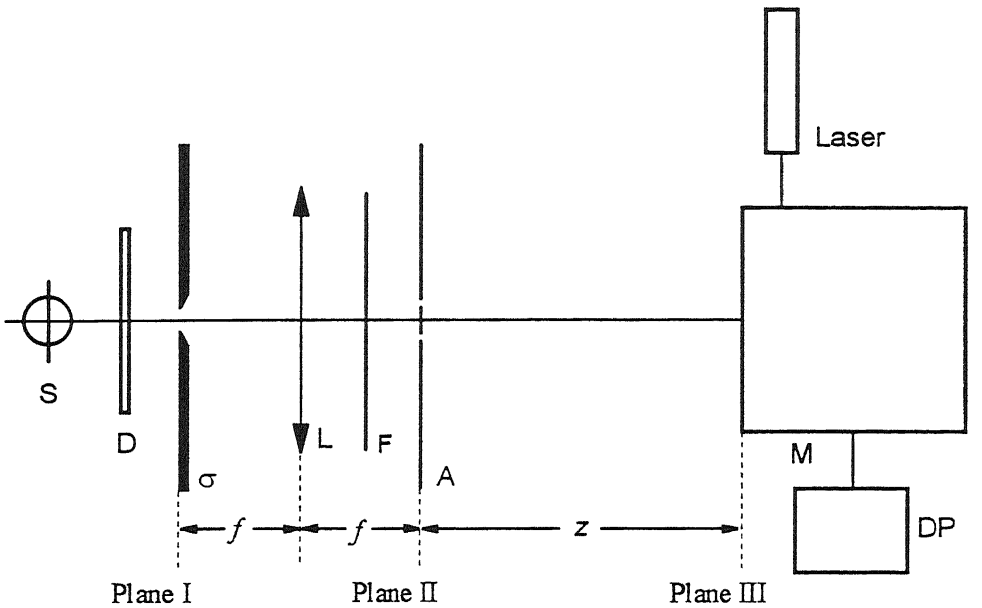

Fig. 2.2 Schematics of the experimental setup used; S-source, D-diffuser, L-Lens, F-filter, A-aperture, M-monochromator, DP-data processing unit.

To observe correlation-induced spectral shifts, circular aperture or annular apertures were introduced at plane II. The radius of the circular aperture used was 328 μm. The variation in outer radius of all annular apertures were within 1.0%, while the central obstructions of the annular apertures were of different radii. The ratios (ε) of radii of the central obstruction to the outer radius for the annular aperture were 0.40, 0.52, 0.60, 0.77 and 0.90. The spectrum of the light emerging from plane II was measured in the far-zone of the apertures (plane III) using a spectrometer. The spectrometer used in this experiment was a SPEX 1404 double grating monochromator M with a cooled photomultiplier detector having GaAs surface as its photocathode. The monochromator used has a focal length of 0.85 m, aperture ratio f/7.8 and gratings of dimensions 110 mm × 110 mm having 1200 lines mm^{-1} blazed at 500 nm. The photomultiplier output was recorded in photon counting mode and was coupled to a data processing system. Measurements were made both for on-axis as well as for off-axis points. To demonstrate correlation-

induced spectral shift, experimental results obtained for interference filter of peak wavelength λ = 534 nm and half bandwidth 15 nm are presented in this chapter.

2.2.1 On-axis measurements

The experimental setup together with the monochromator-detector system was first aligned for on-axis measurements. The spectrum of the light transmitted by the interference filter was measured at a point some distance away from plane II in the absence of the circular aperture or annular in plane II and is assumed to be same at plane II. This spectral distribution is shown by the curve A in Fig. 2.3.

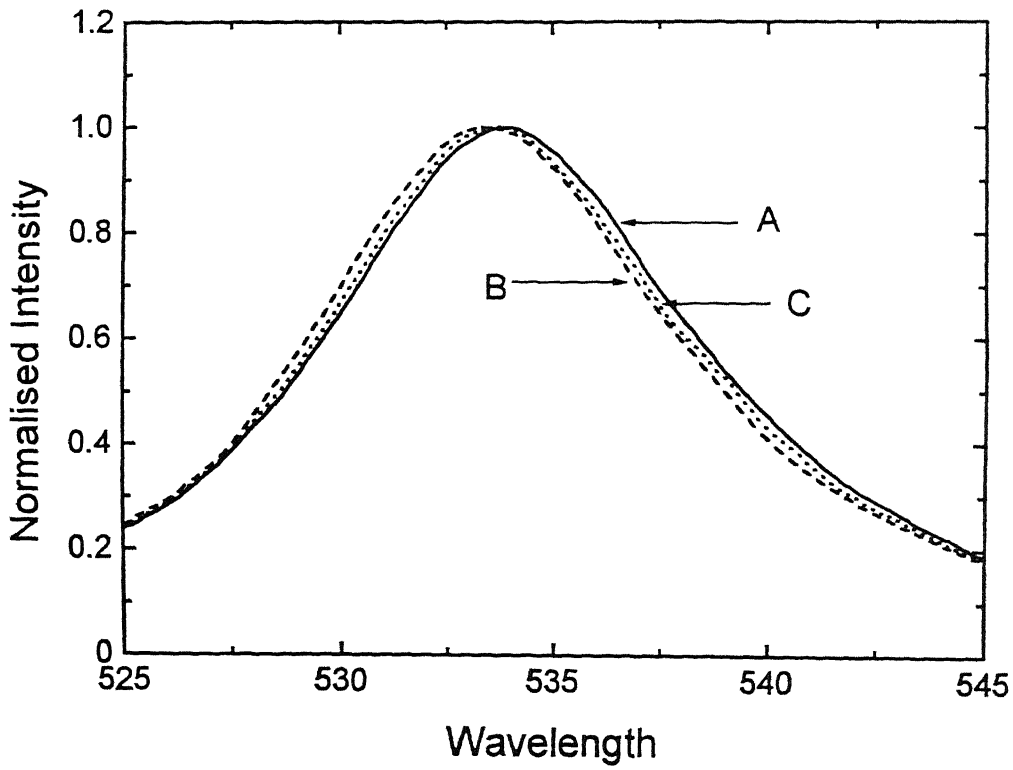

Fig. 2.3 Far-field spectrum at on-axis point, Curve A-source spectrum, Curve B-the spectrum when circular aperture was introduced in plane II, Curve C-the spectrum when annular aperture of central obstruction ε = 0.9 introduced in plane II.

A circular aperture of radius 328 μm was placed in plane II for on-axis measurements without disturbing the alignment of the experimental setup. The spectrum of the light emerging from the aperture was then measured at its far-zone and is shown by curve B in Fig. 2.3. It is observed that in this case the spectrum is blue shifted by 0.6 nm with respect to the spectrum of the source in plane II. These results are consistent with the theoretical predictions by Foley [2] that the spectrum of the light is blue shifted at on-axis point due to source correlation as the correlation length on the circular aperture is much less than the diameter of the aperture. In our experimental setup the effective correlation length of light at plane II was of the order of 130 μm. Other experimental conditions remaining the same, the circular aperture was replaced by an annular aperture of $\varepsilon = 0.9$. The spectrum of the light emerging from the annular aperture was measured at the same on-axis point in the far-zone. The spectral distribution of light is shown by curve C in Fig. 2.3. It is observed that the spectrum is blue shifted by 0.1 nm which is also consistent with the theory.

In order to study the dependence of spectral shift on central obstruction, we made on-axis measurements with different annular apertures under same experimental conditions. The variation of the spectral shift $\Delta\lambda$ with $\varepsilon = 0.40$, 0.52, 0.60, 0.77 and 0.90 for the interference filter having peak wavelength at 534 nm is depicted in Fig. 2.4 which shows that the spectrum is blue shifted in each case with different magnitudes. It is also evident from Fig. 2.4 that on increasing the central obstruction, i.e. on increasing ε for annular apertures, the magnitude of blue shift decreases. In other words for larger obstructions the spectrum of the light tends towards the spectrum of the source. The experiments were repeated under similar experimental conditions with different interference filters and similar results were obtained.

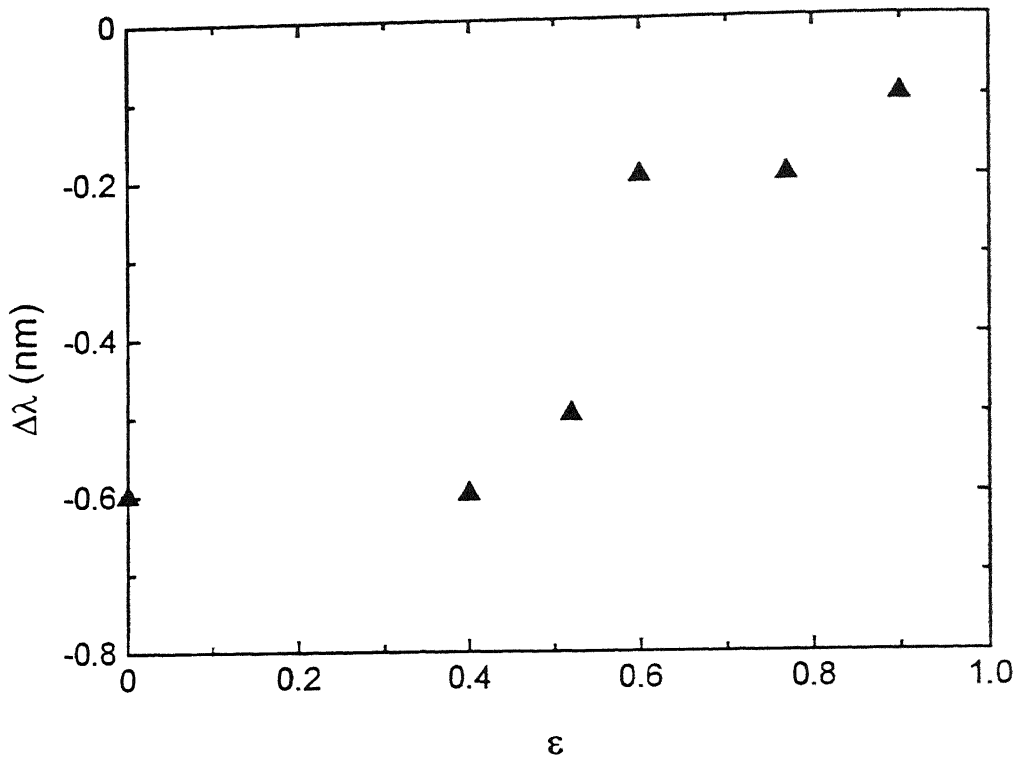

Fig. 2.4 Variation of spectral shift $\Delta\lambda$ with ε $(= b/a)$ for a fixed value $a/\widetilde{L} \cong 2.52$ for on-axis measurements.

2.2.2 Off-axis measurements

The spectral measurements for off-axis points very close to the on-axis points were made in a manner similar to the on-axis measurements. The spectrum of the source was first measured in the absence of any aperture in plane II and is shown by curve A in Fig. 2.5. This spectrum was found to be the same as in the case of on-axis measurements. The circular aperture of radius 328 μm was then placed in plane II without disturbing the alignment of the experimental setup and the spectrum was measured in the far-zone and at an off-axis point. The spectrum was red shifted with respect to the source spectrum by 0.4 nm and is shown by curve B in Fig. 2.5. This experimentally observed redshift was also consistent with the theoretical calculations [2]. We repeated the experiment by replacing the circular aperture by the same annular apertures which were used in the case of on-axis measurements. When circular aperture was replaced by an annular aperture

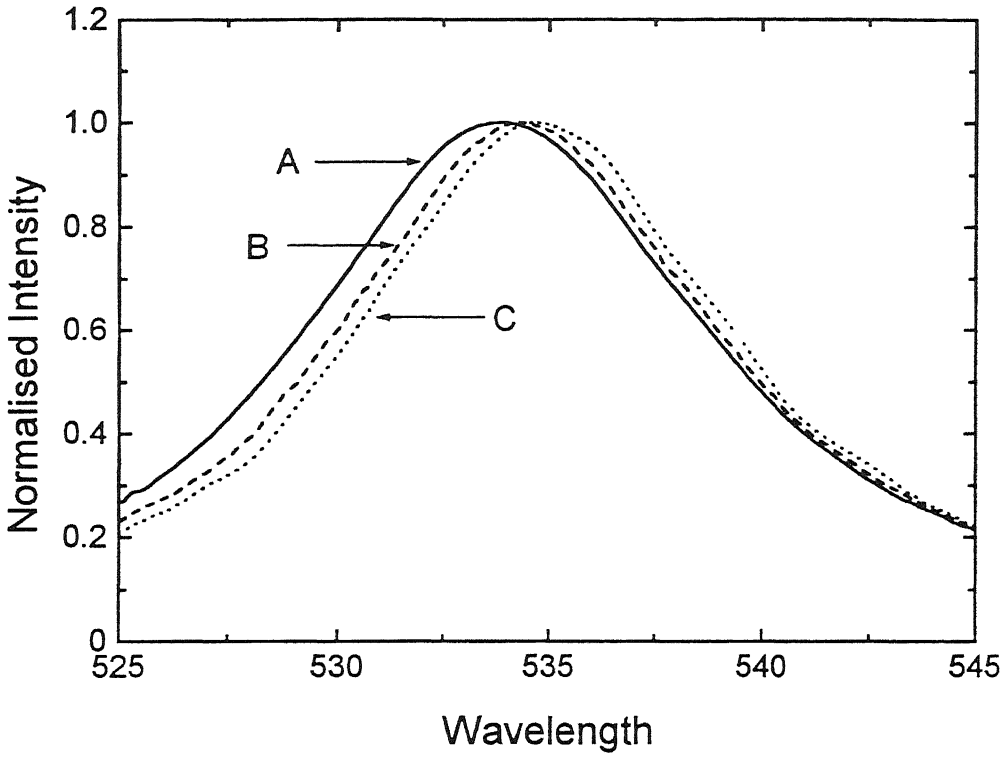

Fig. 2.5 Far-field spectrum at off-axis point, Curve A-source spectrum. Curve B-the spectrum when circular aperture was introduced in plane II, Curve C-the spectrum when annular aperture of central obstruction $\varepsilon = 0.9$ introduced in plane II.

$\varepsilon = 0.90$, and the spectrum was measured at an off-axis point, it was found red shift with respect to the source spectrum by 0.8 nm. The spectral distribution in this case is shown by curve C in Fig. 2.5. We see that in this case the spectrum is shifted more toward the red end of the electromagnetic spectrum than the red shift observed in the case of circular aperture. In this case also, to study the dependence of spectral shift on the ratio of central obstruction of the annular aperture, we repeated this experiments for various annular apertures of different sizes which we used in the on-axis measurements. The measurements were made in each case in the far-zone at off-axis point. The spectrum was found red shifted in each case by different magnitudes. The magnitude of the red shifts observed in these cases were 0.4, 0.5, 0.7, and 0.9 nm for $\varepsilon = 0.4$, 0.52, 0.6, 0.77 and 0.90, respectively. The

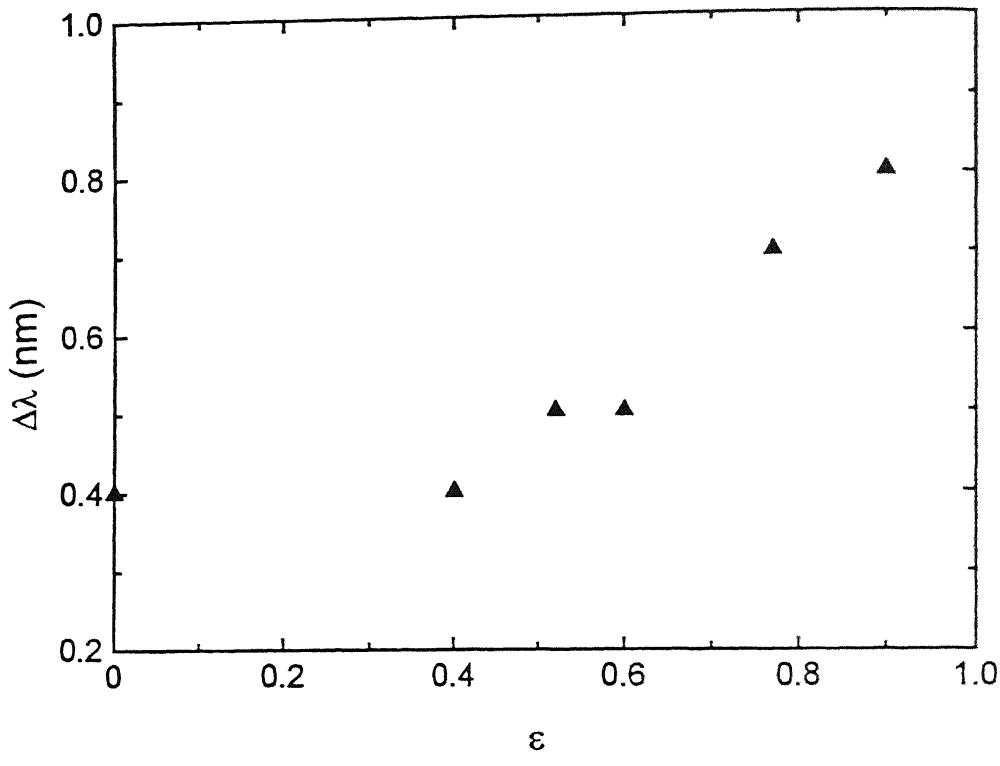

Fig. 2.6 Variation of spectral shift $\Delta\lambda$ with ε $(= b/a)$ for a fixed value $a/\widetilde{L} \cong 2.52$ for off-axis measurements.

variation of the red shift $\Delta\lambda$ with the ratio of central obstruction is shown in Fig. 2.6. From this figure it is seen that the magnitude of the red shift increases on increasing of central obstruction.

Thus this study shows that at off-axis point the spectrum of the light is red shifted while in the case of on-axis it is blue shifted. The experiment was repeated with different filters and spectral shifts of similar nature were observed.

§2.3 Discussion

In these experiments the spectral shift (blue shift) observed with circular aperture for on-axis measurements is due to the violation of the quasi-homogeneous nature of the source at plane II [2]. A quasi-homogeneous source is one in which (i) the intensity distribution is nearly constant, i.e. it is a slow function of position

while the degree of spectral coherence is a fast function of the difference between the two points over the source plane, (ii) the linear dimension of sources is much larger than the correlation length of the source, (iii) linear dimension of the source is much larger than the wavelength and (iv) the correlation length is of the order of wavelength of the light. In this particular study the correlation length is about two orders of magnitude higher than the average peak wavelength of the radiation. Since the radius of the circular aperture is much larger than the correlation length of the light in plane II, the observed shift is due to source correlation and not because of diffraction. In fact, diffraction effects are observed only when the light field is fully coherent over an aperture.

In the case of annular apertures when the central obstruction ε is less than 0.6, the source formed in the annular region violates the quasi-homogeneous condition. Therefore, the observed spectral shift is largest when ε is the smallest and its magnitude decreases as ε increases. When the value of ε is greater than 0.6, the dimension of the opening of the annular ring becomes either equal to or less than the effective correlation length. Therefore the field over the secondary source plane II becomes effectively coherent. The observed shift in the cases when $\varepsilon > 0.6$ is very small because the shift observed in this case will be essentially due to diffraction and the shift produced due to diffraction is quite small. Therefore, the observed spectrum is very close to the spectrum obtained when no aperture is put at plane II.

In the case of off-axis measurements, the spectral shift observed is towards red end of the electromagnetic spectrum. As the solid angle formed by the coherence area in plane II is proportional to the square of the peak wavelength, higher wavelengths will therefore be distributed more towards off-axis points. The

redshift will be more in the peak wavelengths with increase in the central obstruction. As the opening of the annular ring decreases, the annular aperture source lies more towards off-axis points. Therefore red shift observed is maximum when $\varepsilon = 0.9$.

§2.4 Conclusion

It is observed that the experimentally observed shift is comparatively larger than the theoretically expected shift for the parameters used in the experiments. It may be noted that one of the most important devices in these measurements is the monochromator. We have studied the coherence properties of monochromator and the results are reported in the last chapter. On the basis of our studies we are convinced that the coherence of the monochromator plays an important role in the observed spectral shift.

References

[1] E. Wolf, *Phys. Rev. Lett.* **56** (1986) 1370.

[2] J.T. Foley, *Opt. Commun.* **75** (1990) 347.

[3] J.T. Foley, *J. Opt. Soc. Am. A* **8** (1991) 1099.

[4] H C Kandpal, J S. Vaishya and K.C. Joshi, *Opt. Eng.* **33** (1994) 1996, and references cited therein.

[5] E Wolf and D.F.V James, *Rep. Prog. Phys.* **59** (1996) 771, and references cited therein.

[6] J. Pu, *J. Optics (Paris)* **24** (1993) 141.

[7] G.M. Morris and D Faklis, *Opt. Commun.* **62** (1986) 1370.

Chapter 3

Space-frequency equivalence principle in a laboratory version of Michelson's stellar interferometer

One of the best known experiments in elementary physics, to support the wave theory of light, is the double slit interference experiment first described by Thomas Young [1]. An alternative experimental arrangement of Young's interferometer was later introduced by Michelson for determining the angular diameters of stars [2]. Schematics of the Michelson's stellar interferometer are reproduced in Fig. 3.1. Interference fringes are formed at the observation plane by putting two slits at P_1 and P_2 which form Young's double slit. The blurring of the interference fringes in the observation plane is dependent on the variation of the phase difference between the light arriving at two slits from various points on the source plane, which can be done by varying the separation of the mirrors at M and M′. For determining the angular diameter of stars, Michelson moved the mirrors M and M′ (see fig. 3.1) for changing the visibility of the interference fringes. By determining the first zero in the visibility curve on the scale of mirror separation (also known as the baseline length) the angular diameter of the star (α) was determined using the relation $\alpha = 1.22\lambda/L$ where L is the separation of the mirrors M and M′ for which the fringes disappear and λ is an effective wavelength which depends on the wavelength distribution of the intensity of light.

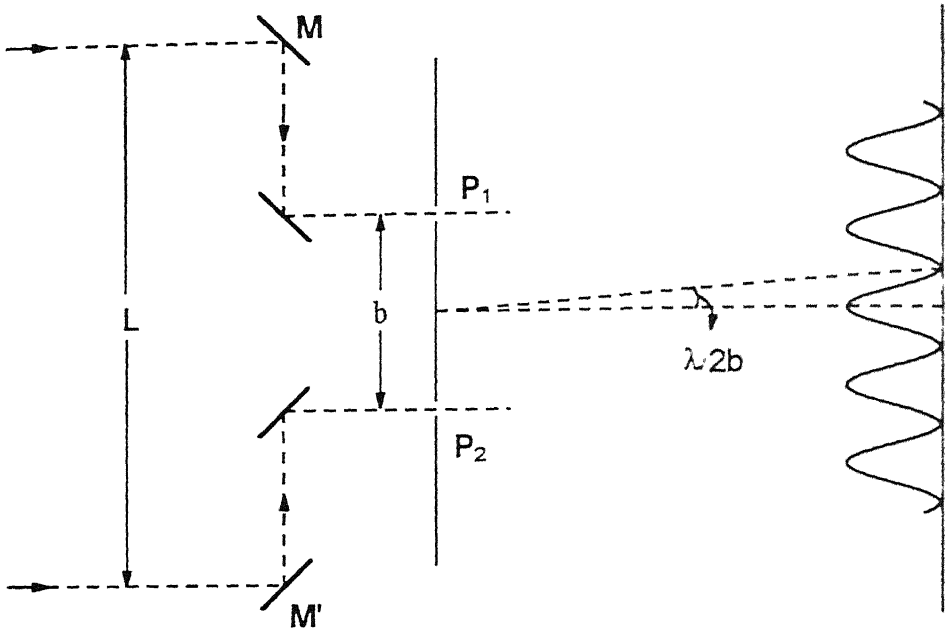

Fig. 3.1 Schematics of Michelson's stellar interferometer.

Zernike [3] theoretically provided linkage between the works of Young and Michelson and revealed more subtle features of light, namely its spatial coherence properties (i.e. partial coherent light). The concept of partial coherence was further investigated experimentally by Thompson and Wolf [4]. Later Michelson's technique formed the basis for interferometric imaging which is one of the most powerful imaging methods currently employed by radio astronomers [5]. In this technique multiple-element interferometers are used for synthetic aperture imaging where a large portion of the incident field is filtered out by a detection system to enable a narrow frequency band to form spatial interference fringe pattern for several baseline lengths. The complex degree of coherence of the field produced by a distant radio source is measured simultaneously in space-time domain and the intensity distribution across astronomical sources (which are assumed to be

essentially spatially incoherent) is determined using classical results of the coherence theory based on van Cittert-Zernike theorem [6].

Until recently interference experiments with broad-band light were not well understood as their quasi-monochromatic counterparts because in a double slit interference experiment with a broad-band radiation, no spatial fringes are formed but spectral interference fringes are produced. However, it has been shown that the spatial coherence properties of broad-band light incident upon a pair of pinholes may significantly modify the spectra in the form of shifting the center frequency or producing modulations in the spectra of light in the region of superposition [7,8]. The phenomenon of producing spectral interference fringes with spatially partially coherent light has received more attention because such spectral changes and the modulations suggest a novel method for determining the spatial coherence properties of light, i.e. the degree of spectral coherence $|\mu_{12}(\omega)|$ from spectroscopic methods [7-12]. In many cases of interest, the degree of spectral coherence of the field in the far-zone of a radiating source obeys the so called space-frequency equivalence principle [13,14]. This principle allows a trade off between the frequency and the distance of separation of pinholes also known as the baseline length [13-15]. Experimental support to the space-frequency equivalence principle under the laboratory conditions has already been provided by measuring the degree of spectral coherence from the spectral changes caused due to spatial coherence produced by the radiating source at the plane of Young's double slit. This information has been utilized to determine intensity distribution across the source and the angular separation of pair of sources [16,17].

In this chapter a method is proposed for determining the angular size of a source by making use of space-frequency equivalence principle in a laboratory

version of Michelson's stellar interferometer. Spectral measurements over a broad frequency range are taken for a single baseline length, i.e. for fixed mirror separation. It is shown that the degree of spectral coherence $\mu_{12}(\omega)$, obtained from the measurements of spectral changes produced due to the correlation existing between the sources formed over the plane of the light collecting mirrors, agrees with its theoretically expected values from the experimental parameters used in van Citter-Zernike theorem. From the zeros of the degree of spectral coherence $|\mu_{12}(\omega)|$ in the frequency scale, the angular size of the source is calculated. The angular size of the source thus determined matches closely with the value obtained from the experimental parameters. This method has the potential of providing a quick and simple technique for determining the angular size of distant sources.

§3.1 Theory

It was shown by Mandel and Wolf [18] and later explicitly by James and Wolf [7], that in Young's double slit experiment, shown in Fig. 3.2, the spectral interference law for the light beams at any state of coherence is given by

$$S(P,\omega)=S^{(1)}(P,\omega)+S^{(2)}(P,\omega) +2\sqrt{S^{(1)}(P,\omega)}\sqrt{S^{(2)}(P,\omega)}|\mu_{12}(\omega)|\cos\left[\omega(R_2-R_1)/c-\beta_{12}(\omega)\right], \qquad (3.1)$$

where $S(P,\omega)$ is the superposed spectrum at point P in the observation plane. $S^{(1)}(P,\omega)$ is the spectrum from one of the pinholes P_1 when the other pinhole at P_2 is closed and $S^{(2)}(P,\omega)$ has a similar meaning with regards to the pinholes at P_2. R_1 and R_2 are the distances of point P in the plane of observation from P_1 and P_2 respectively. $|\mu_{12}(\omega)|$ is the modulus of the spectral degree of the coherence of the radiation produced at the two pinholes, i.e. over the plane of the double slit. $\beta_{12}(\omega)$ is the phase of the spectral degree of coherence $\mu_{12}(\omega)$ and ω is the angular frequency of the radiation.

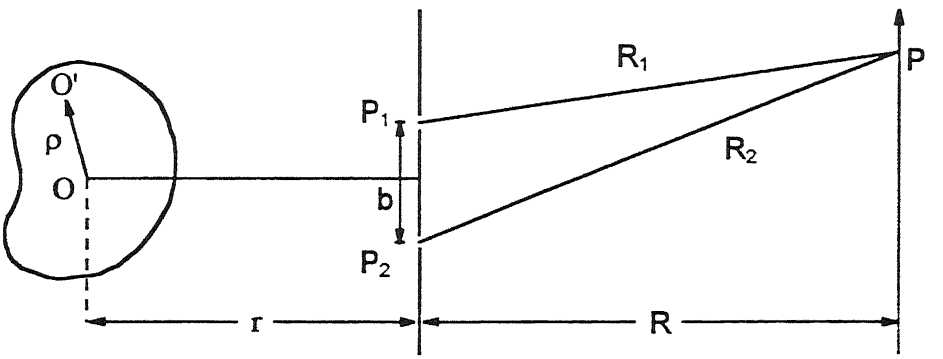

Fig. 3.2 Notation illustrating a quasi-homogeneous extended source illuminating the Young's double slit in its far-zone and the plane of observation in the far-zone of Young's double slit.

James and Wolf [13] by using the second reciprocity relation of Carter and Wolf [19] have shown that the degree of spectral coherence produced by a quasi-homogeneous secondary source can be given as

$$\mu_{12}(\omega)=\frac{\tilde{S}^{(0)}(kb/r,\omega)}{\tilde{S}^{(0)}(0,\omega)}e^{ik(u-b)}, \tag{3 2}$$

where

$$\tilde{S}^{(0)}(K,\omega)=\frac{1}{(2\pi)^2}\int S^{(0)}(\rho,\omega)e^{iK\cdot\rho}d^2\rho. \tag{3.3}$$

In Eqs. (3.2) and (3.3) the parameter K is equal to kb/r, b is the separation between the two pinholes at P_1 and P_2 and for the present experiment b will be replaced by L [the main aim of this study is to see the variation of the degree of correlation with frequency produced over the planes of the outer mirrors of the interferometer (M and M' in Fig. 3.1 and M_3 and M_4 in Fig. 3.3) and by making a trade off between the mirrors' separation and the frequency , the angular diameter of the source will be determined], r is the mean distance from source point O to the

plane of the pinholes and is assumed to be perpendicular to plane of the pinholes. $S^{(0)}(\rho,\omega)$ is the spectral density at some typical point O on the source plane. k is the wave number associated with the angular frequency ω and $\mathbf{u}$ is the unit vector in the direction of $\mathbf{r}$.

If the secondary quasi-homogeneous source is in the form of an infinitely long rectangular slit along y axis but of opening a along x axis, the spectral density $S^{(0)}(\rho,\omega)$ for such a source can be written as

$$S^{(0)}(\rho,\omega) = S^{(0)}(\omega)t(x), \tag{3.4}$$

where $S^{(0)}(\omega)$ is assumed to be same for all point on the secondary source and

$$t(x) = rect|x/a| = 1 \quad \text{for} \quad |x| \le a/2$$
$$= 0 \quad \text{for} \quad |x| > a/2.$$

On substituting from Eq. (3.4) into Eq.(3.3) we get

$$\frac{\tilde{S}^{(0)}(\mathbf{K},\omega)}{\tilde{S}^{(0)}(0,\omega)} = \frac{sin(aK/2)}{aK/2}. \tag{3.5}$$

On substituting Eqs. (3.5) and (3.2) into Eq. (3.1) and assuming that $\mathbf{u}\cdot\mathbf{b} = 0$ (i.e. plane of Young's double slit is perpendicular to the axis of the source), it can be shown that

$$S(P,\omega) = S^{(1)}(P,\omega) + S^{(2)}(P,\omega)$$
$$+2\sqrt{S^{(1)}(P,\omega)}\sqrt{S^{(2)}(P,\omega)}\left|\frac{sin\left(a\omega b/2cr\right)}{\left(a\omega b/2cr\right)}\right| cos\left[\omega(R_2 - R_1)/c + \beta_{12}(\omega)\right], \tag{3.6}$$

where c is the velocity of light, $cos\left[\omega(R_2 - R_1)/c\right]$ is due to off-axis measurement which is a fast varying function of frequency ω, however for on axis measurements

$cos[\omega(R_2 - R_1)/c]$ can be put equal to 1, $\beta_{12}(\omega)$ will be 0 or π if the source is placed symmetrically with respect to P_1 and P_2. Equation (3.6) can be also written in the form

$$S(P,\omega) = S^{(1)}(P,\omega) + S^{(2)}(P,\omega) + 2\sqrt{S^{(1)}(P,\omega)}\sqrt{S^{(2)}(P,\omega)}|\mu_{12}(\omega)|, \qquad (3.7)$$

where

$$|\mu_{12}(\omega)| = \left|\left\{\frac{\sin\left(a\omega b / 2cr\right)}{\left(a\omega b / 2cr\right)}\right\}\right|. \qquad (3.8)$$

For an experimental setup shown in Fig. 3.3 where the correlation is developed over the outer mirrors M_3 and M_4 of the interferometer, in Eq. (3.8) b has been replaced by L which is the distance between the mirrors M_3 and M_4 and Eq. (3.8) changes to

$$|\mu_{12}(\omega)| = \left|\left\{\frac{\sin\left(a\omega L / 2cr\right)}{\left(a\omega L / 2cr\right)}\right\}\right|. \qquad (3.9)$$

§3.2 Experimental procedure and results

The schematic of the experimental setup which is a laboratory version of Michelson's stellar interferometer is shown in Fig. 3.3. A 750 Watt tungsten halogen lamp operated by highly stabilized (1 part of 10^4) d.c. power supply alongwith a transmitting ground glass diffuser (D) was used to illuminate uniformly, symmetrically and incoherently a rectangular slit which forms a quasi-homogenous secondary source. The width a of this rectangular slit was 1.2 mm. It is a well known fact that spatial coherence is developed during propagation of radiation and the coherence area depends on the square of the distance of the field plane from the source plane. In order to increase the distance of the plane of the light collecting mirrors from the source, we folded the beam of light at very small angles at plane

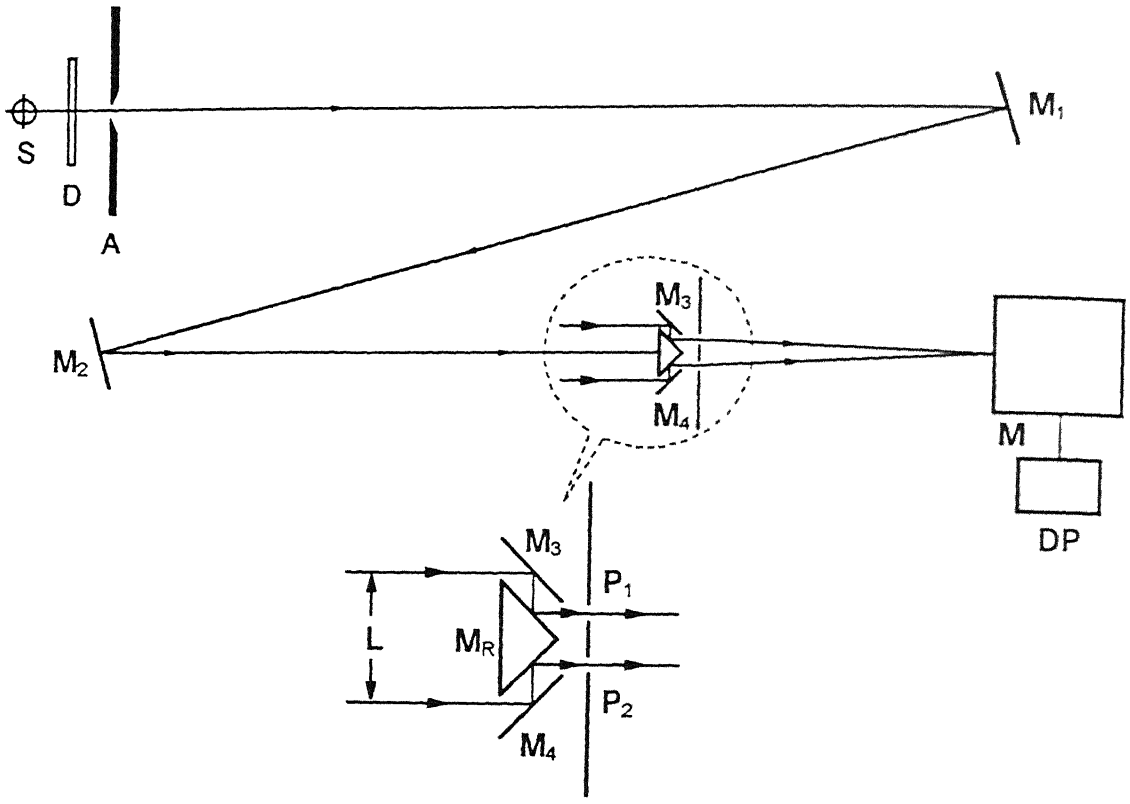

Fig. 3.3 Schematics of the experimental setup used in Laboratory version of Michelson's stellar interferometer for observing spectral changes. S - source, D - diffuser, A - aperture, M_1, M_2, M_3 and M_4 - plane mirrors, M_R - rectangular mirror prism, DS - double slit, M - monochromator and DP - data processing unit.

mirrors M_1 and M_2 of very good reflectivity and a large distance of 4.5 m was achieved. The light was made incident on two light collecting mirrors M_3 and M_4 which are also referred as the outer mirrors of the interferometer. The first area of coherence and radius of coherence produced by the source of size = 1.2 mm over the plane mirrors for average wavelength of 600 nm are 5.06 mm^2 and 2.25 mm respectively. To achieve the separation of 2.25 mm we need very thin mirrors . With the help of very thin mirrors the average distance between the mirrors M_3 and M_4 was put ≈2.9 mm for one set of measurements and ≈2.7 mm for another set of measurement with the help of micrometers so that we can have access to the second

area of coherence. The light reflected by M_3 and M_4 was made incident on a rectangular mirror M_R with its the silvered surfaces (each surface having width of approximately 1.5 mm) facing M_3 and M_4. The light reflected from M_R was made incident on a Young's double slit DS which was aligned parallel to the source plane The separation between P_1 and P_2 is approximately 1 mm. Care was taken that the radiation collected by mirror M_3 falls on the slit at P_1 and that by M_4 falls on the slit at P_2 so that the degree of correlation between P_1 and P_2 is the same as that between M_3 and M_4 The spectra of radiation were recorded in the far-zone of DS when one of the slits at P_1 was open and the other one at P_2 was kept closed and vice versa The spectrum of the superposed radiation was recorded when both the slits of the DS were open. The instruments used and experimental procedure for measuring the spectra have been described in *chapter two.*

Keeping the separation of the Young's slits and also the separation of the mirrors M_3 and M_4 fixed, spectroscopic measurements of the radiation were made for on-axis point of observation. The spectra shown in Fig. 3.4 correspond to L = 2.9 mm and that shown in Fig. 3.5 correspond to L = 2.7 mm respectively. These spectra show a dip because the spectra are the product of the spectral response of the source, response of the grating and also the response of the detector. In these figures, curve A shows the spectrum when one of the slits (at P_1) in DS was open and other one (at P_2) was closed and curve B is the spectrum when the slit at P_1 was

Keeping the separation of the Young's slits and also the separation of the mirrors M_3 and M_4 fixed, spectroscopic measurements of the radiation were made for on-axis point of observation. The spectra shown in Fig. 3.4 correspond to L = 2.9 mm and that shown in Fig. 3.5 correspond to L = 2.7 mm respectively. These

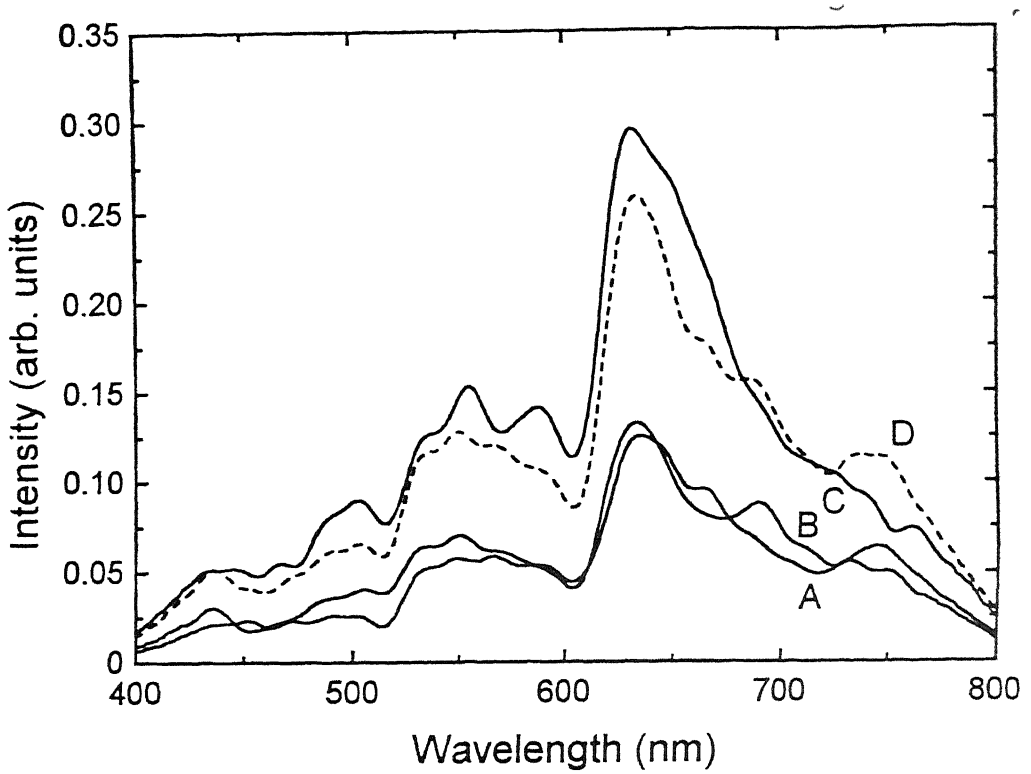

Fig. 3.4 Far-field spectrum at on-axis observation point when a = 1.2 mm, L = 2.9 mm and r = 4.5 m. Curve A is the spectrum radiated when slit P_1 was open and slit P_2 was closed. Curve B is the spectrum when slit P_2 was open and slit P_1 was closed. Curve C is the superposed spectrum when both the slit were open. Dotted curve D is the summation of curves A and B.

spectra show a dip because the spectra are the product of the spectral response of the source, response of the grating and also the response of the detector. In these figures, curve A shows the spectrum when one of the slits (at P_1) in DS was open and other one (at P_2) was closed and curve B is the spectrum when the slit at P_1 was closed and the one at P_2 was kept open. Curve C is the spectrum of the superposed radiation, i.e. when both the slit at P_1 and P_2 were kept open. Curve D was computed as the sum of intensities obtained for curve A and curve B. A look at Figs. 3.4 and 3.5 reveals that the intensity of the spectral distribution from individual slits of the Young's double slit (curve A and curve B) are nearly identical, while the magnitude and the spectral distribution in the superposed spectrum (curve C) is modified due to correlations existing between the source at P_1 and P_2 of the

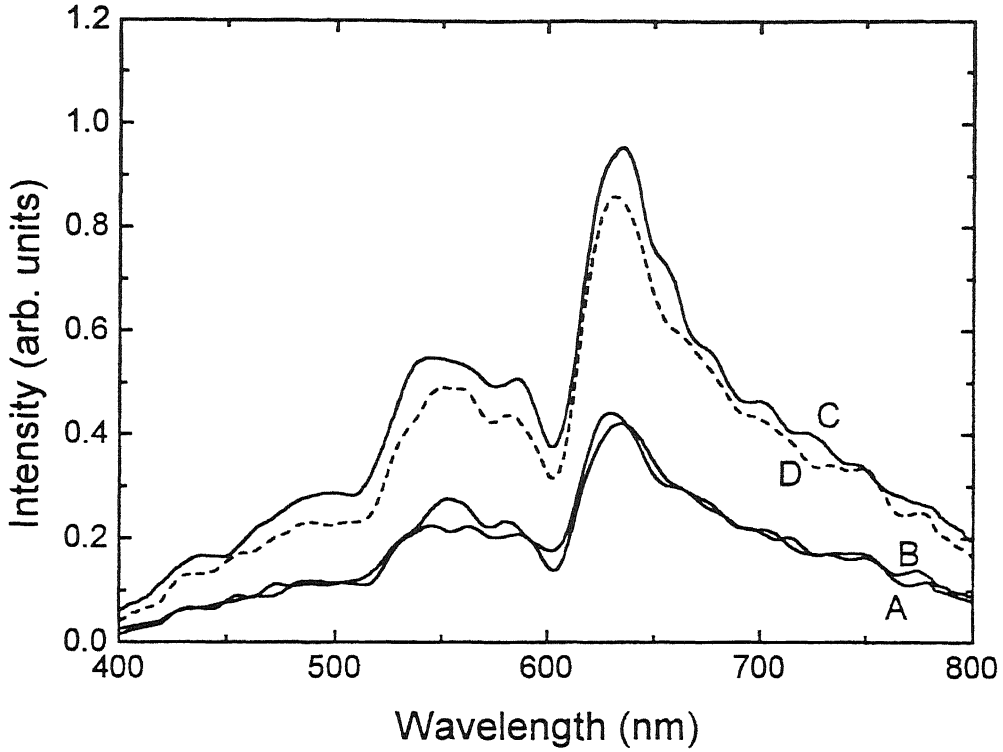

Fig. 3.5 Far-field spectrum at on-axis observation point when a = 1.2 mm. L = 2.9 mm and r = 4.5 m. Curve A is the spectrum radiated when slit P_1 was open and slit P_2 was closed. Curve B is the spectrum when slit P_2 was open and slit P_1 was closed. Curve C is the superposed spectrum when both the slit were open. Dotted curve D is the summation of curves A and B

double slit or more precisely between the mirrors M_3 and M_4. This can also be seen by comparing curve D with curve C in the Figs. 3.4 and 3.5.

The spectral data shown in Fig. 3.4 obtained experimentally were used to calculate the degree of spectral coherence $|\mu_{12}(\omega)|$ using Eq. (3.7). The values of the degree of spectral coherence thus determined are shown in Fig. 3.6 by solid dots with error bars. The theoretical values of degree of spectral coherence were obtained for the experimental parameters a = 1.2 mm, r = 4.5 m, L = 2.9 mm and R_2-R_1 = 0 using Eq. (3.9) and the curve is shown in Fig. 3.6 by a solid line. The same process was repeated to get the values of the degree of spectral coherence from the spectral data shown in Fig. 3.5 and also the theoretical values for

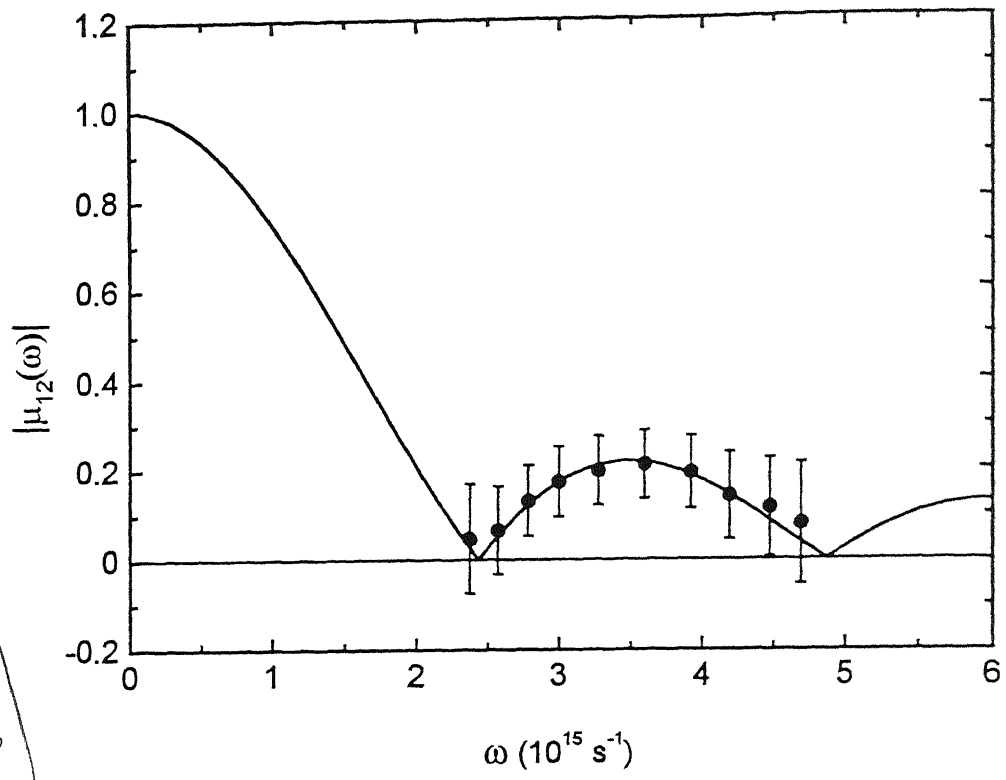

Why error bars so big

Fig. 3.6 Variation of degree of spectral coherence with frequency. Solids dots with error bars are the values obtained experimentally from the spectral distributions shown in Fig. 3.4. Solid curve is the theoretically expected curve using experimental parameters a = 1.2 mm, L = 2.9 mm and r = 4.5m.

a = 1.2 mm, r = 4.5 m, L = 2.7 mm and R_2-R_1 = 0. The experimental and theoretical values of the degree of spectral coherence are shown in Fig. 3.7. The experimentally determined values are in good agreement with the theoretical values within experimental errors.

§3.3 Discussion

In the experiments conducted in this study, we kept the separation of the light collecting mirrors M_3 and M_4 fixed. The spectra of the radiation from individual slits of DS and their superposed spectra were recorded. From the spectral data, the degree of spectral coherence was calculated using Eq. (3.7). Thus we have made use of the new interferometric-equivalence principle that measuring the complex degree of coherence over several base line lengths (mirror separation)

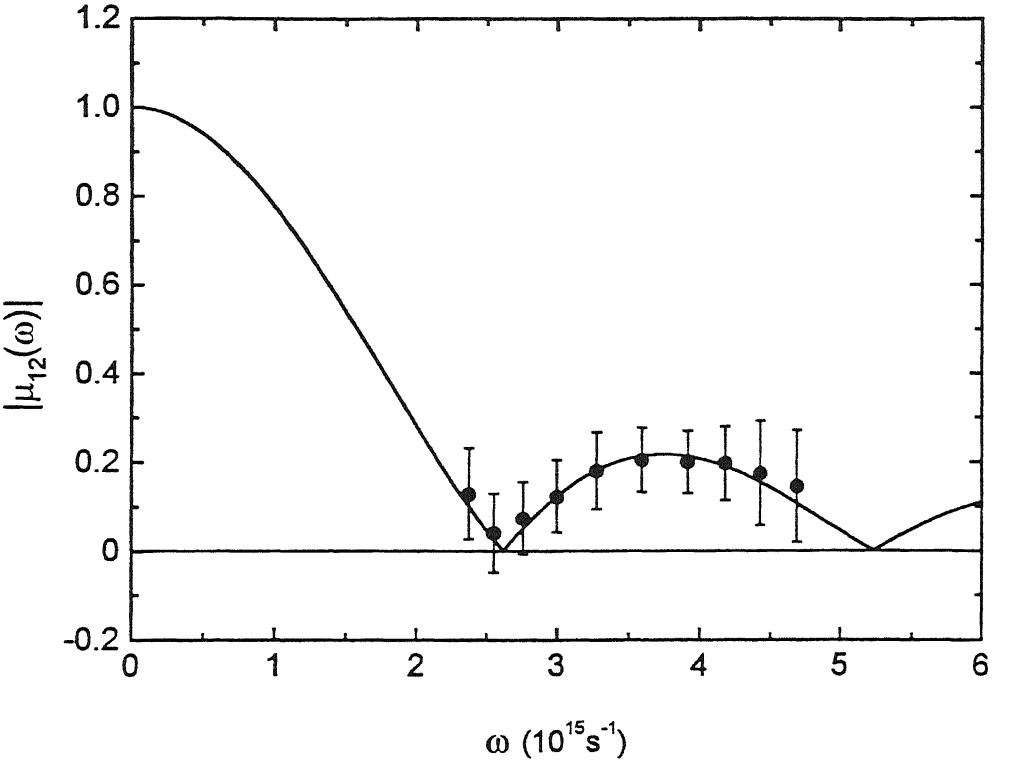

Fig. 3.7 Variation of degree of spectral coherence with frequency. Solids dots with error bars are the values obtained experimentally from the spectral distributions shown in Fig. 3.4. Solid curve is the theoretically expected curve using experimental parameters a = 1.2 mm, L = 2.7 mm and r = 4.5m.

from the visibility of the interference fringes obtained by filtering the incoming radiation to obtain a narrow-band radiation is equivalent to measuring the degree of spectral coherence over a fixed baseline length (mirror separation) for large frequencies using broad-band radiation. One important point to note in this study, unlike in conventional methods, no radiation is lost due to prior filtering.

The degrees of spectral coherence calculated using Eq. (3.7) from spectral measurements shown in Figs. 3.4 and 3.5 and the theoretically expected results for two sets of experimental parameters (*i*) a = 1.2 mm, r = 4.5 m, L = 2.9 mm, R_2-R_1 = 0 and (*ii*) for a = 1.2 mm, r = 4.5 m, L = 2.7 mm, R_2-R_1 = 0 using Eq. (3.9) are shown in Figs. 3.6 and 3.7 respectively. These figures show clearly the agreement between the theoretically expected results and the experimental results for degree of

spectral coherence obtained from spectroscopic measurements within experimental errors. The factors which may contribute to measurement uncertainties are (a) the difference in the widths of the light images formed by mirrors M_3 and M_4 which were incident on the Young's double slit, (b) the difference in the reflectivities of the mirrors used in the experiment, (c) the Young's double slit was placed symmetrically in front of the rectangular mirror M_R and also with respect to the plane containing the rectangular slit A, (d) the nonlinearity of detector (though the detector used is a photomultiplier with a GaAs surface as its cathode has a flat response in the visible region of electromagnetic spectrum) and (e) the electronics of the data acquisition and processing system. With all these factors considered, the measured value of the degree of spectral coherence would show some scatter for repeated spectral measurements. For a few measurements, the scatter in the experimental values for the degree of spectral coherence is shown as error bars while the average value is shown by solid circles in Figs. 3.6 and 3.7.

The values of the frequencies for which the degree of spectral coherence $|\mu_{12}(\omega)|$ becomes zero in the frequency scale were obtained from Figs. 3.6 and 3.7. A look at Figs. 3.6 and 3.7 reveals that the product of ωL (ω is the frequency for which $|\mu_{12}(\omega)|$ is zero and L is the base line length) comes out to be the same. From the information of these frequencies the angular size (a/r) of the source was determined putting the value of $|\mu_{12}(\omega)| = \left| \frac{\sin\left(a\omega L / 2cr\right)}{a\omega L / 2cr} \right| = 0$ or $\left(a\omega L / 2rc\right) = n\pi$ (where n is an integer). The mean value of the angular size comes out to be 2.46×10^{-4} radians, which is very close to 2.6×10^{-4} radians obtained from the experimental parameters a = 1.2 mm and r = 4.5 m and also the average value of $\alpha = 1.22\lambda/L$ gives the average angular size equal to 2.6×10^{-4} radians for average L=2.8 mm and average wavelength 0f 600 nm.

§3.4 Conclusion

In this chapter we have determined angular size of a source by calculating the degree of spectral coherence over the planes of the light collecting mirrors of a laboratory version of Michelson's stellar interferometer from spectroscopic measurements. It is shown that one can get the angular separation of a source by very simple and quick spectral measurements over a fixed base line length. This approach of obtaining the degree of spectral coherence from spectral measurements over a fixed base line length may replace the conventional methods which are used at present to determine the size of stellar objects from measurements of visibility of interference fringes over several base line lengths by filtering the incoming radiation. Thus one may overcome the complications arising in the conventional experiments due to moving of the mirrors or using arrays of detecting systems.

References

[1] T. Young, *Phil. Trans. Roy. Soc.* **xcii** 12 (1802) 387; *Young's Works*, Vol. 1, pp. 140, 170.

[2] A.A. Michelson, *Phil. Mag.* 30 (1890) 1..

[3] F. Zernike, *Physica* **5** (1938) 785.

[4] B.J. Thompson, and E. Wolf,. *J. Opt. Soc. Am.* **47** (1957) 895.

[5] A.R. Thompson, J.M. Moran, and G.W Swenson, *"Interferometry and Synthesis in Radio Astronomy"* (Wiley, New York, 1986).

[6] M. Born and E. Wolf, *"Principles of Optics"* (Pergamon Press, Oxford, Sixth ed., 1980).

[7] D.F.V. James and E. Wolf, *Phys. Lett. A* **157** (1991) 6.

[8] D.F V. James and E. Wolf, *Opt. Commun.* **81** (1991) 150.

[9] H.C. Kandpal, J.S. Vaishya, M. Chander, K. Saxena, D.S. Mehta and K.C. Joshi, *Phys. Lett. A* **167** (1992) 114.

[10] H.C. Kandpal, J.S. Vaishya, M. Chander, K. Saxena and K.C. Joshi, *Phys. Lett. A* **167** (1992) 120.

[11] K. Saxena, D.S. Mehta, H.C. Kandpal, J.S. Vaishya, and K.C. Joshi, *Opt. Commun.* **111** (1994) 423.

[12] M. Santarsiero and F. Gori, *Phys. Lett. A* **167** (1995) 123.

[13] D.F.V. James and E. Wolf, *Radio Sci.* **26** (1991) 1239.

[14] W.E. Kock and J.L. Stone, *Proc. IRE* **46** (1958) 499.

[15] D.F.V. James, H.C. Kandpal and E. Wolf, *Astrophys. J.* **445** (1995) 406.

[16] H.C. Kandpal, K. Saxena, D.S. Mehta, J.S. Vaishya and K.C. Joshi, *J. Mod. Opt.* **42** (1995) 447.

[17] H.C. Kandpal, J.S. Vaishya, K. Saxena, D.S. Mehta and K.C. Joshi, *J. Mod. Opt.* **42** (1995) 455.

[18] L. Mandel and E. Wolf, *J. Opt. Soc. Am.* **66** (1976) 529.

[19] W.H. Carter and E. Wolf, *J. Opt. Soc. Am.* **67** (1977) 785.

Chapter 4

Reconstruction of optical source-profile from spectral measurements in Young's interference experiment

In a two beam interference experiment, specially in Young's interference experiment, it has been shown that the spatial coherence of the wavefield leads to spectral changes and measurement of on-axis spectrum provides information about the spectral degree of coherence of the light over the pinholes [1-3]. It has also been shown that the degree of coherence produced in the far-zone of a globally incoherent source is proportional to the spatial Fourier transform of the spectrum of the source [4-5]. For a source whose normalised spectrum is independent of the position, one can reconstruct the source-intensity distribution by making Fourier inversion of degree of spectral coherence determined from on-axis spectral measurements at all frequencies in a fixed-baseline Young's interference experiment. In practice, complete reconstruction is not possible with such a fixed-baseline interferometer because of the finite radiation bandwidth of conventional (optical) sources.

In this chapter, the reconstruction of optical source-profile from spectral measurements in Young's interference experiment is described. Experimental results are discussed with modifications for overcoming the drawback that are encountered due to experimental limitation of the spectra obtained for sources radiating at optical and near-infrared frequencies.

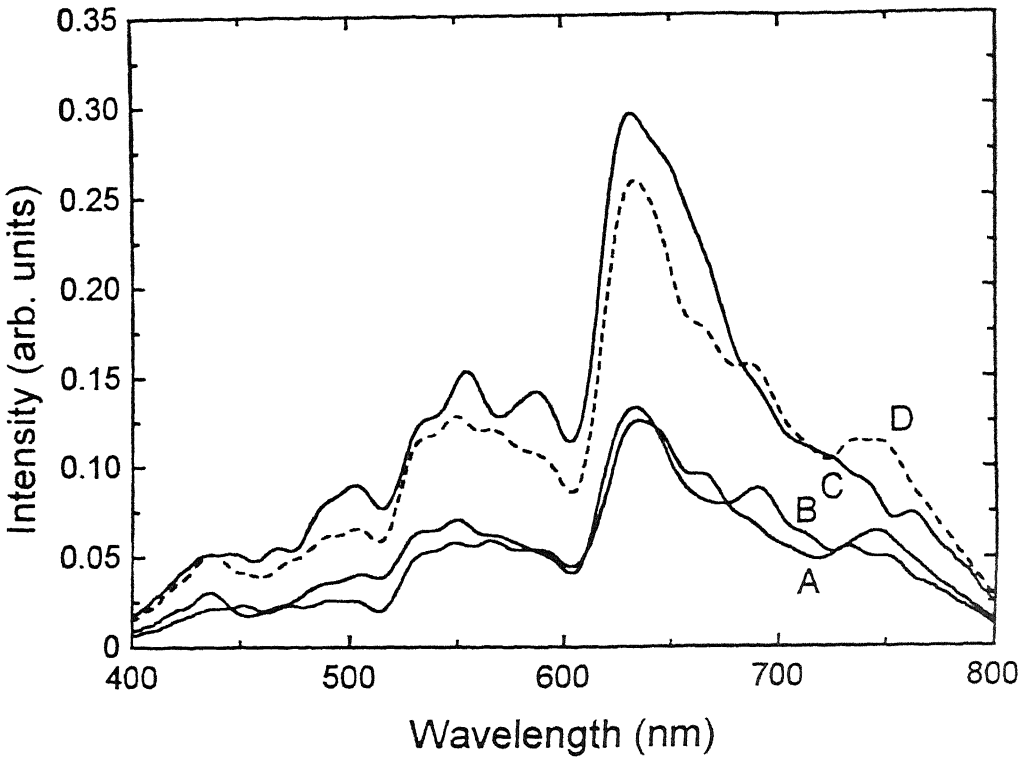

Fig. 3.4 Far-field spectrum at on-axis observation point when a = 1.2 mm, L = 2.9 mm and r = 4.5 m. Curve A is the spectrum radiated when slit P_1 was open and slit P_2 was closed. Curve B is the spectrum when slit P_2 was open and slit P_1 was closed. Curve C is the superposed spectrum when both the slit were open. Dotted curve D is the summation of curves A and B.

spectra show a dip because the spectra are the product of the spectral response of the source, response of the grating and also the response of the detector. In these figures, curve A shows the spectrum when one of the slits (at P_1) in DS was open and other one (at P_2) was closed and curve B is the spectrum when the slit at P_1 was closed and the one at P_2 was kept open. Curve C is the spectrum of the superposed radiation, i.e. when both the slit at P_1 and P_2 were kept open. Curve D was computed as the sum of intensities obtained for curve A and curve B. A look at Figs. 3.4 and 3.5 reveals that the intensity of the spectral distribution from individual slits of the Young's double slit (curve A and curve B) are nearly identical, while the magnitude and the spectral distribution in the superposed spectrum (curve C) is modified due to correlations existing between the source at P_1 and P_2 of the

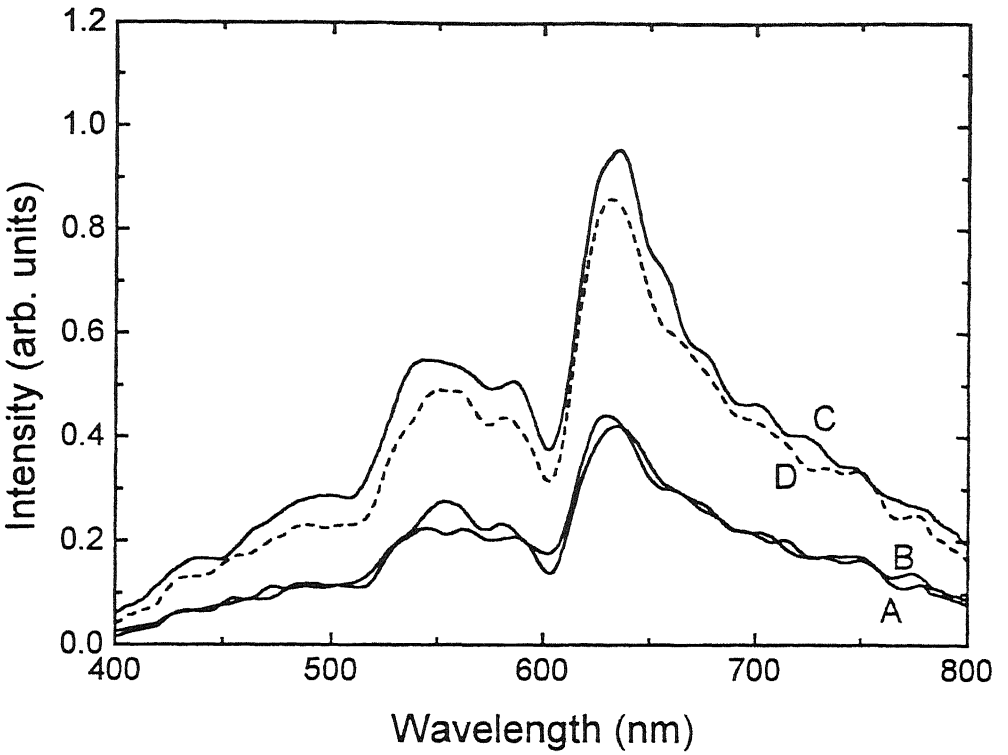

Fig. 3.5 Far-field spectrum at on-axis observation point when a = 1.2 mm, L = 2.9 mm and r = 4.5 m. Curve A is the spectrum radiated when slit P_1 was open and slit P_2 was closed. Curve B is the spectrum when slit P_2 was open and slit P_1 was closed. Curve C is the superposed spectrum when both the slit were open. Dotted curve D is the summation of curves A and B.

double slit or more precisely between the mirrors M_3 and M_4. This can also be seen by comparing curve D with curve C in the Figs. 3.4 and 3.5.

The spectral data shown in Fig. 3.4 obtained experimentally were used to calculate the degree of spectral coherence $|\mu_{12}(\omega)|$ using Eq. (3.7). The values of the degree of spectral coherence thus determined are shown in Fig. 3.6 by solid dots with error bars. The theoretical values of degree of spectral coherence were obtained for the experimental parameters a = 1.2 mm, r = 4.5 m, L = 2.9 mm and R_2-R_1 = 0 using Eq. (3.9) and the curve is shown in Fig. 3.6 by a solid line. The same process was repeated to get the values of the degree of spectral coherence from the spectral data shown in Fig. 3.5 and also the theoretical values for

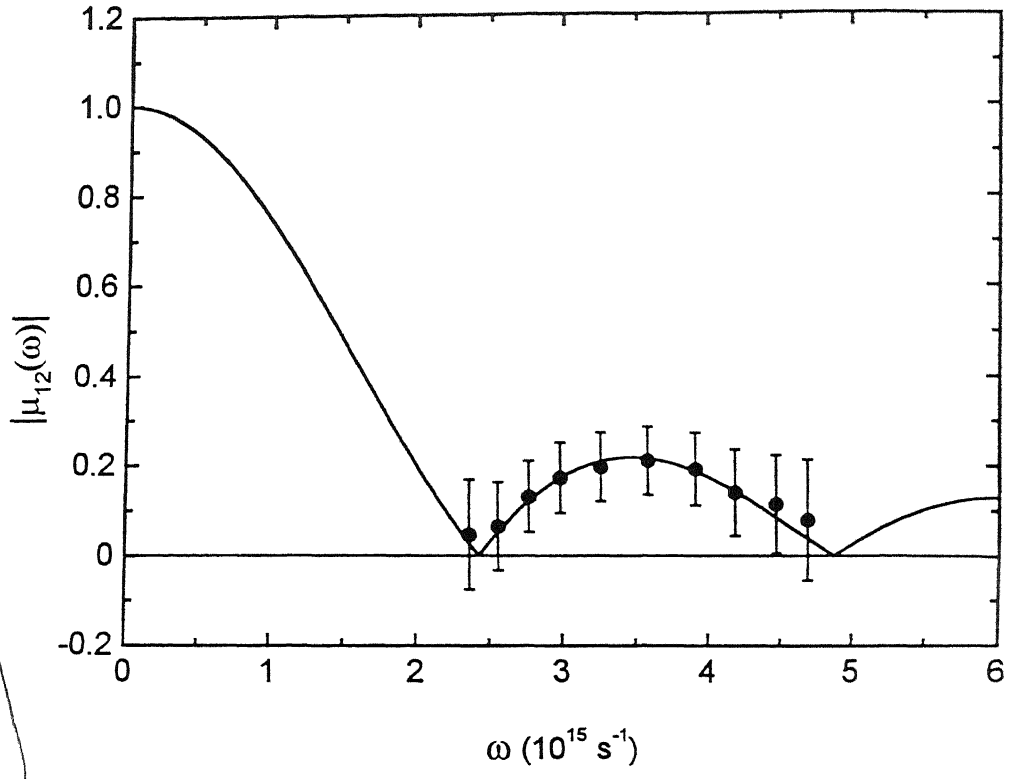

Why error bars so big

Fig. 3.6 Variation of degree of spectral coherence with frequency. Solids dots with error bars are the values obtained experimentally from the spectral distributions shown in Fig. 3.4. Solid curve is the theoretically expected curve using experimental parameters a = 1.2 mm, L = 2.9 mm and r = 4.5m.

a = 1.2 mm, r = 4.5 m, L = 2.7 mm and R_2-R_1 = 0. The experimental and theoretical values of the degree of spectral coherence are shown in Fig. 3.7. The experimentally determined values are in good agreement with the theoretical values within experimental errors.

§3.3 Discussion

In the experiments conducted in this study, we kept the separation of the light collecting mirrors M_3 and M_4 fixed. The spectra of the radiation from individual slits of DS and their superposed spectra were recorded. From the spectral data, the degree of spectral coherence was calculated using Eq. (3.7). Thus we have made use of the new interferometric-equivalence principle that measuring the complex degree of coherence over several base line lengths (mirror separation)

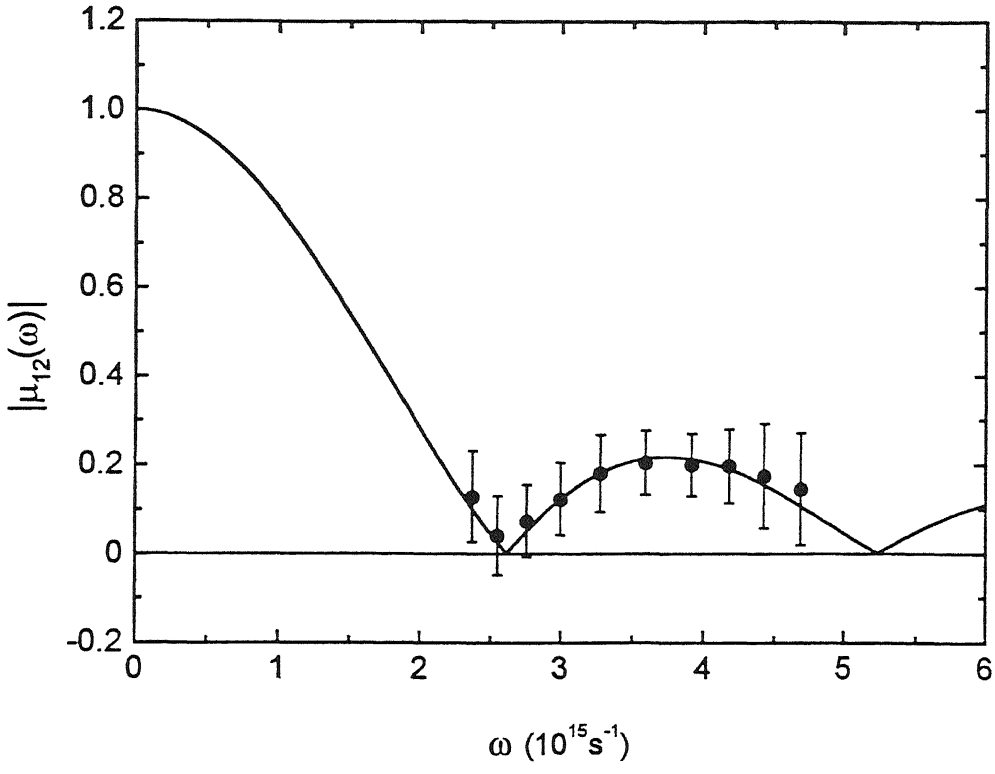

Fig. 3.7 Variation of degree of spectral coherence with frequency. Solids dots with error bars are the values obtained experimentally from the spectral distributions shown in Fig. 3.4. Solid curve is the theoretically expected curve using experimental parameters a = 1.2 mm, L = 2.7 mm and r = 4.5m.

from the visibility of the interference fringes obtained by filtering the incoming radiation to obtain a narrow-band radiation is equivalent to measuring the degree of spectral coherence over a fixed baseline length (mirror separation) for large frequencies using broad-band radiation. One important point to note in this study, unlike in conventional methods, no radiation is lost due to prior filtering.

The degrees of spectral coherence calculated using Eq. (3.7) from spectral measurements shown in Figs. 3.4 and 3.5 and the theoretically expected results for two sets of experimental parameters (*i*) a = 1.2 mm, r = 4.5 m, L = 2.9 mm, R_2-R_1 = 0 and (*ii*) for a = 1.2 mm, r = 4.5 m, L = 2.7 mm, R_2-R_1 = 0 using Eq. (3.9) are shown in Figs. 3.6 and 3.7 respectively. These figures show clearly the agreement between the theoretically expected results and the experimental results for degree of

spectral coherence obtained from spectroscopic measurements within experimental errors. The factors which may contribute to measurement uncertainties are (a) the difference in the widths of the light images formed by mirrors M_3 and M_4 which were incident on the Young's double slit, (b) the difference in the reflectivities of the mirrors used in the experiment, (c) the Young's double slit was placed symmetrically in front of the rectangular mirror M_R and also with respect to the plane containing the rectangular slit A, (d) the nonlinearity of detector (though the detector used is a photomultiplier with a GaAs surface as its cathode has a flat response in the visible region of electromagnetic spectrum) and (e) the electronics of the data acquisition and processing system. With all these factors considered, the measured value of the degree of spectral coherence would show some scatter for repeated spectral measurements. For a few measurements, the scatter in the experimental values for the degree of spectral coherence is shown as error bars while the average value is shown by solid circles in Figs. 3.6 and 3.7.

The values of the frequencies for which the degree of spectral coherence $|\mu_{12}(\omega)|$ becomes zero in the frequency scale were obtained from Figs. 3.6 and 3.7. A look at Figs. 3.6 and 3.7 reveals that the product of ωL (ω is the frequency for which $|\mu_{12}(\omega)|$ is zero and L is the base line length) comes out to be the same. From the information of these frequencies the angular size (a/r) of the source was determined putting the value of $|\mu_{12}(\omega)| = \left|\frac{\sin\left(a\omega L/2cr\right)}{a\omega L/2cr}\right| = 0$ or $\left(a\omega L/2rc\right) = n\pi$ (where n is an integer). The mean value of the angular size comes out to be 2.46×10^{-4} radians, which is very close to 2.6×10^{-4} radians obtained from the experimental parameters a = 1.2 mm and r = 4.5 m and also the average value of $\alpha = 1.22\lambda/L$ gives the average angular size equal to 2.6×10^{-4} radians for average L=2.8 mm and average wavelength 0f 600 nm.

§3.4 Conclusion

In this chapter we have determined angular size of a source by calculating the degree of spectral coherence over the planes of the light collecting mirrors of a laboratory version of Michelson's stellar interferometer from spectroscopic measurements. It is shown that one can get the angular separation of a source by very simple and quick spectral measurements over a fixed base line length. This approach of obtaining the degree of spectral coherence from spectral measurements over a fixed base line length may replace the conventional methods which are used at present to determine the size of stellar objects from measurements of visibility of interference fringes over several base line lengths by filtering the incoming radiation. Thus one may overcome the complications arising in the conventional experiments due to moving of the mirrors or using arrays of detecting systems.

References

[1] T. Young, *Phil. Trans. Roy. Soc.* **xcii** 12 (1802) 387, *Young's Works*, Vol. 1, pp. 140, 170.

[2] A.A. Michelson, *Phil. Mag.* **30** (1890) 1..

[3] F. Zernike, *Physica* **5** (1938) 785.

[4] B.J. Thompson, and E. Wolf,. *J. Opt. Soc. Am.* **47** (1957) 895.

[5] A.R. Thompson, J.M. Moran, and G.W Swenson, *"Interferometry and Synthesis in Radio Astronomy"* (Wiley, New York, 1986).

[6] M. Born and E. Wolf, *"Principles of Optics"* (Pergamon Press, Oxford, Sixth ed., 1980).

[7] D.F.V. James and E. Wolf, *Phys. Lett. A* **157** (1991) 6.

[8] D.F.V. James and E. Wolf, *Opt. Commun.* **81** (1991) 150.

[9] H.C. Kandpal, J.S. Vaishya, M. Chander, K. Saxena, D.S. Mehta and K.C. Joshi, *Phys. Lett. A* **167** (1992) 114.

[10] H.C. Kandpal, J.S. Vaishya, M. Chander, K. Saxena and K.C. Joshi, *Phys Lett. A* **167** (1992) 120.

[11] K. Saxena, D.S. Mehta, H.C. Kandpal, J.S. Vaishya, and K.C. Joshi, *Opt. Commun.* **111** (1994) 423.

[12] M. Santarsiero and F. Gori, *Phys. Lett. A* **167** (1995) 123.

[13] D.F.V. James and E. Wolf, *Radio Sci.* **26** (1991) 1239.

[14] W.E. Kock and J.L. Stone, *Proc. IRE* **46** (1958) 499.

[15] D.F.V. James, H.C. Kandpal and E. Wolf, *Astrophys. J.* **445** (1995) 406.

[16] H.C. Kandpal, K. Saxena, D.S. Mehta, J.S. Vaishya and K.C. Joshi, *J. Mod. Opt.* **42** (1995) 447.

[17] H.C. Kandpal, J.S. Vaishya, K. Saxena, D.S. Mehta and K.C. Joshi, *J. Mod. Opt.* **42** (1995) 455.

[18] L. Mandel and E. Wolf, *J. Opt. Soc. Am.* **66** (1976) 529.

[19] W.H. Carter and E. Wolf, *J. Opt. Soc. Am.* **67** (1977) 785.

Chapter 4

Reconstruction of optical source-profile from spectral measurements in Young's interference experiment

In a two beam interference experiment, specially in Young's interference experiment, it has been shown that the spatial coherence of the wavefield leads to spectral changes and measurement of on-axis spectrum provides information about the spectral degree of coherence of the light over the pinholes [1-3]. It has also been shown that the degree of coherence produced in the far-zone of a globally incoherent source is proportional to the spatial Fourier transform of the spectrum of the source [4-5]. For a source whose normalised spectrum is independent of the position, one can reconstruct the source-intensity distribution by making Fourier inversion of degree of spectral coherence determined from on-axis spectral measurements at all frequencies in a fixed-baseline Young's interference experiment. In practice, complete reconstruction is not possible with such a fixed-baseline interferometer because of the finite radiation bandwidth of conventional (optical) sources.

In this chapter, the reconstruction of optical source-profile from spectral measurements in Young's interference experiment is described. Experimental results are discussed with modifications for overcoming the drawback that are encountered due to experimental limitation of the spectra obtained for sources radiating at optical and near-infrared frequencies.

§4.1 Theory

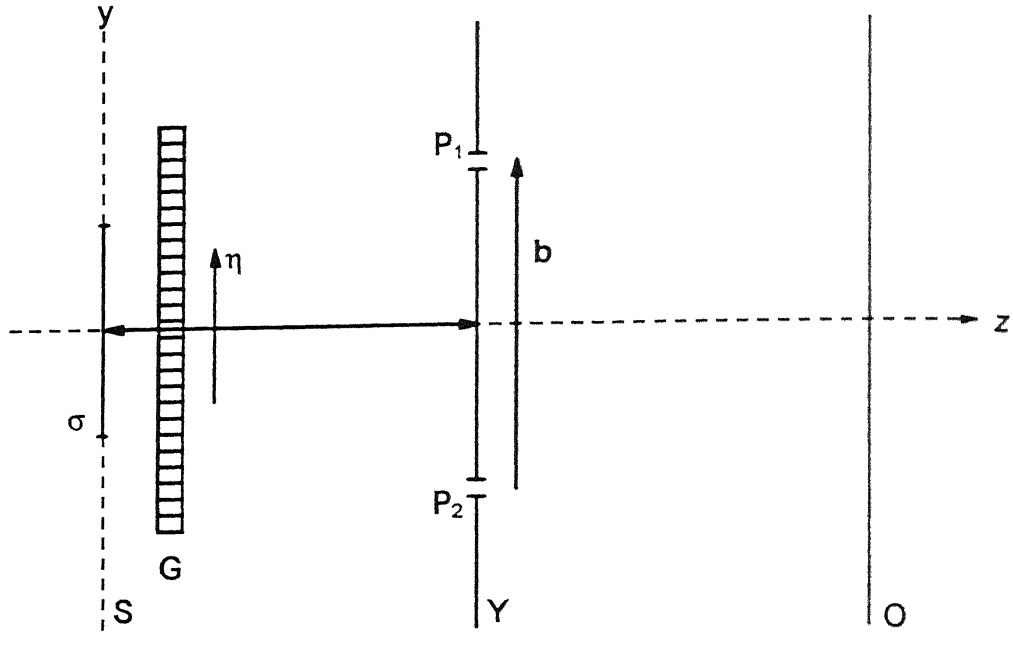

Fig. 4.1 Notation specifying various planes and distance in the setup of amplitude grating masked Young's double slit interference experiment. S - source plane, G - amplitude grating mask, Y - Young double slit plane (P_1 and P_2 are pinholes), η and **b** - the spatial frequency vector of the mask (grating) and pinhole separation vector, respectively.

Let us consider, for example, an arrangement shown in Fig. 4.1. The spectrum analyzer located on-axis in the observation plane O measures the superposed spectrum $S(\omega)$ of the radiation from Young's pinholes/slits, and single slit spectrum $S^{(1)}(\omega)$ produced by light that has passed through pinhole P_1 when P_2 is closed and $S^{(2)}(\omega)$ when P_2 open and P_1 closed. The spectral degree of coherence, $\mu_{12}(\omega)$, of the light at the two pinholes/slits in plane Y can be given by the formula [1]

$$Re\{\mu_{12}(\omega)\} = \frac{S(\omega) - S^{(1)}(\omega) - S^{(2)}(\omega)}{2\sqrt{S^{(1)}(\omega)S^{(2)}(\omega)}}, \tag{4.1}$$

where Re denotes the real part. If the source σ in plane S has the same normalized spectrum at every source point ρ, then

$$I^{(0)}(\rho) = \int_0^\infty S^{(0)}(\rho,\omega)d\omega \tag{4.2}$$

denotes the spatial distribution of the optical intensity across the source. The spectral degree of coherence, between the light field at pinholes 1 and 2 in Young's plane Y lying in the far zone of a secondary globally incoherent, quasi-homogeneous source, is proportional to the spatial Fourier transform of the spectrum of the source which in turn is proportional to the Fourier transform of the intensity distribution across the source, is given by the formula [4,5]

$$\mu_{12}(\omega) = \frac{\tilde{I}^{(0)}\left(kb/r\right)}{\tilde{I}^{(0)}(0)} \tag{4.3}$$

where b is the vector normal to the z axis, pointing from pinholes P_1 to P_2, r is the distance from the source plane S to the pinholes plane Y, $k = \omega/c$, is the wavenumber associated with frequency ω and

$$\tilde{I}^{(0)}(\mathbf{f}) = \frac{1}{(2\pi)^2}\int_\sigma I^{(0)}(\rho)\exp(-i\mathbf{f}\cdot\rho)d^2\rho\,. \tag{4.4}$$

If it is assumed that the source intensity is rotationally symmetric about z-axis, then the Fourier transform of $\tilde{I}^{(0)}(\mathbf{f})$ is real and depends only on the magnitude $f = |\mathbf{f}|$. On inverting Eq. (4.4) and putting Eq. (4.3) into Eq. (4.4) we get

$$I^{(0)}(\rho) = \tilde{I}^{(0)}(0)\int_0^\infty \mu_{12}(\omega)\exp(i\mathbf{f}\cdot\rho)d^2f \tag{4.5}$$

where

$$f = kb/r = \omega b/cr\,. \tag{4.6}$$

Hence by determining the degree of spectral coherence over the plane of Young's slits from spectral measurements, one can reconstruct the source intensity profile using Eq. (4.5).

In the very first experiment conducted to verify space-frequency equivalence in coherence theory and also to reconstruct the intensity distribution of a source [6], the baseline length 'b' and r were kept fixed. In that experiment, a rectangular slit source was illuminated incoherently and symmetrically so that the slit acted like a quasi-homogenous source. The spectral degree of coherence over the double slit plane was determined from the measurements of the superposed spectrum $S(\omega)$ and single slit spectrum $S^{(i)}(\omega)$ (i = 1,2 referring to pinholes P_1 or P_2) and it was found to be in close agreement with that obtained by applying the generalised form of van Cittert-Zernike theorem at the far-zone a quasi-homogeneous source [as there was a prior knowledge of the source intensity distribution]. Due to the experimental limitations the spectra could be recorded only over a finite bandwidth, i.e. in the range from $\omega_1 = 2.36\times10^{15}$ s^{-1} to $\omega_2 = 4.71\times10^{15}$ s^{-1} (wavelength range from λ =0.8 μm to 0.4 μm). Spectral degree of coherence $\mu_{12}(\omega)$ could be determined within this frequency range. According to Eq. (4.6), the minimum and the maximum accessible (radial) frequencies of the source intensity distribution were

$$f_1 = \left(\frac{b}{cr}\right)\omega_1 \qquad (4.7a)$$

and

$$f_2 = \left(\frac{b}{cr}\right)\omega_2 \qquad (4.7b)$$

respectively. For optical and near-infrared sources the main problem is that the spatial optical frequencies at or near the origin $f = 0$ of the spatial frequency plane, which determine the overall distribution of the source intensity from Eq. (4.5), can

not be recovered over such a fixed-baseline interferometer. For these reasons, the Fourier inversion of the measured degree of spectral coherence over the accessible frequencies can not reconstruct the intensity profile of the source. Therefore in reference 6, the source intensity profile was determined indirectly by the resemblance of the theoretically expected degree of coherence with that found experimentally from spectral measurements.

It is obvious that better reconstruction of sources-intensity profile is possible with sources of wider spectral widths. For an optical source having a temperature T = 3000 K which radiates in a spectral range from λ = 0.25 μm to 2.5 μm, though much wider spectral range can be measured with some experimental difficulty than that measured in reference 6, but one can never reach zero spatial frequency. Therefore, it is obvious that the filtered intensity reconstruction obtained using Eq. (4.5) will bear no resemblance to the actual source intensity.

Recently, it has been shown theoretically by Friberg and Fischer [7] that by placing a deterministic mask with an amplitude transmission function in front of the source, it is possible to map the low spatial frequencies of the source intensity onto accessible optical frequencies. Consequent, to the above findings access to the zero spatial frequency of the source intensity is possible with suitable experimental parameters and one can reconstruct the source intensity distribution. It has been shown that if a mask having an amplitude transmission function proportional to $\left|\cos(\eta\cdot\rho)\right|$ where η is the two dimensional spatial frequency vector of the grating (Fig. 4.1), the degree of coherence, $\mu_{12}(\omega)$, calculated over the two pinholes/slits under certain assumption (for details see reference 7) is given by the formula

$$\mu_{12}(\omega)=\frac{\tilde{I}^{(0)}\left(\frac{kb}{r}-2\eta\right)+2\tilde{I}^{(0)}\left(\frac{kb}{r}\right)+\tilde{I}^{(0)}\left(\frac{kb}{r}+2\eta\right)}{\tilde{I}^{(0)}(-2\eta)+2\tilde{I}^{(0)}(0)+\tilde{I}^{(0)}(2\eta)}. \qquad (4.8)$$

For rotationally symmetric sources that is effectively bandlimited to the domain $|\mathbf{f}| \le \eta$, and the source radiates in or is filtered to the frequency range $\omega_1 \le \omega \le \omega_2$ and the source intensity distribution also satisfies some more inequality conditions, $\left(2\eta - f_{max} \le \frac{\omega b}{rc} \le 2\eta\right)$ which have been described in detail in reference 7, Eq. (4.8) reduces to

$$\mu_{12}(\omega) = \frac{\tilde{I}^{(0)}\left(\frac{kb}{r} - 2\eta\right)}{2\tilde{I}^{(0)}(0)}. \tag{4.9}$$

Equation (4.9) shows that a range of spatial frequency components of $\tilde{I}^{(0)}(\mathbf{f})$ can be scanned as ω varies from ω_1 to ω_2 It has also been shown that η can be chosen in such a way that

$$\eta = \frac{\omega_2 b}{2cr} \tag{4.10}$$

and the highest accessible frequency ω_2 can be mapped onto zero spatial frequency of the source intensity, i.e. $f_1 = 0$. From Eq. (4.9) one obtains $\mu_{12}(\omega) \le \mu_{12}(\omega_2) = 1/2$ and Eq. (4.10) helps in choosing the experimental parameters, i.e. η, b and r. The highest accessible spatial frequency of the source intensity, for which ω_1 is the lower limit, can be determined as

$$f_2 = (\Delta\omega)\frac{b}{cr}, \tag{4.11}$$

where $\Delta\omega = \omega_2 - \omega_1$. By this method one can access to the (radial) frequencies of the source intensity $I^{(0)}(\rho)$ in the range $f_1 = 0 < f < f_2$ and the reconstruction of the source intensity is then done by using the relation

$$I_{rec}^{(0)}(\rho) = 2\pi\int_0^{f_2} \tilde{I}^{(0)}(f) J_0(\rho f) f df. \tag{4.12}$$

In this chapter we have made experimental demonstration of these theoretical findings. Source intensity profile is reconstructed from spectral measurements in a fixed baseline Young's double slit experiment. Amplitude transmission gratings of different spatial frequencies are used to mask a secondary quasi-homogeneous source of known source intensity profile. Double slits of different baseline lengths are chosen depending on the requirement of the experiment. Spectral degree of coherence produced by a rectangular slit source masked with an amplitude grating is determined by making spectral measurements for a fixed-baseline Young's double slit placed in the far-zone of the source. The mask placed over the slit acts as a low frequency grating. Spectral measurement are made in the frequency range $\omega_1 = 2.36\times10^{15}$ s^{-1} to $\omega_2 = 4.71\times10^{15}$ s^{-1} (λ =0.8 μm to 0.4 μm). The spectral degree of coherence over the plane of a double slit is determined by measuring the spectra from both the slits and from one of the slits of the double slit. The theoretically expected degree of coherence obtained for the experimental parameters is matched with the experimental results. The highest radiation frequency is mapped onto zero spatial frequency of the source intensity and the source intensity profile is reconstructed by the Fourier inversion of the spectral degree of coherence [cf. Eq. (4.12)]

$$I_{rec}^{(0)}(\rho) = 2\pi\tilde{I}^{(0)}(0)\left(\frac{b}{cr}\right)^2 \int_0^{f_2} \mu_{12}\left(\frac{fcr}{b}\right) J_0(\rho f) f df \,. \tag{4.13}$$

§4.2 Experimental procedure and results

The experimental setup is shown in Fig. 4.2. S is a 750 W tungsten halogen source which is operated with a highly stabilized (1 part in 10^4) direct current power supply. D is a diffuser which illuminated uniformly and symmetrically an aperture A which is in the form of a variable rectangular slit and acts as a globally incoherent

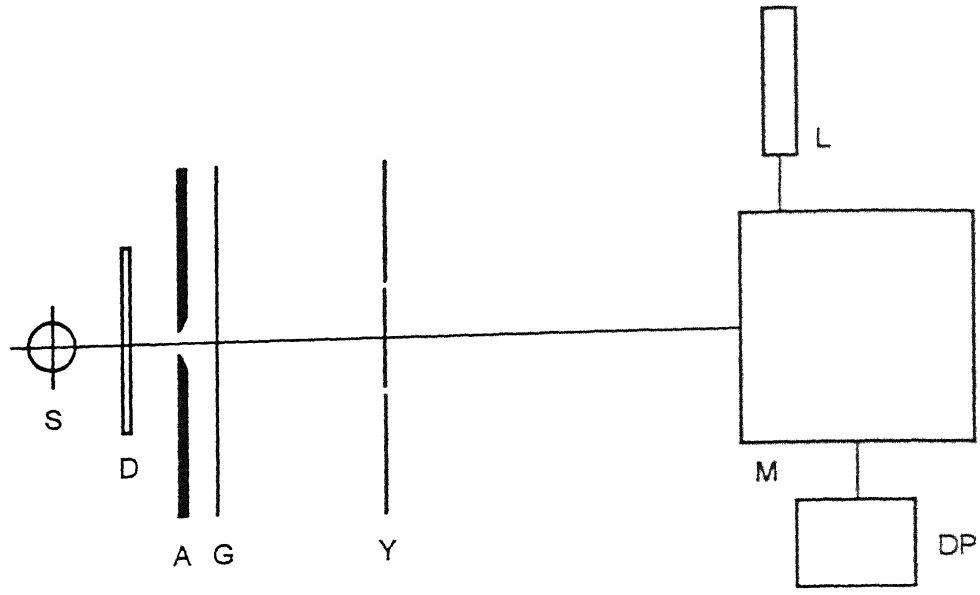

Fig. 4.2 Schematics of the experimental setup used. S - source, D - diffuser, A - aperture, G - Mask grating, Y - double slit, L - Laser, M - monochromator and DP - Data processing unit.

quasi-homogeneous secondary source. The intensity profile of this aperture is reconstructed. The spectral coherence length of a quasi-homogeneous source (σ_g) being approximately equal to the average wavelength of the radiation [8], is approximately equal to 0.5 μm in the present case. Just in front of the source an amplitude grating with spatial frequency η is put. Care is taken that the masked source remains quasi-homogeneous, i.e. the condition that $\eta\sigma_g << 1$ is always fulfilled otherwise the generalised form of van Cittert-Zernike theorem cannot be applied in the far-zone of the rectangular source. For a particular η, a double slit with fixed baseline length b is taken. The distance r between the secondary source plane S and double slit plane Y is calculated using the value of η and b in Eq. (4.10). Since the double slit should lie in the far-zone of the aperture A, of opening '*a*', the value of r calculated from Eq. (4.10) must satisfy the condition $a \leq \sqrt{\lambda r}$, where λ is the average wavelength of the radiation. The spectra of the radiation are recorded with a SPEX 1404 double grating monochromator coupled with a cooled

photomultiplier. To have good signal to noise ratio in the frequency range $\omega_1 = 2.36\times10^{15}$ s^{-1} to $\omega_2 = 4.71\times10^{15}$ s^{-1} (λ =0.8 μm to 0.4 μm) two gratings of 1200 lines/mm with size 110 mm×110 mm blazed at 0.5 μm are used. For on-axis positioning of the experimental setup the alignment of the monochromator and the optical setup was done with the help of a He-Ne laser fixed at one of the exit slits of the monochromator (Fig. 4.2).

To verify the theoretical results reported in reference 7, we have used a rectangular slit of opening a = 0.5 mm rather than a circular disk of diameter 0.5 mm for intensity consideration. An amplitude grating with η = 31.3 lines/mm and a double slit with b = 2.015 mm are used. Putting the values of η, b and ω_2 in Eq. (4.10), the value of r comes out to be 50.54 cm which also satisfies the far-zone condition for the slit taken in the experiment.

The superposed spectrum $S(\omega)$ of the radiation from the double slit (both slits open) and the single slit spectra $S^{(1)}(\omega)$ and $S^{(2)}(\omega)$ are recorded when one of the slits in plane Y is open and other one closed and vice versa. When the spectrometer is properly aligned with the on-axis position of the source and double slit, it is found the spectra of the radiation recorded from the each of the slits are almost the same (Fig. 4.3). Therefore, the degree of coherence over the plane of double slit from these spectral measurements is calculated using Eq. (4.1). Experimentally obtained value of degree of coherence at few selected frequencies is shown in Fig. 4.4(a) by solid dots along with error bars.

The spectral degree of coherence $\mu_{12}(\omega)$ for a rectangular slit of width 'a' masked with an amplitude grating of frequency η used in the present experimental

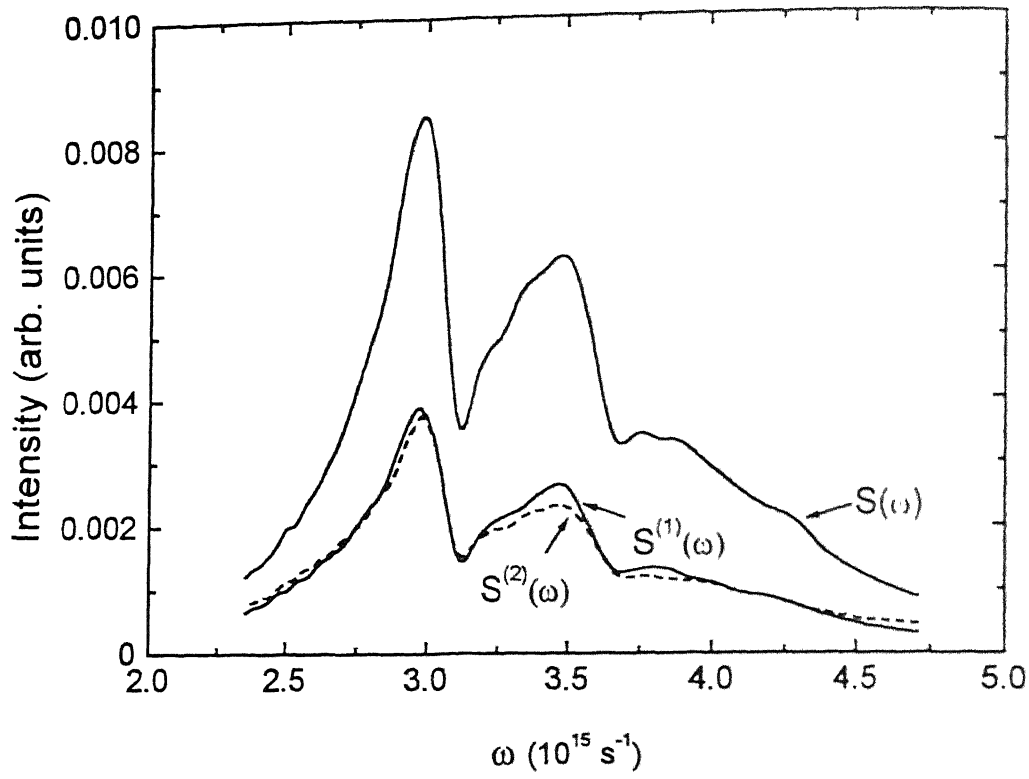

Fig. 4.3 Far field spectrum at on-axis observation point. $S^{(1)}(\omega)$ is the spectrum radiated when slit P_1 was open and slit P_2 was closed. $S^{(2)}(\omega)$ is the spectrum when slit P_2 was open and slit P_1 was closed. $S(\omega)$ is the superposed spectrum when both the slit were open.

setup is calculated using Eq. (4.8) which in the case of rectangular slit comes out to be

$$\mu_{12}(\omega)=\frac{1}{2}\left\{\frac{\sin\frac{a}{2}(f+2\eta)}{\frac{a}{2}(f+2\eta)}\right\}+\frac{\sin\left(\frac{a}{2}f\right)}{\left(\frac{a}{2}f\right)}+\frac{1}{2}\left\{\frac{\sin\frac{a}{2}(f-2\eta)}{\frac{a}{2}(f-2\eta)}\right\}. \qquad (4.14)$$

The degree of coherence obtained experimentally using Eq. (4.1) is in good agreement with the theoretically expected values (solid line curve in Fig. 4.4(a)) obtained, for the experimental parameters a =0.5 mm, b = 2.015 mm, r = 50.54 cm

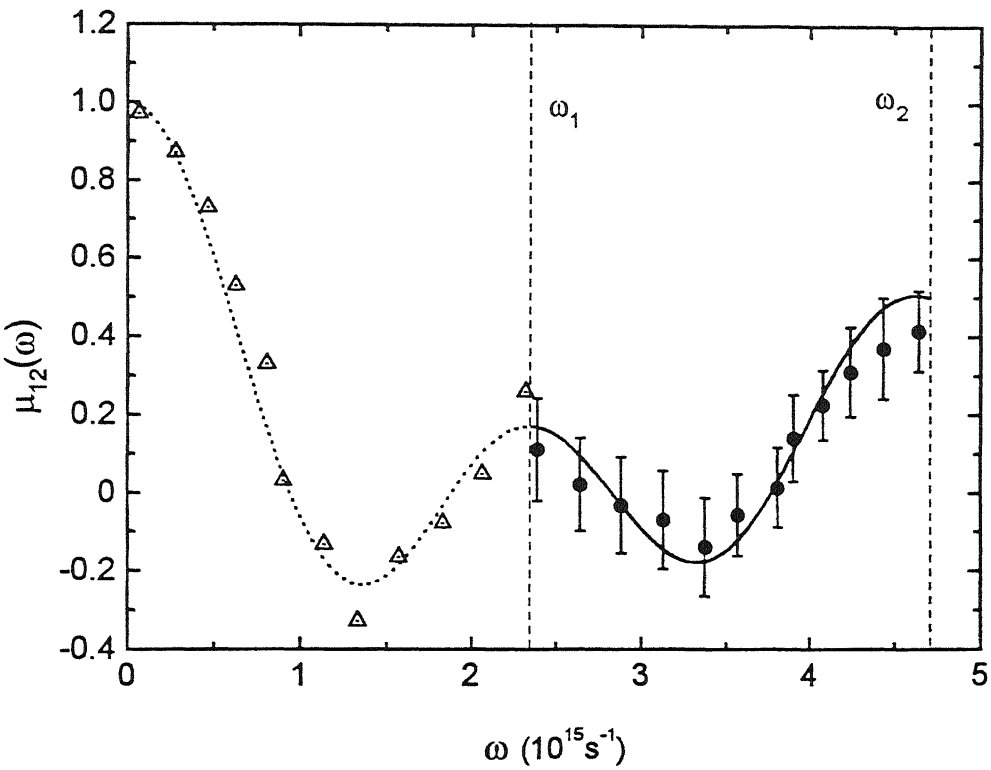

Fig. 4.4(a) Solid dots with error bars represent the experimental results of degree of spectral coherence, $\mu_{12}(\omega)$ obtained from spectral measurements in the frequency range $\omega_1 = 2.36\times10^{15}$ s^{-1} to $\omega_2 = 4.71\times10^{15}$ s^{-1}. Mapping of the experimental points (solid dots) are shown by triangles with dots inside. The theoretically expected value of $\mu_{12}(\omega)$ (solid line curve in the accessible region and by dotted line curve in the mapped region respectively)is obtained for the experimental parameters $a = 0.5$ mm, $b = 2.015$ mm, $r = 50.54$ cm and $\eta = 31.3$ lines/mm.

and $\eta = 31.3$ lines/mm, using Eq. (4.14). To determine source intensity profile, we have mapped the spectral degree of coherence obtained over the accessible frequency range such that the highest radiation frequency maps onto the zero spatial frequency and the other radiation frequencies to the corresponding low spatial frequencies. The mapping of experimental values of degree of spectral coherence at selected frequencies is shown by triangles and it is found to be in close agreement

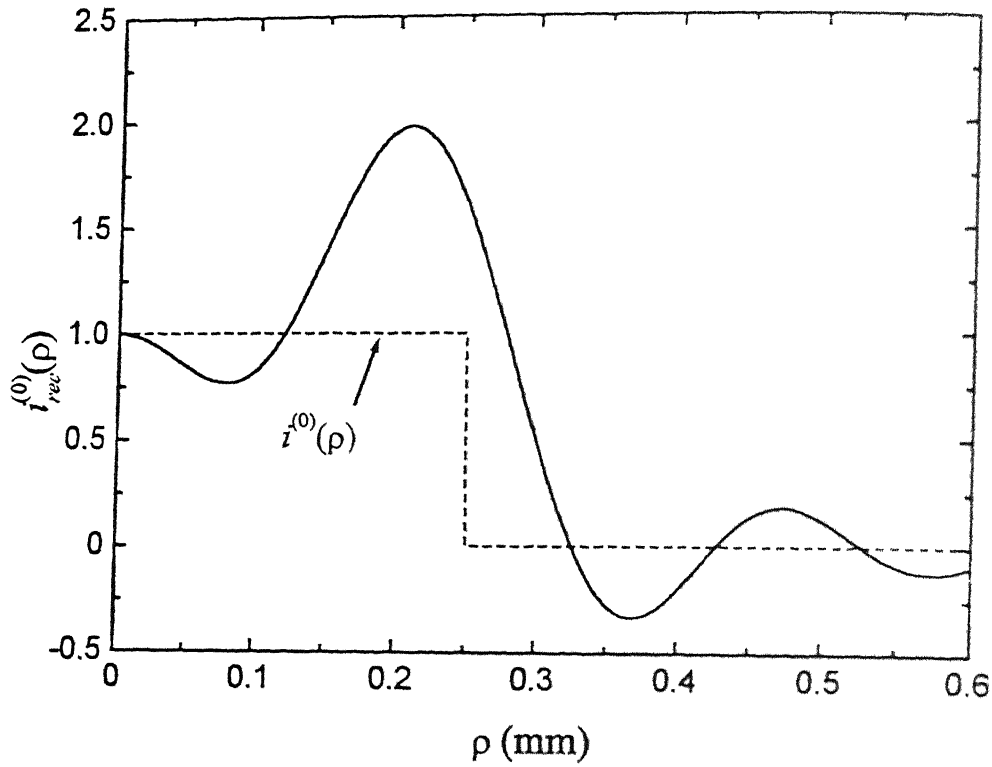

Fig. 4.4(b) Solid line curve shows the reconstructed intensity $i_{rec}^{(0)}(\rho) = I_{rec}^{(0)}(\rho)/\tilde{I}^{(0)}(0)$. The dotted line curve shows the actual source profile

with the dotted line curve obtained using Eq. (4.14). It is also noted that contribution to $\mu_{12}(\omega)$ in the accessible frequency range $\omega_1 = 2.36\times10^{15}$ s^{-1} to $\omega_2 = 4.71\times10^{15}$ s^{-1} for the selected experimental parameters is mainly due to the last term in Eq. (4.14) as discussed in the previous section [cf. Eq.(4.9)]. The Fourier inversion of the mapped degree of coherence in the spatial frequency range from 0 to f_2 is done by using Eq. (4.13). The reconstructed intensity profile is shown in Fig. 4.4(b). The dotted line curve in Fig. 4.4(b) gives the half width of the size of the actual source profile $i^{(0)}(\rho)$. The experiment is repeated for another set of the experimental parameters namely a = 0.5 mm, η = 42.2 lines/mm, b = 1.25 mm and

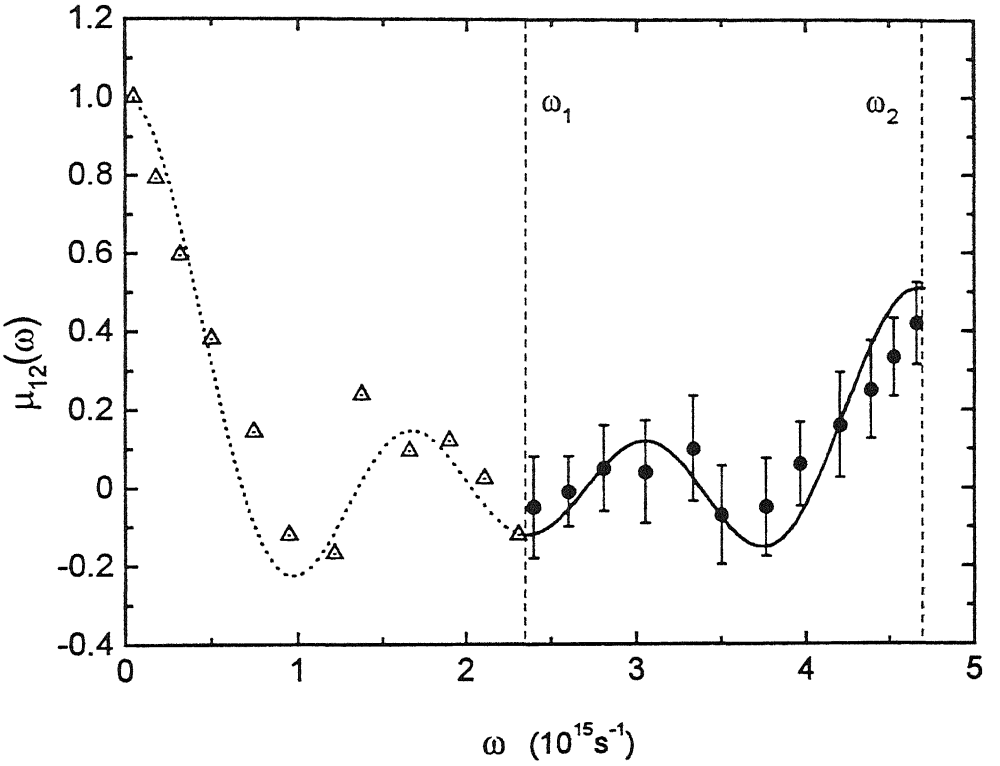

Fig. 4.5(a) Solid dots with error bars represent the experimental results of degree of spectral coherence, $\mu_{12}(\omega)$ obtained from spectral measurements in the frequency range $\omega_1 = 2.36\times10^{15}$ s^{-1} to $\omega_2 = 4.71\times10^{15}$ s^{-1}. Mapping of the experimental points (solid dots) are shown by triangles with dots inside. The theoretically expected value of $\mu_{12}(\omega)$ (solid line curve in the accessible region and by dotted line curve in the mapped region respectively)is obtained for the experimental parameters a = 0.5 mm, b = 1.25 mm, r = 23.3 cm and η = 42.2 lines/mm.

r = 23.3 cm. Typical results for the degree of spatial coherence obtained experimentally from the spectral measurements (solid dots with error bars in Fig. 4.5(a)) match within experimental errors with the theoretically expected degree of coherence (solid line curve in Fig. 4.5(a)). The mapping of the experimental value of the degree of spatial coherence at highest radiation frequency onto zero spatial frequency and the lowest radiation frequency onto f_2 is shown in Fig. 4.5(a) by

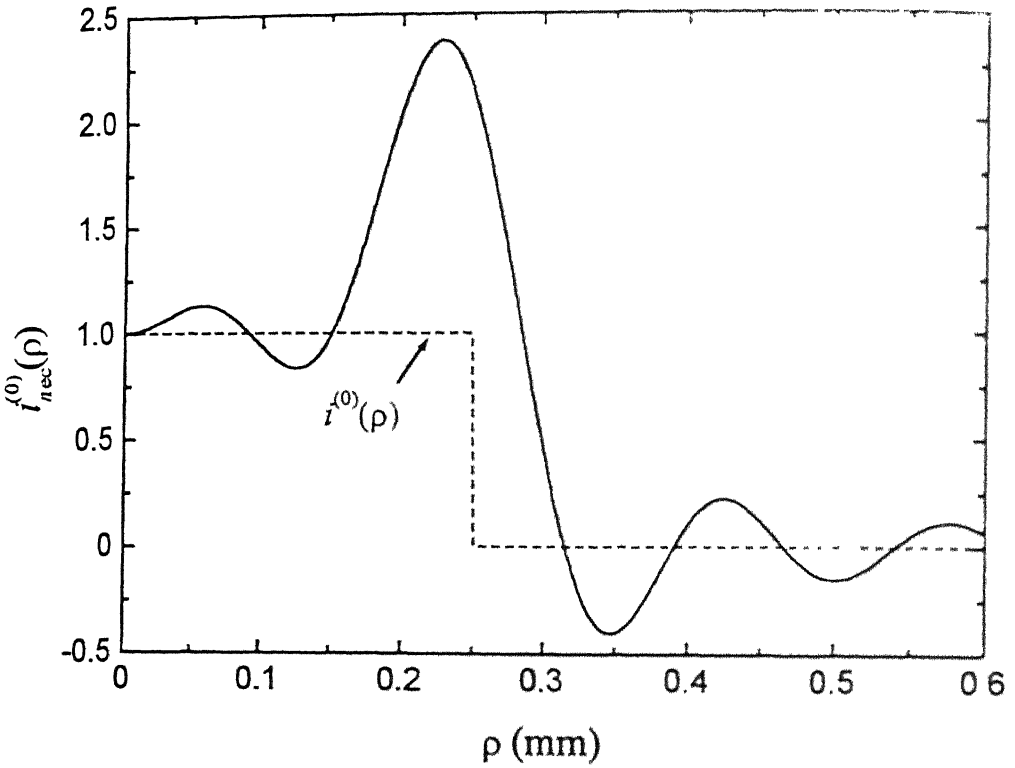

Fig. 4.5(b) Solid line curve shows the reconstructed intensity $i_{rec}^{(0)}(\rho)$ The dotted line curve shows the actual source profile.

triangles while the theoretically calculated value of the degree of spectral coherence (obtained using Eq. (4.14)) is shown by dotted line curve in Fig. 4.5(a). The reconstructed intensity is shown in Fig 4.5(b).

Experiments are also conducted with different sizes of the aperture '*a*' with different values of η, *b* and *r* such that r is always in the far zone of the secondary source. Experimental results for the degree of spectral coherence and the reconstructed intensity obtained with the procedure described above are also shown in Fig. 4.6 and 4.7. Figures 4.6(a) and 4.6(b) correspond to the degree of coherence

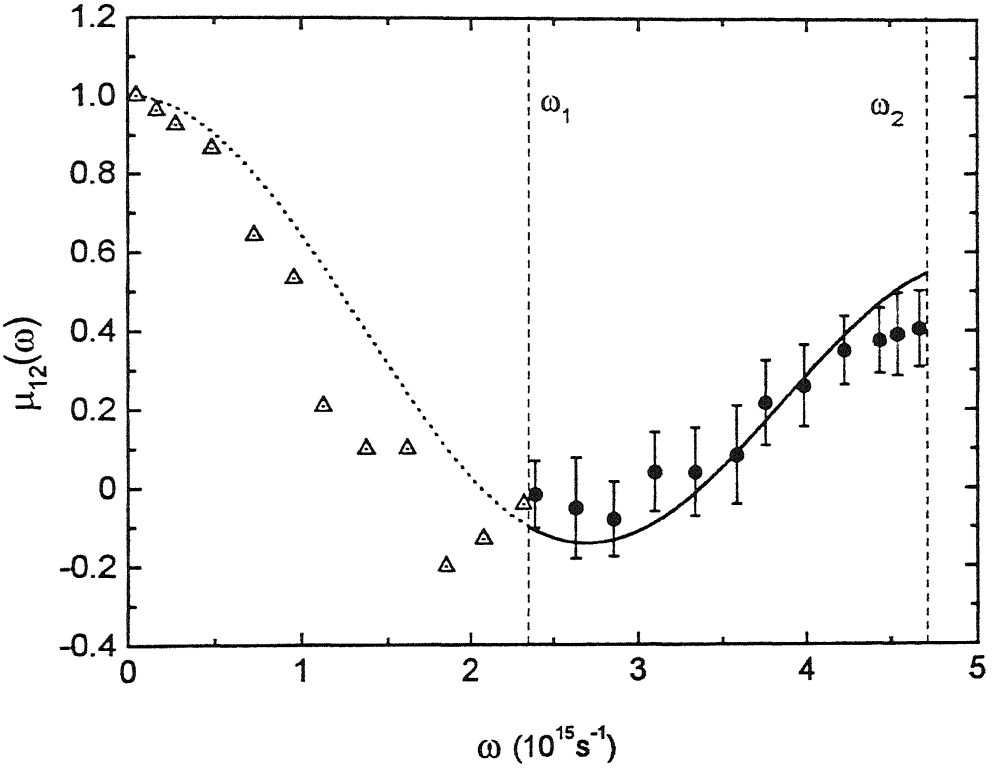

Fig. 4.6(a) Solid dots with error bars represent the experimental results of degree of spectral coherence, $\mu_{12}(\omega)$ obtained from spectral measurements in the frequency range $\omega_1 = 2.36\times10^{15}$ s^{-1} to $\omega_2 = 4.71\times10^{15}$ s^{-1}. Mapping of the experimental points (solid dots) are shown by triangles with dots inside. The theoretically expected value of $\mu_{12}(\omega)$ (solid line curve in the accessible region and by dotted line curve in the mapped region respectively)is obtained for the experimental parameters $a = 0.28$ mm, $b = 2.015$ mm, $r = 50.54$ cm and $\eta = 31.3$ lines/mm.

and the reconstructed intensity, respectively for $a = 0.28$ mm, $r = 50.54$ cm, $b = 2.015$ mm and $\eta = 31.3$ lines/mm. Figures 4.7(a) and 4.7(b) correspond to the degree of coherence and the reconstructed intensity, respectively for $a = 0.28$ mm, $r = 66.74$ cm, $b = 2.015$ mm and $\eta = 23.7$ lines/mm. It is found that due to experimental limitations in these cases as discussed in the next section the

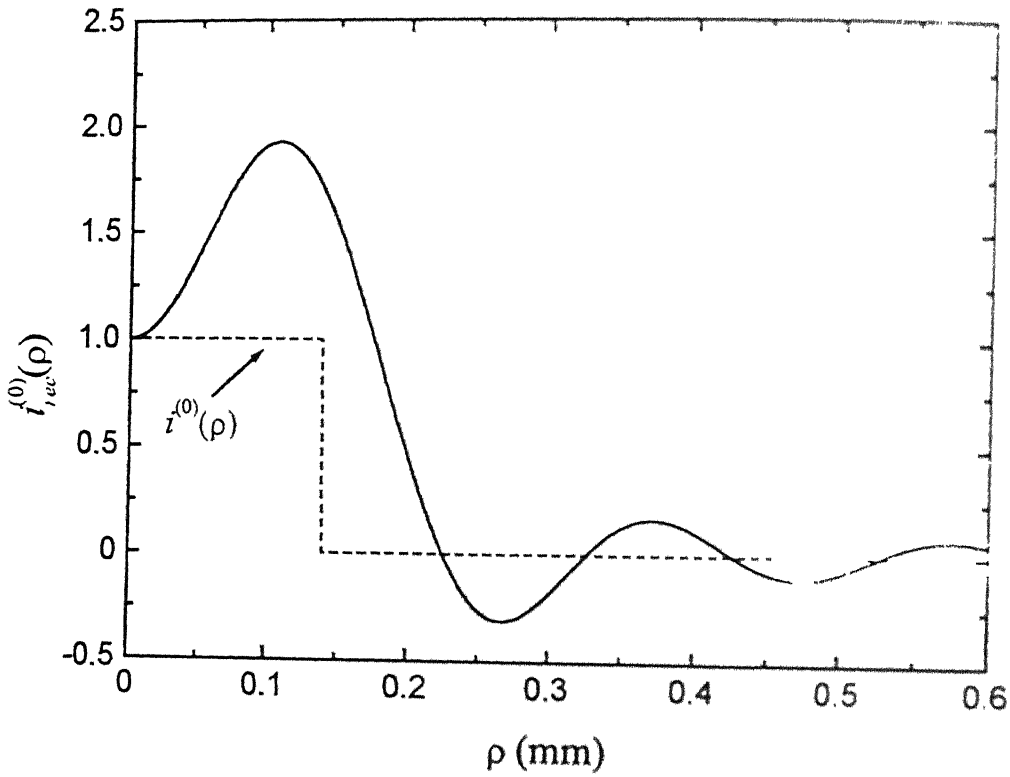

Fig. 4.6(b) Solid line curve shows the reconstructed intensity $I_{rec}^{(0)}(\rho)$ The dotted line curve shows the actual source profile.

reconstructed intensity-profile does not match closely to the actual source intensity profile $I^{(0)}(\rho)$.

§4.3 Discussions

In this experimental study we have considered the reconstruction of source intensity profile of rectangular slit source of varying sizes (namely a = 0.5 mm and a = 0.28 mm) using a technique suggested by Friberg and Fischer [7]. The source is masked by appropriate amplitude grating. The degree of spectral coherence

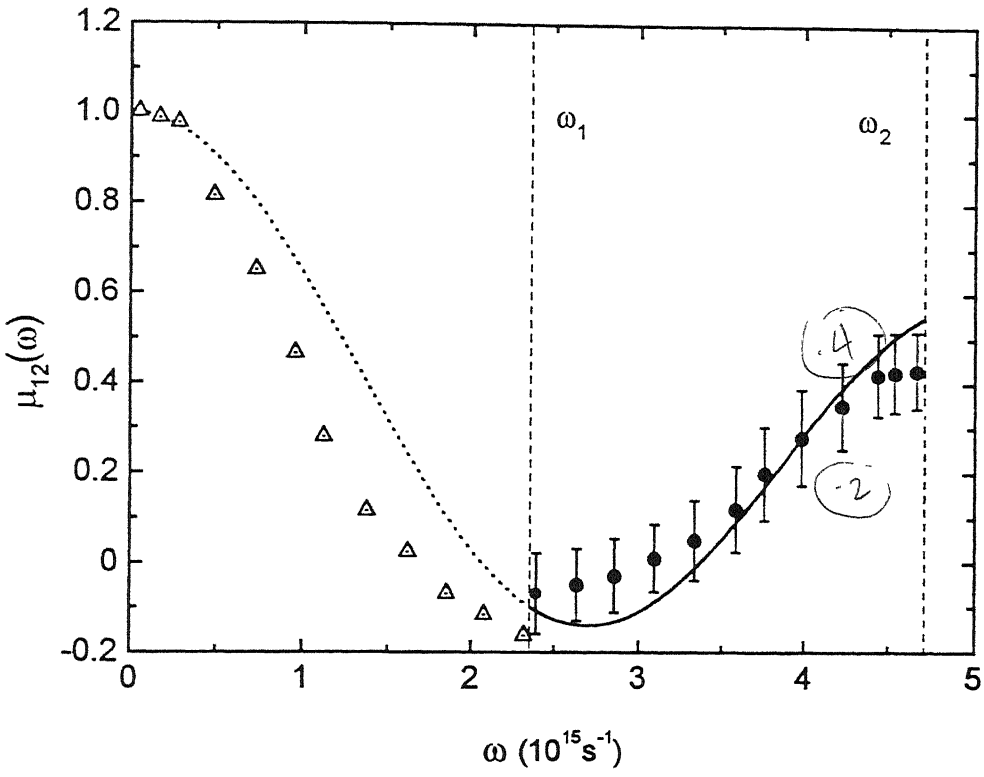

Fig. 4.7(a) Solid dots with error bars represent the experimental results of degree of spectral coherence, $\mu_{12}(\omega)$ obtained from spectral measurements in the frequency range $\omega_1 = 2.36\times10^{15}$ s^{-1} to $\omega_2 = 4.71\times10^{15}$ s^{-1}. Mapping of the experimental points (solid dots) are shown by triangles with dots inside. The theoretically expected value of $\mu_{12}(\omega)$ (solid line curve in the accessible region and by dotted line curve in the mapped region respectively)is obtained for the experimental parameters a = 0.28 mm, b = 2.015 mm, r = 66.74 cm and η = 23.7 lines/mm.

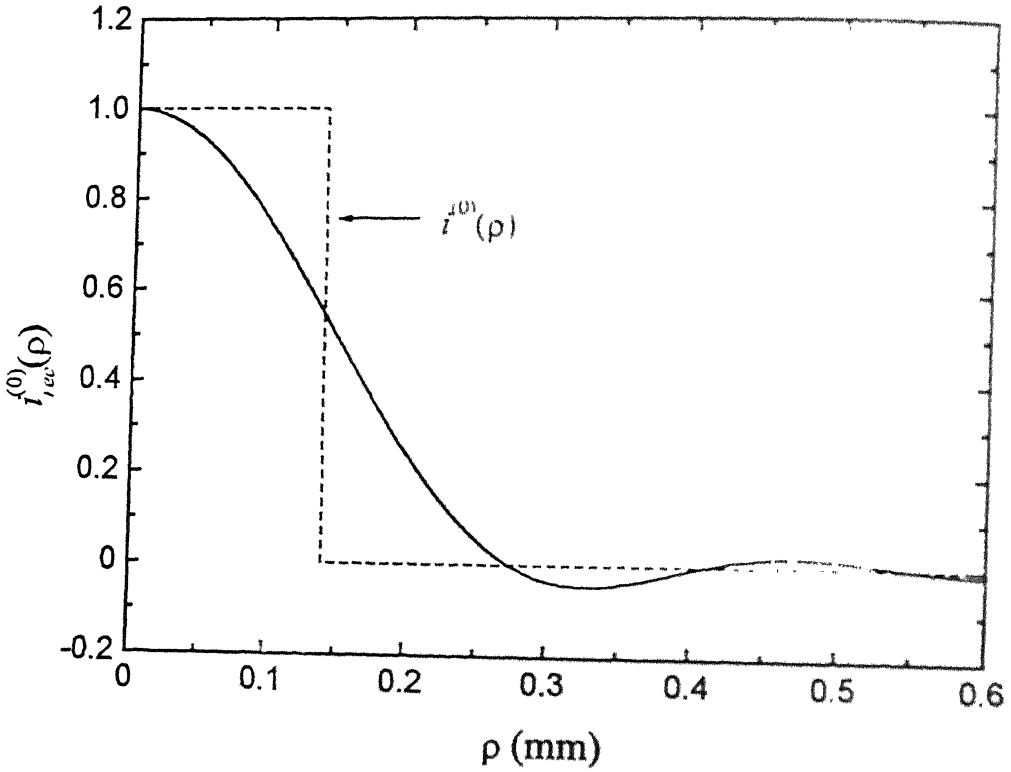

Fig. 4.7(b) Solid line curve shows the reconstructed intensity $I^{(0)}_{ave}(\rho)$. The dotted line curve shows the actual source profile.

produced by the masked source in its far-zone on the plane of Young's double slit is determined by making spectral measurements over the optical frequency region from $\omega_1 = 2.36\times10^{15}$ s^{-1} to $\omega_2 = 4.71\times10^{15}$ s^{-1} ($\lambda = 0.8$ μm to 0.4 μm). It has been found experimentally that in almost all the cases the value of the spectral degree of coherence $\mu_{12}(\omega)$ at ω_2 comes close to 1/2 but not equal to 1/2 as expected theoretically. This may be due to experimental errors in placement of Young's double slit in front of the masked source on the optics axis. The other factors which may contribute to measurement uncertainties are (a) the nonlinearity of detector (though the detector used is a photomultiplier with a GaAs surface as its cathode

has a flat response in the visible region of electromagnetic spectrum) and (b) the electronics of the data acquisition and processing system. It is noted that the experimental values of degree of spectral coherence obtained using Eq. (4.1) match closely to the theoretical expected values of $\mu_{12}(\omega)$ from Eq. (4.8). The measured degree of spectral coherence is mapped such that highest radiation frequency ω_2 maps onto zero spectral frequency and lowest radiation frequency ω_1 onto f_2 given by Eq. (4.11). The mapped degree of spectral coherence at selected frequencies is shown by triangles and it is found to be in close agreement with the dotted line curve obtained using Eq. (4.14) in Fig. 4.4(a) to 4.7(a). Source intensity is reconstructed by Fourier inversion of the mapped degree of coherence using Eq (4.13). It is seen that none of the reconstruction of the source intensity is exact This is because the spatial Fourier transform of the source intensity distribution has substantial high frequency content that is not accessible at visible wavelengths. It is also seen that reconstruction becomes worse when the source size is reduced from 0.5 mm to 0.28 mm. However, in all cases considered, it is noted that one can make an estimate of the source shape to a good approximation from the reconstructed source intensity.

A characteristic feature that is implicit in the application of this technique is that we should have a prior knowledge of the source intensity and the spectrum, and also that the source has a sufficiently broad-band spectrum so that the recovery of all the spatial frequency components of the source intensity is possible. The mask, the double slit and the spectrum analyser can be chosen appropriately if we have the knowledge of the source intensity and the spectrum. Under the conditions discussed earlier, there may be a good match between the experimentally measured degree of coherence and the theoretically expected values for the experimental parameters and a proper reconstruction of the source intensity-profile is possible, provided that the

spectral measurements are taken over the first order of the spectrum due to the grating (mask). It is observed that due to the low spatial frequency of the mask grating different orders of the grating spectra can not be separated out. This is one of the limitations of this experimental technique. The other problem encountered with such an experiment is that the radiation coming out of the Young's slits in some situations becomes so coherent that superposition of the radiation from the two slits does not take place. If some optical components are used to superpose these two sources, e.g., a lens at the entrance slit of the monochromator, the images formed at the first light collecting mirror of the monochromator do not fall at its centre. Hence, the spectra recorded for the two sources come out to be very different because of different angular positions of the sources. Extreme care should be taken so that the radiation from single slit and the superposed radiation from the Young's plane fall at the centre of the light collecting mirror of the monochromator (Fig. 4.2). Reducing the separation of young's slits overcomes this difficulty. But this is done at the cost of η and r, which in turn puts restriction on the size of the source intensity profile.

§4.4 Conclusion

It is the first time we have shown experimentally that intensity reconstruction to a good approximation of a source-profile masked with an amplitude grating can be performed with fixed baseline two pinholes/double slits interference experiments. Spectral measurements of superposed radiation and radiation from only a single slit are required. However, a prior knowledge of the intensity and the spectrum of the source is required. With this technique, it is possible to obtain optical intensity of quasi-homogeneous sources which form a rather large class of sources. Though in such an experiment some intensity is lost due to scattering at the mask and the double slit but with the improved detection techniques it should not be a serious

concern. In the present study, the source taken is a rotationally symmetric source. But this technique can be extended to other class of sources if some additional measurements resulting from the axial symmetry of the spectral degree of coherence are made. Such experiment may have useful practical applications, e.g., in automated inspection [7].

References

[1] D.F.V. James and E. Wolf, *Optics Commun.* **81** (1991) 150

[2] H.C. Kandpal, J.S. Vaishya, M. Chander, K. Saxena, D.S. Mehta and K.C. Joshi, *Phys. Lett. A* **167** (1992) 114

[3] M. Santarsiero and F. Gori, *Phys. Lett. A* **167** (1992) 123

[4] W.H. Carter and E. Wolf, *J. Opt. Soc. Am.* **67** (1977) 785

[5] D.F.V. James and E. Wolf, *Radio Science* **26** (1991) 1237

[6] H.C. Kandpal, K. Saxena, D.S. Mehta, J.S. Vaishya and K.C. Joshi, *J. Mod. Opt.* **42** (1995) 455.

[7] A.T. Friberg and D.G. Fischer, *Appl. Opt.* **33** (1994) 5426

[8] E. Wolf, *J. Opt. Soc. Am.* **68** (1978) 6.

Chapter 5

Spectroscopy of partially coherent fields at geometrical-image plane and Fourier transform plane of a lens

In a recent theoretical study it has been shown that the spectrum of a partially coherent field radiated by a Gaussian Schell-model beam after passage through a lens will be blueshifted for on-axis points of observation and maximum blueshift in the spectra occurs at the back focal plane and no shift occurs at the geometrical-image plane of the lens [1].

In this chapter the results of an experimental study on the spectra of radiated field after passage through a lens by taking a Gaussian Schell-model beam produced by a He-Ne multimode laser, a secondary source of high degree of coherence produced at the far-zone of an incoherent source and a quasi-homogeneous source are reported. It is found experimentally that the spectra are blue shifted when detecting system is in the Fourier plane and no shift is observed in the geometrical-image plane of the lens. The amount of observed shift has been found to depend on the bandwidth of the source. For a broad-band source the observed shift is larger than the shift observed for narrow-band source.

It has been shown by Palma and Cincotti[1] that when such a field impinges on a lens of focal length f, whose transmission for paraxial approximation is given by

$$\tau(r;\nu) = exp\left(-\imath\frac{\pi\nu r^2}{cf}\right), \tag{5.3}$$

the field after the lens at a distance z_2, again in paraxial approximation, gives the spectral intensity $S(0,z_2;\nu)$ (the spectrum) on the optical z-axis ($r_1 = r_2 = 0$) as

$$S(0,z_2;\nu) = S(0;\nu)M(z_1,z_2;\nu), \tag{5.4}$$

where

$$M(z_1,z_2;\nu) = \frac{1}{\left(1-\frac{z_2}{f}\right)+\left(\frac{cM^2}{\pi\nu w_0^{\,2}}\right)^2\left(z_1+z_2-\frac{z_1z_2}{f}\right)^2}. \tag{5.5}$$

If we consider a case when z_1 is at the front focal plane of a lens and z_2 is at the back focal plane or the Fourier transform plane of the lens, i.e. $z_1 = f$ and $z_2 = f$, Eqs. (5.4) and (5.5) give

$$S(0,z_2;\nu) = S(0;\nu)\left(\frac{\pi w_0^2}{cM^2 f}\right)^2\nu^2. \tag{5.6}$$

Equation (5.6) shows that the spectrum of the field at z_2 will be modified and shifted with respect to the source spectrum $S(0;\nu)$.

In a typical case when $z_1 = 2f$ and $z_2 = 2f$, the geometrical-image plane with respect to each other (this case is specially discussed here because in spectroradiometric measurements, this combination of distances is taken for unit magnification of the source image formed at the entrance slit of the monochromator

using lens or mirror optical system), the spectrum at z_2 as obtained from Eqs. (5.5) and (5.6) is $S(0,z_2;\nu)=S(0,\nu)$. This means that the normalized spectrum at the geometrical-image plane would be the same as the normalized spectrum at the source plane.

§5.2 Experimental setup and results

Keeping in view the aforesaid calculations, we have performed spectral measurement in the Fourier plane and in the geometrical-image plane of a lens for two different sources namely (1) multimode He-Ne laser source and (2) a quasi homogeneous source with different degrees of spatial coherence.

5.2.1 Gaussian Schell-model beam radiated by a multimode He-Ne green laser

The experimental setup (shown in Fig. 5.1) was built up on a vibration isolation table. The room temperature was maintained constant within ± 1°C to ensure that no significant drift takes place in the spectrum of laser radiation due to temperature variation. Spectral analysis of the laser radiation was made in two cases. First the spectrum of the radiation emitted by the laser source was taken without any auxiliary optics in between the source and the spectrometer. The instruments used and experimental procedure for measuring the spectra have been described in chapter 2. Curve A in Fig. 5.2 shows the spectrum of radiation from the multimode He-Ne green laser. Then the aperture of the laser source and the entrance slit of the monochromator were put at the front and back focal planes of a thin double convex lens (f = 30 cm) as shown in Fig. 5.1. The spectrum of the laser radiation transmitted by the lens was recorded and is shown by a dotted line curve B in Fig. 5.2. A comparison of the two spectra (curves A and B in Fig. 5.2) reveals that the spectrum of the laser radiation in Fourier plane of the lens is shifted towards blue end of the electromagnetic spectrum and the magnitude of the observed relative

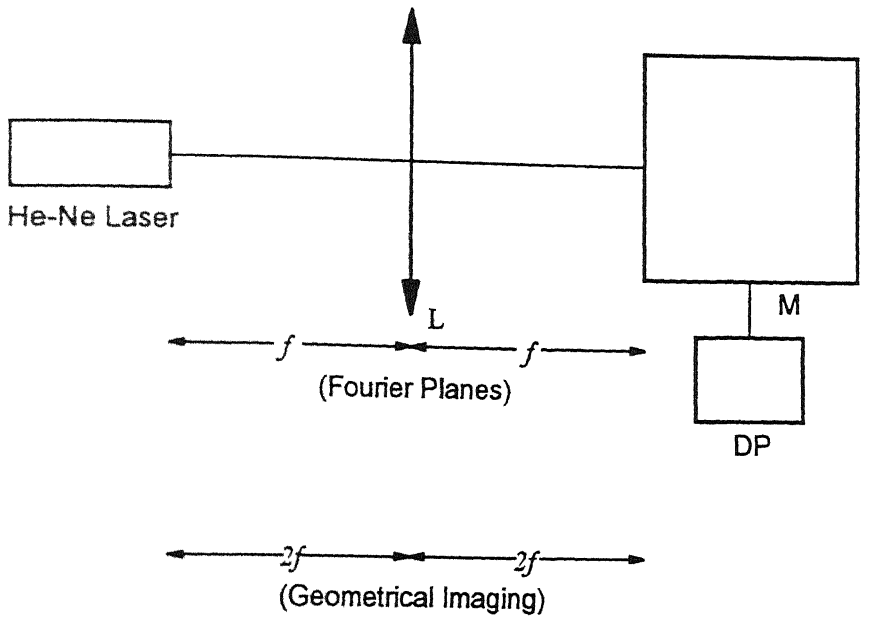

Fig. 5.1 Schematics of the experimental setup for measuring the spectra of laser radiation. L - lens, M - Monochromator, and DP - data processing unit.

shift $\Delta\lambda/\lambda \approx 10^{-5}$. This observation is consistent with the theoretical value obtained using Eq. (5.6). The aperture of the laser source and the entrance slit of the monochromator were then put at the geometrical-image plane of the lens (i.e. both laser source and the entrance slit of the monochromator were at a distance $2f = 60$ cm from the lens as shown in Fig. 5.1). The spectrum of the laser source recorded for this experimental setup is shown by curve C in Fig. 5.2. It is seen that this spectrum (Curve C) almost overlaps with the laser spectrum (Curve A).

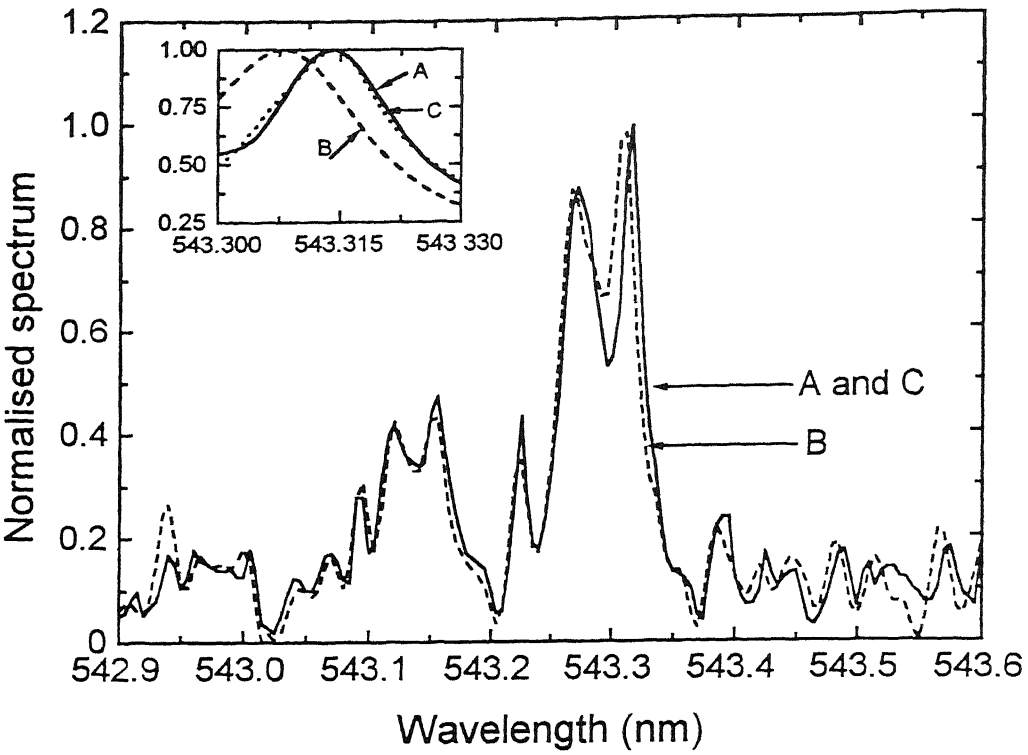

Fig. 5.2 Spectrum of laser radiation (A) when no lens is put in between the laser source and the entrance slit of the monochromator. (B) when the aperture of laser source and the entrance slit of the monochromator are at the front and back focal planes of the lens. and (C) when the aperture of laser source and the entrance slit of the monochromator are at the front and back geometrical-image planes of the lens. The inset shows an exploded view of a small spectral region to show the difference between curves A, B and C.

5.2.2 A quasi-homogeneous source with different degrees of spatial coherence

Quasi-homogeneous secondary sources with different degrees of spatial coherence were generated using a tungsten halogen lamp with a diffuser. Two specific cases are described below in which a quasi-homogeneous secondary source having widely different degrees of spatial coherence were used.

(I) A quasi-homogeneous source with low degree of spatial coherence was produced by illuminating a rectangular slit with a diffuser source having uniform luminance. The schematics of the experimental setup is shown in Fig. 5.3. S is a 450 W tungsten halogen lamp source having a planar filament, D is a diffuser, A is

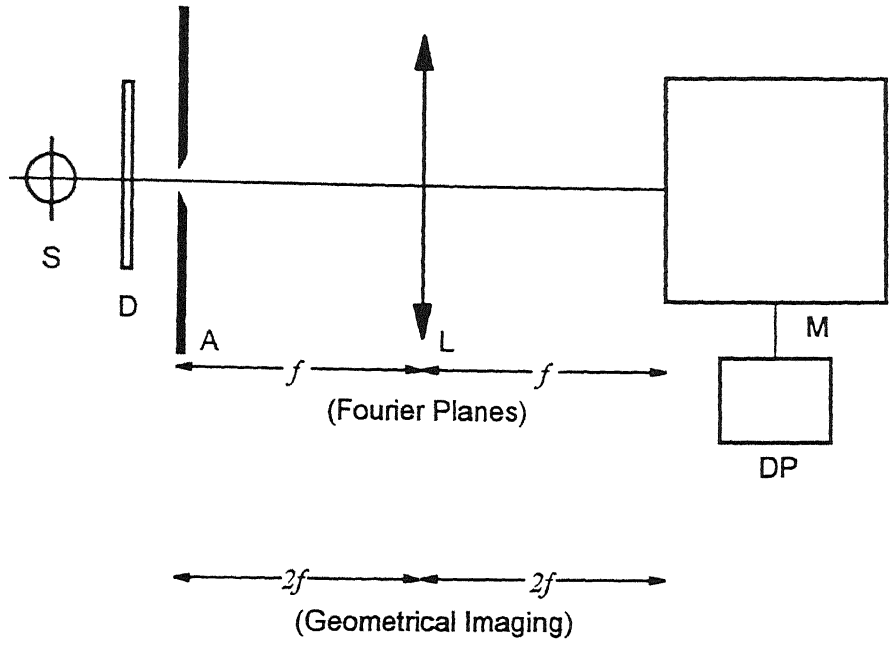

Fig. 5.3 Schematics of the experimental setup for measuring the spectra of the broad-band source formed at slit A. S - source, D - diffuser, A - rectangular slit, and M - monochromator. A and M are put at a distance f from the lens L in one experimental setup and at $2f$ from the lens L in another experimental setup, and DP - data processing unit.

the one dimensional rectangular slit which acts as a quasi-homogeneous secondary source having a low degree of spatial coherence, L is a thin double convex lens, and M is a monochromator. The spectrum of the radiation emitted by the rectangular slit A was recorded without any auxiliary optics in between the source and the monochromator. The recorded spectrum is shown by curve A in Fig 5.4. The spectrum recorded by placing the lens in between the source and the detecting system, when both (the source and the detecting system) were at the front and back Fourier transform planes of the lens, is shown by curve B in Fig. 5.4. This spectrum (Curve B) is blue shifted with respect to the spectrum (Curve A) obtained without lens and it is also observed that the blue shift becomes more pronounced at the higher wavelengths. The experiment was also conducted with the lens placed in such a manner that the image of the slit obtained at the entrance slit of the

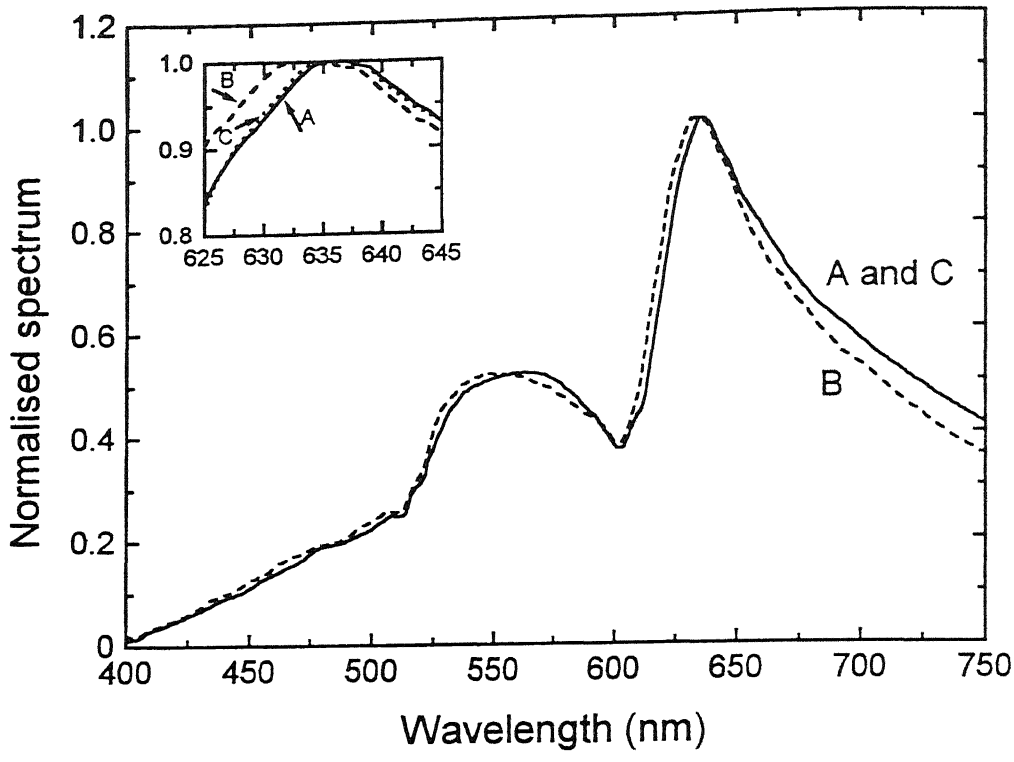

Fig. 5.4 Spectrum of radiation from the rectangular slit A. (A) when no lens is put in between the source slit A and the entrance slit of the monochromator, (B) when the source slit A and the entrance slit of the monochromator are at the front and back focal planes of the lens, and (C) when the source slit A and the entrance slit of the monochromator are at the front and back geometrical-image planes of the lens L. The inset shows an exploded view of a small spectral region to show the difference between curves A, B and C.

monochromator with unit magnification, i.e. the source and the detector were at the front and back geometric planes of the lens (each being at $2f$ distance from the lens). It is found that the spectrum recorded in this case (curve C in Fig. 5.4) comes out to be nearly the same as obtained without any lens in between the slit A and the monochromator. A look at Fig. 5.4 reveals as if curve A and curve C are exactly identical. In a scale where wavelengths from 400 nm to 700 nm are shown, it is very difficult to visualize the difference curve A and curve C. Therefore, a small wavelength region is also shown in exploded form to show the difference among the curves distinctly.

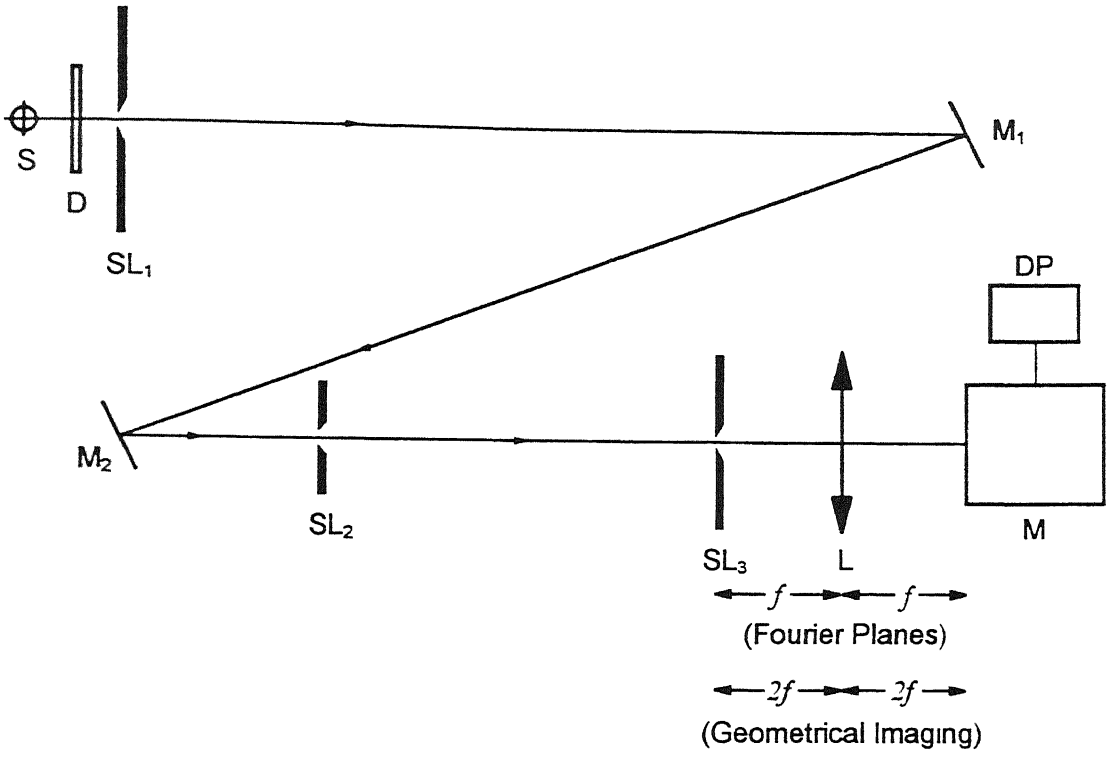

Fig. 5.5 Schematics of the experimental setup for measuring the spectra of the broad-band source formed at slit SL_1. S - source, D - diffuser, SL_1, SL_2 and SL_3 - rectangular slit, L - lens, M - monochromator, and DP - data processing unit.

(II) A secondary source of high degree of spatial coherence was produced at the far-zone of an incoherent source. According to van Cittert-Zernike theorem, the nature of the degree of spatial coherence at the far-zone of an incoherent source of aperture size d is similar to the diffraction caused by the aperture and one can get the information about the areas of coherence from the wavelength of the radiation λ, and the size of the aperture d. The effective coherence length as determined from the nature of the spatial coherence function and from the first zero of the sinc function for a rectangular slit of size d is given by $R\lambda/d$ [5], where R is the distance from the source plane to the plane where the degree of coherence is measured. The experimental setup used in this study is shown in Fig. 5.5. An infinitely long rectangular slit SL_1 along y-axis and having dimension d = 1 mm along x-axis was

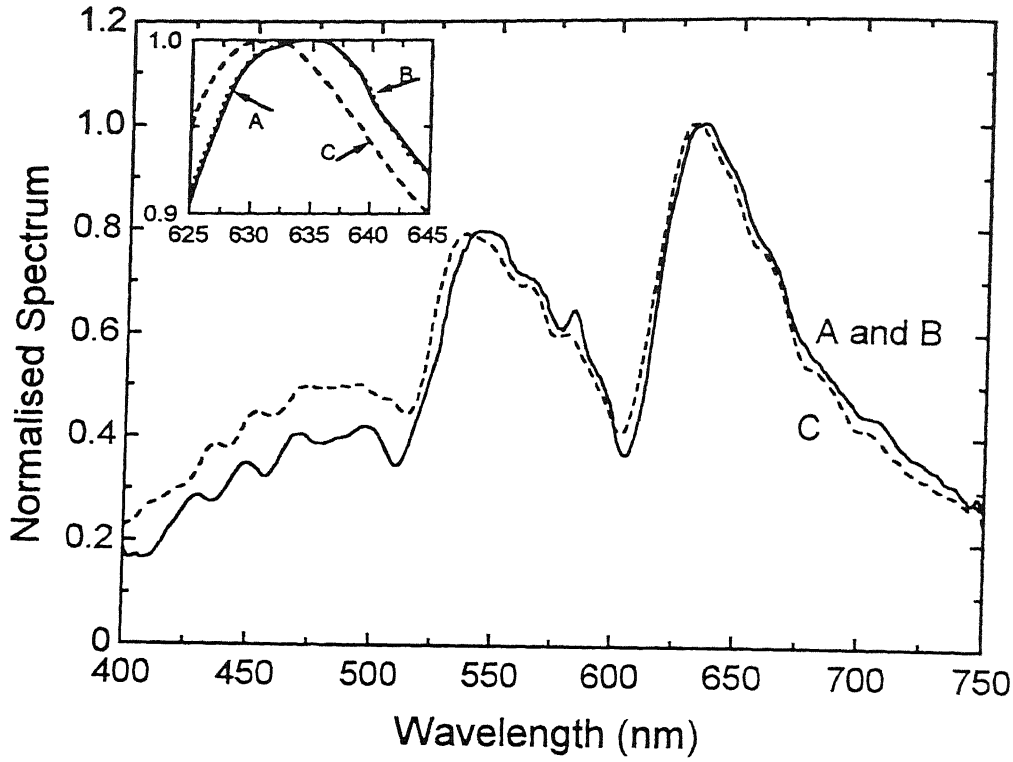

Fig. 5.6 Spectrum of radiation from the slit SL_2. (A) When no optical system is put in between SL_2 and M. (B) when SL_3 is put in between SL_2 and M, and (C) when SL_3 and the entrance slit of the monochromator are at the front and back focal planes the lens L. The inset shows an exploded view of a small spectral region to show the difference between curves A, B and C.

kept close to the diffuser D illuminated by using a tungsten halogen source S. The coherence length at a distance of 9.1 m from SL_1 comes out to be 2.73 mm for an average wavelength = 600 nm. At this position another one-dimensional rectangular slit SL_2 of opening of 0.75 mm which is much smaller than the coherence length was put. Therefore, a field of high degree of coherence was obtained over slit SL_2. The spectrum of radiation emitted by the slit SL_2 was measured without any auxiliary optics in between this slit and the monochromator and is shown by curve A in Figs. 5.6 and 5.7. To observe the effect of an auxiliary optics in between this secondary source (slit SL_2) and the monochromator, a lens of focal length $f = 30$ cm and a rectangular slit SL_3 was used. The radiation from the slit SL_2 was made incident on

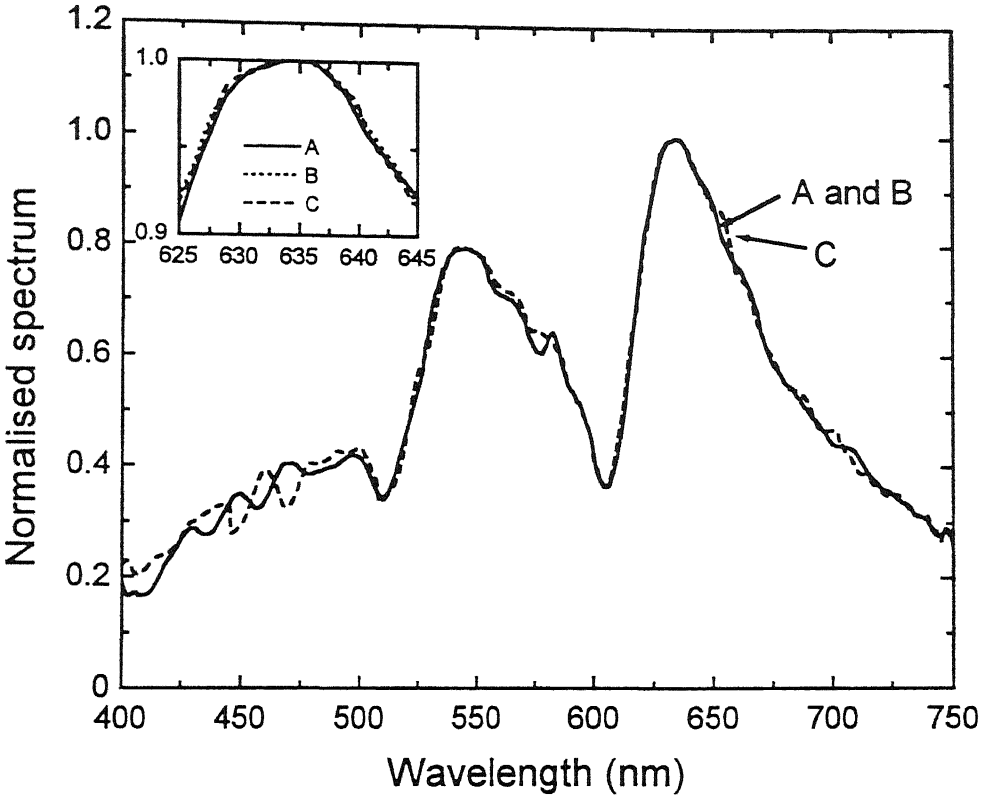

Fig. 5.7 Spectrum of radiation from the slit SL_2. (A) When no optical system is put in between SL_2 and M, (B) when SL_3 is put in between SL_2 and M, and (C) when SL_3 and the entrance slit of the monochromator are at the front and back geometrical-planes of the lens L. The inset shows an exploded view of a small spectral region to show the difference between curves A, B and C.

slit SL_3 of opening equal to 0.5 mm. The source formed at SL_3 departs considerably from maintaining quasi-homogeneity condition as coherence length is much larger than the size of the slit SL_3 The normalized spectrum of the radiation emitted by SL_3 is shown by curve B in Figs. 5.6 and 5.7 and it is found to be the same as the normalized spectrum (curve A) of radiation from SL_2. The spectra of the radiation transmitted by the lens placed in between the SL_3 and detector were recorded in two cases.

(*i*) In the first case, the slit SL_3 was put at the front focal plane of this lens (f = 30 cm) and the monochromator slit was at the back focal plane (the Fourier transform plane) of the lens (as shown in Fig. 5.5). The spectrum of the radiation

recorded by the monochromator is shown by curve C in Fig. 5.6. A comparison of curve B with curve C in Fig. 5.6 shows that this spectrum (curve C) is shifted towards the blue region of the electromagnetic spectrum with respected to the spectrum (curve B). This observation is consistent with the theoretical findings To show distinction between curves A, B and curve C, an exploded view of a small wavelength region is also shown in Fig. 5.6.

(*ii*) In the second case the slit SL_3 and the entrance slit of the monochromator were put at a distance of $2f = 60$ cm from the lens such that the slit SL_3 and the monochromator slit were at the front and back geometrical-image planes of the lens. The spectrum of the radiation recorded is shown by dotted line curve C in Fig. 5.6. It is seen that the curves A and C in Fig. 5.7 are nearly the same with in experimental errors. The same process of distinguishing curves A, B and curve C is repeated in Fig. 5.7. Curve A and curve B in Figs. 5.6 and 5.7 are identical as they were taken under identical conditions.

§5.3 Conclusions

These experimental studies show that the spectra on the optical z-axis of a lens are different at different positions. In the geometrical-image plane these observations show that no spectral shift occurs and the normalized spectrum of the imaged source is the same as that of the source observed without any optics. However, the spectrum is blue shifted when the spectrum is taken at the back focal plane of the lens and maximum blue shift takes place when the source and the detecting system are at the front and the back focal planes of the lens, i.e. the source and the detecting system are at the Fourier transform planes. Our observations show that while performing spectral measurements with unit magnification in the geometrical-image plane, absence of spectral shift provides the best situation for

spectral measurement. This also has been shown by a theoretical calculation that in the geometrical-image plane of the lens the spectral modifier (Eq. 5.5) becomes independent of frequency ν and thus the observed spectrum is modified by a constant factor only. Therefore the normalized spectra of the source and that of the field at the geometrical-image plane are exactly the same. However, the worst situation will be obtained when the spectral measurement are made at the back focal plane of a lens when the source and detection planes are the Fourier transform planes. These studies might be useful in spectral measurements relating to metrology

References

[1] C. Palma and G. Cincotti, *Opt. Lett.* **22** (1997) 671.

[2] F. Gori, *Opt. Commun.* **34** (1980) 301.

[3] F. Gori, *Opt. Commun.* **46** (1983) 149.

[4] A. Siegman, *"Lasers"* (University Science Mill Valley, Calif. 1986).

[5] A.S. Marathay, *"Elements of Optical Coherence Theory"* (John Wiley and Sons, 1982) p 112.

Chapter 6

Study on coherence properties of light fields as influenced by a monochromator

In *chapter one* it has already been discussed that the change in the spectrum of a source is dependent on the state of coherence of the source. In the experiments which have been performed, so far, secondary sources of varying degrees of coherence are produced and the far-field spectra are analyzed using a monochromator as a spectrum analyzer. In all these studies it has been found that the spectral shift observed using a monochromator as a spectrum analyser is more than the calculated for the experimental parameters. In *chapter two* we, on the basis of our observations. have made a conclusion that the coherence properties of the light field are modified by a monochromator. In many spectroscopic studies, for example. in detector calibration for spectral responsivity, selective excitation spectroscopy, etc., a monochromator is used as a spectral filter. The secondary source synthesized using a monochromator may produce such coherence properties of the secondary source that its far-field spectra may be different from the source spectrum. The aim of the present chapter is to study experimentally the effect of a monochromator on the spatial coherence properties of the light field incident at its entrance slit which after passing through the apertures, diffraction gratings and other auxiliary optics of the monochromator synthesizes a secondary source at the exit slit of the monochromator. Experiments are performed with light fields of different states of spatial coherence incident at the entrance slit of monochromator.

The degree of spectral coherence or spectral degree of coherence (SDC) at the entrance and exit slits of the monochromator are determined using the spectral interference law by measuring the spectra of radiation from a Young's double slit (YDS) placed at the position of the entrance and exit slits of the monochromator. It is found that the SDC at the exit slit of the double monochromator is more than the SDC at the exit slit of a single monochromator and also much more than that at the entrance slit. It is, therefore, proposed that the change in spatial coherence property of the incident field must be studied carefully while synthesizing a secondary source at the exit slit of a monochromator.

In the present study different experimental conditions, of producing varying degree of spatial coherence of the incident field at the entrance slit of a monochromator depending on the optics, are considered. These conditions are studied in detail and the effect of monochromator on the coherence properties of the light fields is analyzed by measuring the spectra of the radiation from the YDS placed at the exit slit of the monochromator.

§6.1 Experimental setup and results

6.1.1 Partially coherent beam-like field incident at the entrance slit

The experimental setup used for determining the SDC at the exit slit of a monochromator is shown in Fig. 6.1. The source S is a 40W tungsten-halogen lamp that is operated with a DC power supply of very high stability (1 part in 10^4). A is an infinitely long rectangular aperture of 1 mm width and D is a diffuser which is kept just before the aperture A so that it gets uniformly and incoherently illuminated. Aperture A acts as an incoherent secondary source and is put at the front focal plane of lens L. At the back focal plane of the lens L, the entrance slit of a double monochromator M_1 is kept so that partially coherent beam-like field is

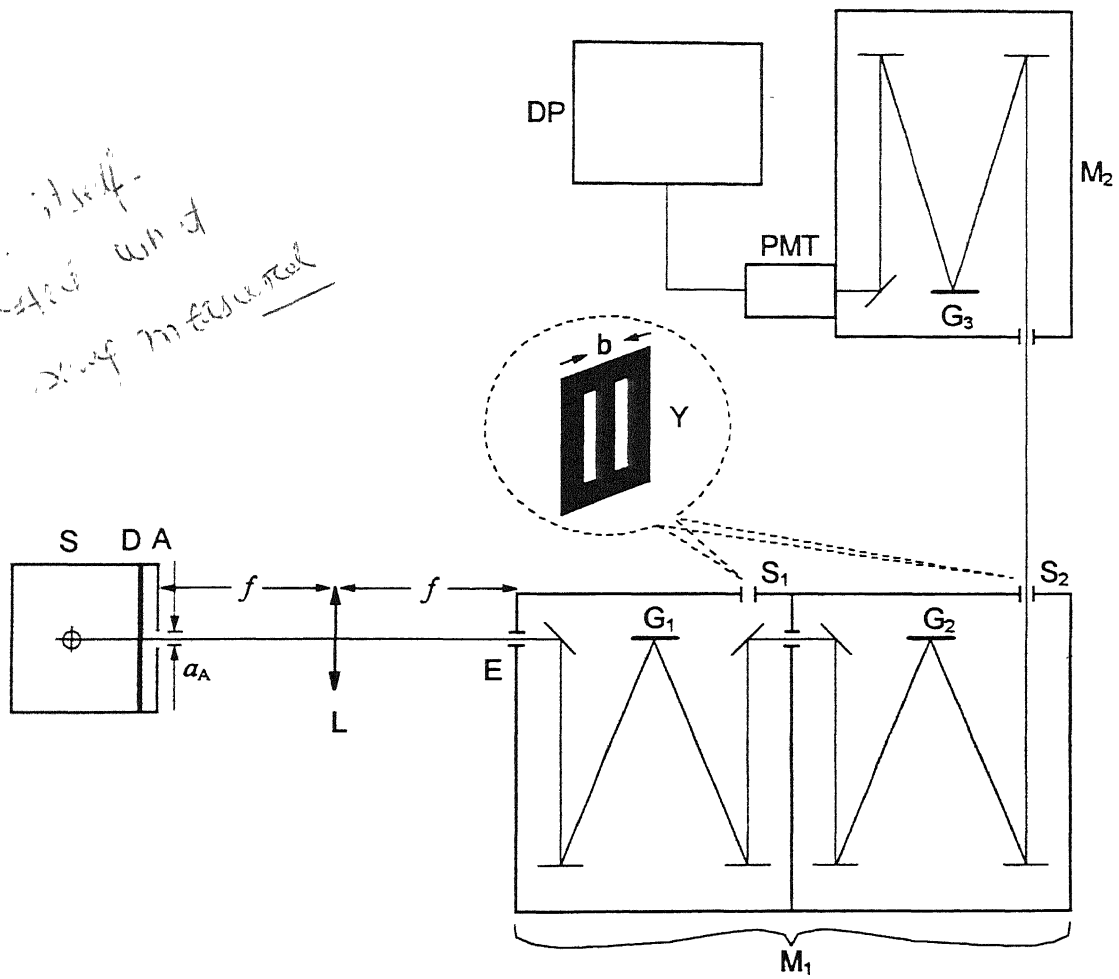

Fig. 6.1 Experimental setup for measuring the spectral degree of coherence at the exit slits S_1 and S_2 when partially coherent beam like field is incident at the entrance slit of monochromator M_1. S - source, D - diffuser, L - lens, M_1 - double monochromator consisting of two single monochromator placed in juxtaposition, E - entrance slit of M_1, S1 and S_2 - exit slits of single and double monochromator respectively. Y - Young's double slit, M_2 - single monochromator used to measure the spectra of the radiation emanating from S_1 and S_2 or the double slit. G_1, G_2 and G - gratings of M_1 and M_2 respectively, PMT - photomultiplier detector and DP - data processing unit.

incident at M_1. The double monochromator is a combination of two single monochromators placed in juxtaposition so that output spectra from the exit slit S_1 of the single monochromator as well as from the exit slit S_2 of the double monochromator can be obtained. This monochromator is used as a tunable filter so that spectral profiles of different bandwidths at a fixed or at different wavelengths can be obtained. The spectra of the radiation emerging from the exit slits S_1 and S_2 are analyzed using another single monochromator M_2 coupled with a cooled photomultiplier and data processing system. The gratings used in M_1 and M_2 have 1200 lines/mm and are blazed at 300 nm.

To obtain spectral profiles of considerably large bandwidth, experiments with varying slit widths of the monochromator are done. Within the experimental limitations spectral profiles having full width at half maximum (FWHM)

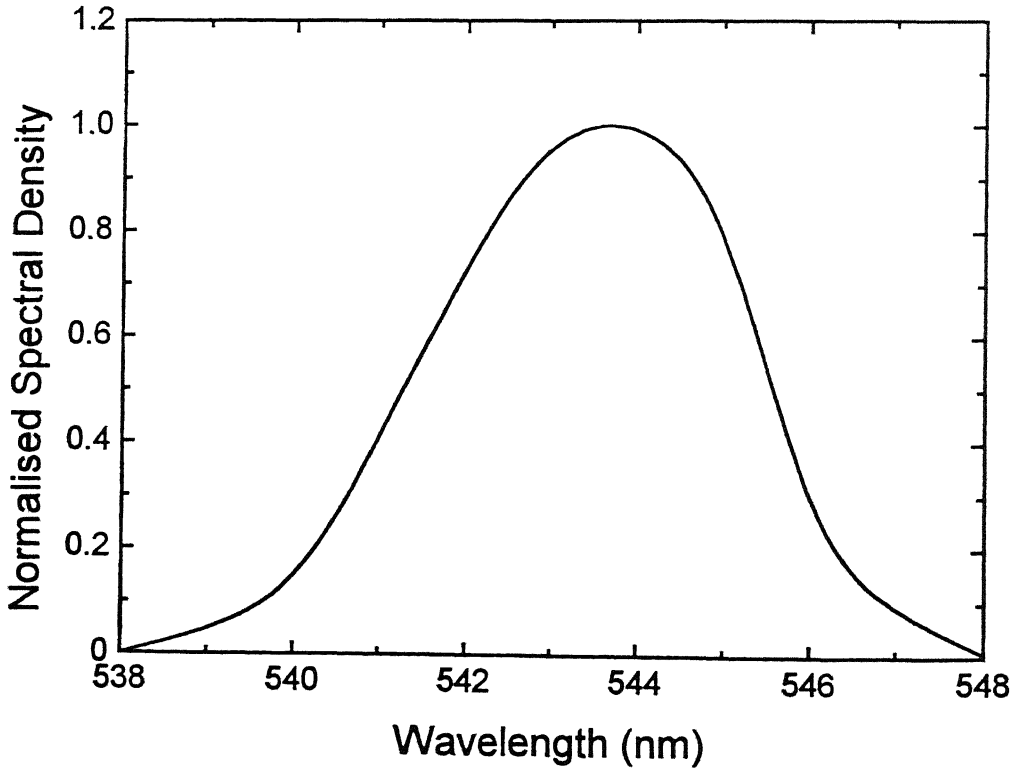

Fig. 6.2 The normalised spectral density for the spectral profile peaking at about 544 nm.

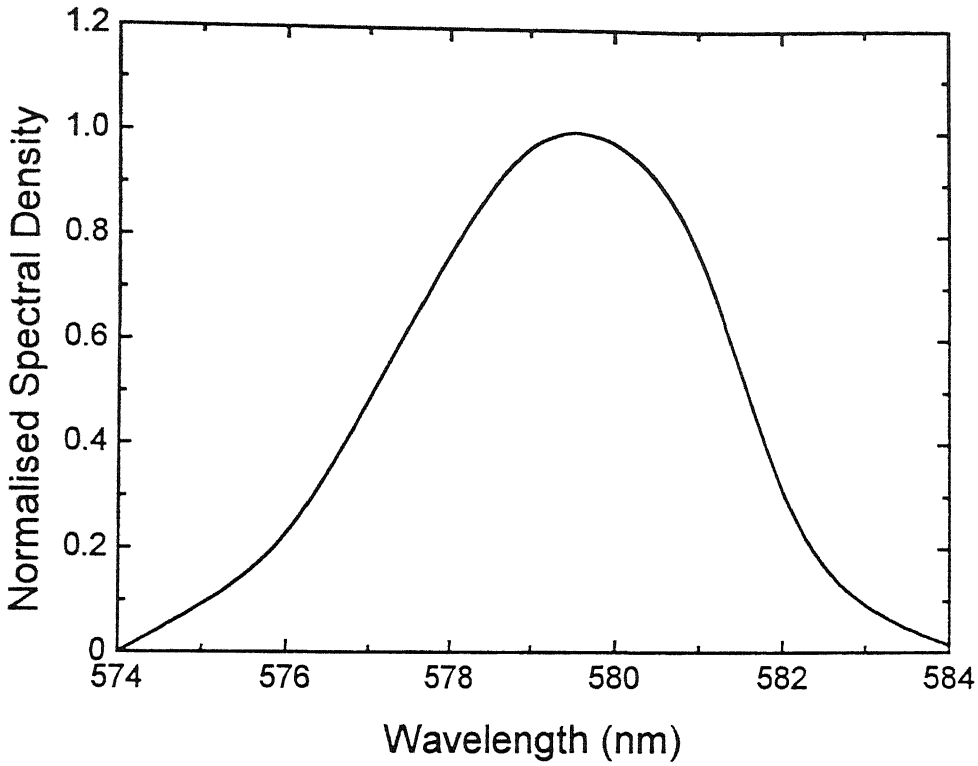

Fig. 6.3 The normalised spectral density for the spectral profile peaking at about 580 nm.

approximately equal to 4 nm, when the opening of the entrance and exit slits S_1 and S_2 of the monochromator M_1 are 2 mm each, are obtained. The normalized spectra of two spectral profiles peaking at 544 nm and 580 nm are shown in Figs. 6.2 and 6.3. To determine the spectral degree of coherence at the exit slits of the monochromator, double slits (which will be referred to as Young's slit) is used at each of the exit slits S_1 and S_2 of the monochromator M_1.

For YDS experiment, the spectral interference law as derived by James and Wolf [1] is

$$S(Q,\lambda) = 2S^{(1)}(Q,\lambda)\left\{1+\left|\mu_{12}(\lambda)\right| cos\left[\frac{2\pi}{\lambda}(R_2 - R_1)+\beta_{12}(\lambda)\right]\right\}, \qquad (6.1)$$

where $S(Q,\lambda)$ is the superposed spectrum at point Q (which is the entrance slit of M_2) in the observation plane. $S^{(1)}(Q,\lambda)$ is the spectrum from one of the slits of YDS

when the other one is closed and it is assumed that the spectra obtained from each of the slits of YDS are identical. This may be a drastic assumption. However, for a grating monochromator with linear dispersion, in the present case, the spectra of the radiation from the two slits having axial separation ≈ 458 μm may not differ much. This was verified experimentally in the present study. $|\mu_{12}(\lambda)|$ is the modulus of the complex degree of coherence produced over the plane of the YDS. R_1 and R_2 and are the distances of Q from P_1 and P_2 respectively (In the present study it is assumed that $R_1 = R_2$ because the slits are symmetrically placed). $\beta_{12}(\lambda)$ is assumed to be 0 or π due to the symmetry of the source and that of the experimental system. The SDC at the slits S_1 and S_2 of the monochromator M_1 is determined by measuring the superposed spectrum (when both the YDS are open) and the spectrum from the individual slit (when one slit is open and the other one is closed and vice versa) with monochromator M_2 and putting the data in Eq. (6.1). The SDCs determined for the two spectral profiles (one extending from 538 nm to 548 nm peaking at about 544 nm and the other from 574 nm to 584 nm peaking at about 580 nm) are shown by curve A over the plane of the slit S_1 and by curve B over the plane of the slit S_2 in Figs. 6.4 and 6.5 respectively.

The SDC at the entrance slit of the monochromator M_1 (which is at the back focal plane of the lens L) due to a rectangular source of width 'a_A' can be calculated using the following relation

$$|\mu_{12}(\lambda)| = \left| \frac{\sin\left(\frac{\pi a_A |\rho_2 - \rho_1|}{\lambda f}\right)}{\left(\frac{\pi a_A |\rho_2 - \rho_1|}{\lambda f}\right)} \right|, \qquad (6.2)$$

where $|\rho_2 - \rho_1|$ is the modulus of the difference of the position vectors of two points on the entrance slit of the monochromator M_1 which is chosen to be equal to

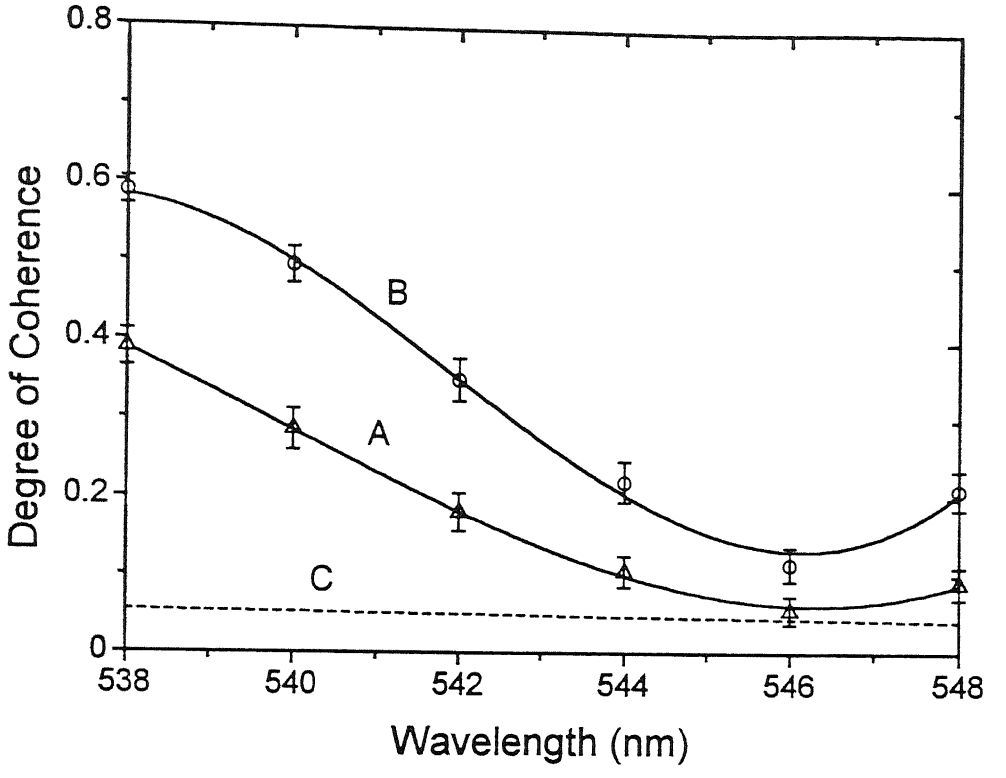

Fig. 6.4 Curves A and B - the spectral degree of coherence obtained experimentally at S_1 and S_2 respectively for the spectral profile extending from 538 to 548 nm. Curve C - the spectral degree of coherence obtained for the experimental parameters, viz. a_A = 1 mm, f = 20 cm, $|\rho_2 - \rho_1|$ = 458 μm and λ for the spectral range.

458 μm because, in the present study, the average separation between the YDS is equal to 458 μm. a_A = 1 mm is the size of the aperture A, f is the focal length of lens L (f = 20 cm) and λ is the wavelength of the field. The SDCs calculated using Eq. (6.2) for the wavelength ranges from 538 nm to 548 nm and from 574 nm to 584 nm are shown by dotted curves C in Figs. 6.4 and 6.5 respectively. It is seen that the SDC calculated using Eq. (6.2) is in close agreement with that obtained experimentally. These figures also reveal that the SDCs at slits S_1 and S_2 are more than the SDC at the entrance slit of the monochromator M_1 and the SDC at S_2 is more than SDC at S_1.

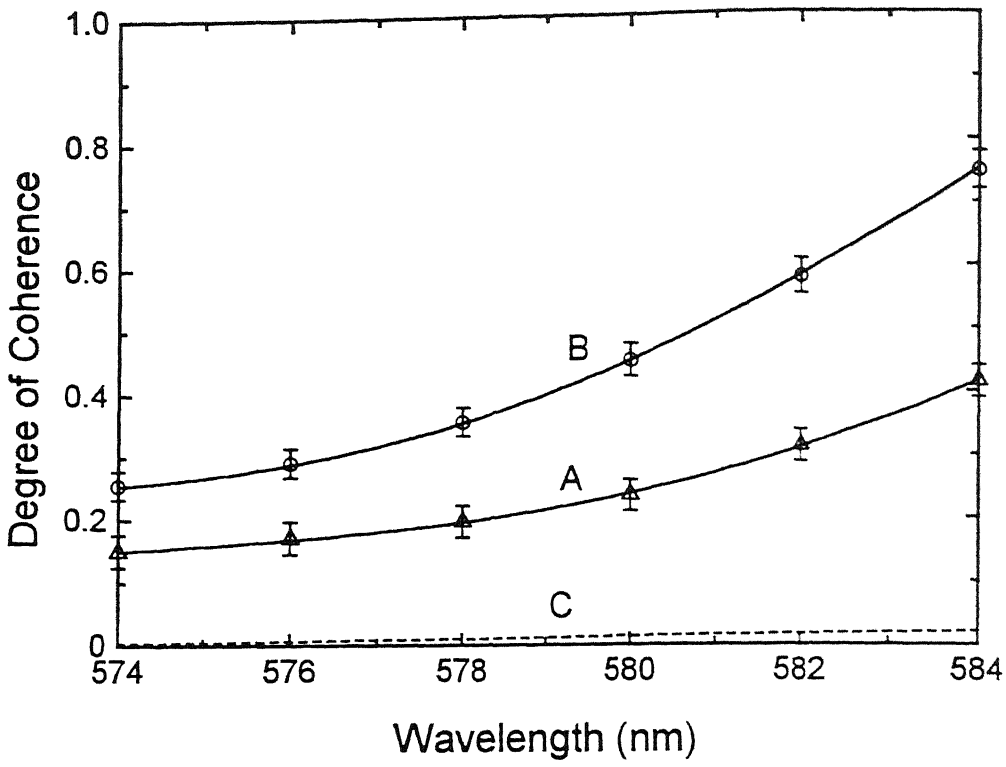

Fig. 6.5 Curves A and B - the spectral degree of coherence obtained experimentally at S_1 and S_2 respectively for the spectral profile extending from 574 to 584 nm. Curve C - the spectral degree of coherence obtained for the experimental parameters, viz. a_A = 1 mm, f = 20 cm, $|\rho_2 - \rho_1|$ = 458 μm and λ for the spectral range.

6.1.2 Secondary source imaged at the entrance slit of the monochromator

In most of the measurements, for example spectroscopic measurements and also in spectroradiometric measurements, a secondary source in the form of a circular or a rectangular aperture is imaged at the entrance slit of a monochromator. The secondary source which is an incoherent or a quasi-homogeneous source (which is a globally incoherent source) if imaged, the coherence properties of the image may be assumed to be nearly the same as that of the secondary source. Though the coherence spread function of the image may not be the same as that of the source, yet, to a good degree of assumption, this can be treated as an incoherent source.

The spectral properties of this imaged source are analyzed by YDS and monochromator M_2 whose description are given in 6.1.1. It is found that the imaged source is also an incoherent source since the superposed spectrum from both slits of YDS is just an algebraic sum of the two spectra from individual slits of YDS.

Occasionally, It is assumed that the optics of a monochromator acts only as an imaging system which images the source (at its entrance slit) at the exit slit after dispersion through the grating(s) so that the coherence property of the field at the image plane is the same as that of the field at the entrance slit. This assumption may not be correct. To verify this an experimental setup shown in Fig. 6.6 is employed. The description of the source and the other ancillary used is the same as in section 6.1.1. Aperture A act as an incoherent secondary source and is imaged with unit magnification with the help of a lens L at the entrance slit of the monochromator M_1. The SDCs at the slits S_1 and S_2 of the monochromator M_1 are determined by measuring the superposed spectrum from both the slits of YDS and the spectrum from the individual slit (when one slit is open and other one is closed and vice versa) with monochromator M_2 and putting the data in Eq. (6.1) under the same assumption as made in section 6.1.1. The SDCs measured (for the spectral profiles extending from 538 to 548 nm and for the spectral profile extending from 574 to 584 nm) are shown by curve A over the plane of S_1 and by curve B over the plane of slit S_2 in Figs. 6.7 and 6.8 respectively. Figures 6.7 and 6.8 indicate that high degree of coherence is generated at the slits S_1 and S_2.

§6.3 Discussion

The experimental observations from different experiment performed in the present study show obviously that the processes of synthesizing a secondary source using a monochromator has to be looked into very carefully. The auxiliary optics of

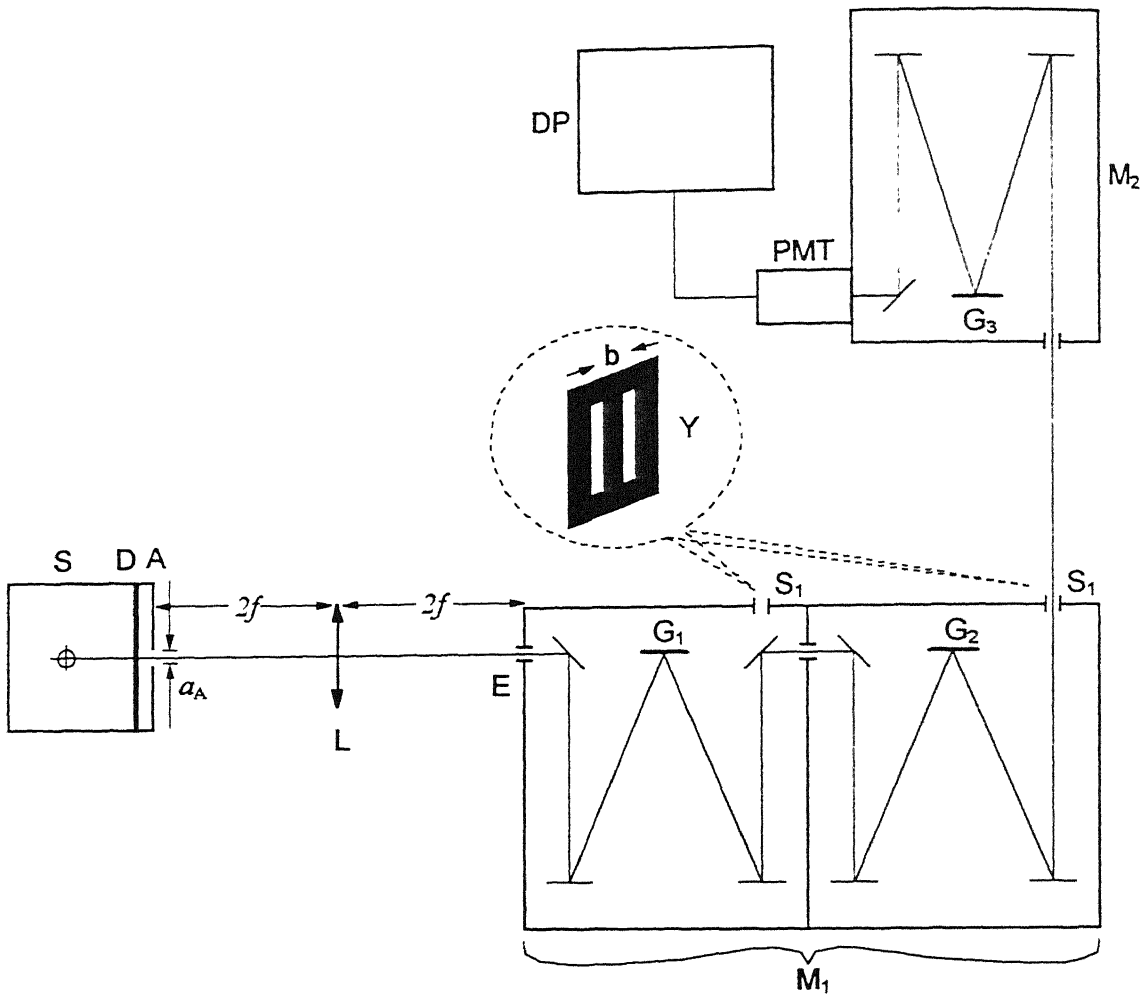

Fig. 6.6 Experimental setup for measuring the spectral degree of coherence at the exit slits S_1 when secondary source is imaged at the entrance slit of the monochromator M_1. S - source, D - diffuser, L - lens, M_1 - double monochromator consisting of two single monochromator placed in juxtaposition, E - entrance slit of M_1, S_1 and S_2 - exit slits of single and double monochromator respectively. Y - Young's double slit, M_2 - single monochromator. G_1, G_2 and G - gratings of M_1 and M_2 respectively, PMT - photomultiplier detector and DP - data processing unit.

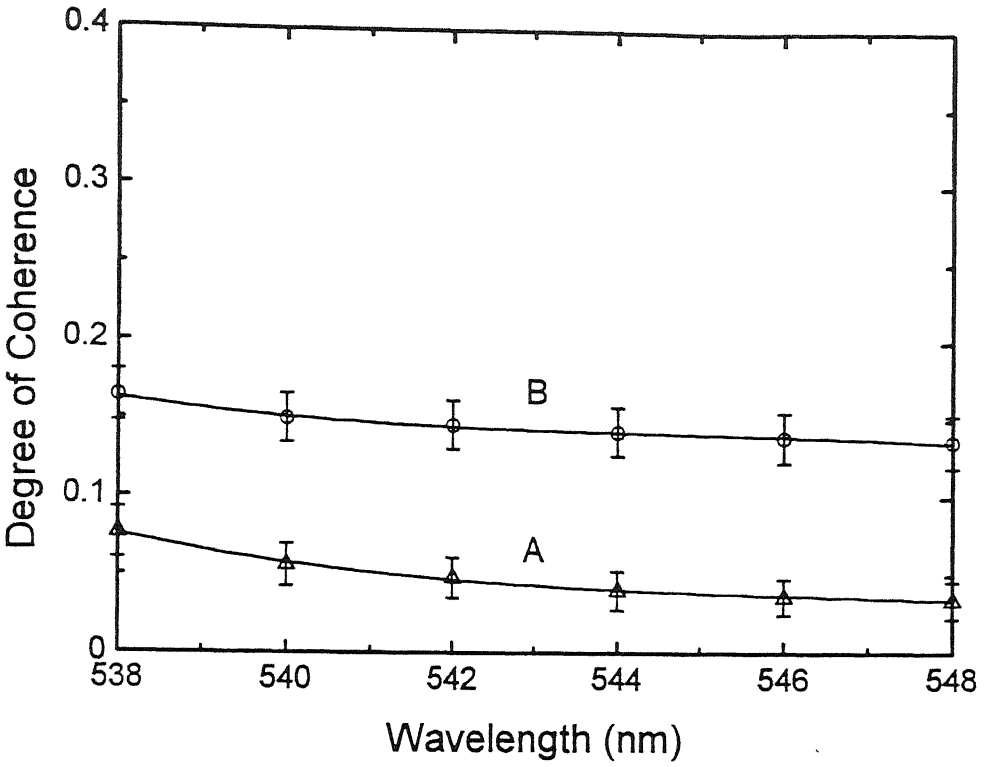

Fig. 6.7 Curves A and B - the spectral degree of coherence obtained experimentally at S_1 and S_2 respectively for the spectral profile extending from 538 to 548 nm.

the monochromator augments the SDC whether a partially coherent beam like field and an incoherent field is incident at the entrance slit of a monochromator. If we look very carefully into the process of image formation in a monochromator, the optical elements like apertures (entrance or exit slits), the gratings and the mirrors or the lenses make the light field more and more coherent. It is clear from the results of the different experiments that the SDC at the exit slit S_2 of double monochromator is more than the SDC at the exit slit S_1 of a single monochromator and is also much more than the degree of coherence at the entrance slit E of the monochromator.

Wolf [2], while discussing the invariance of the spectrum on propagation of tion, derived an expression for the far-zone normalized spectral density of a

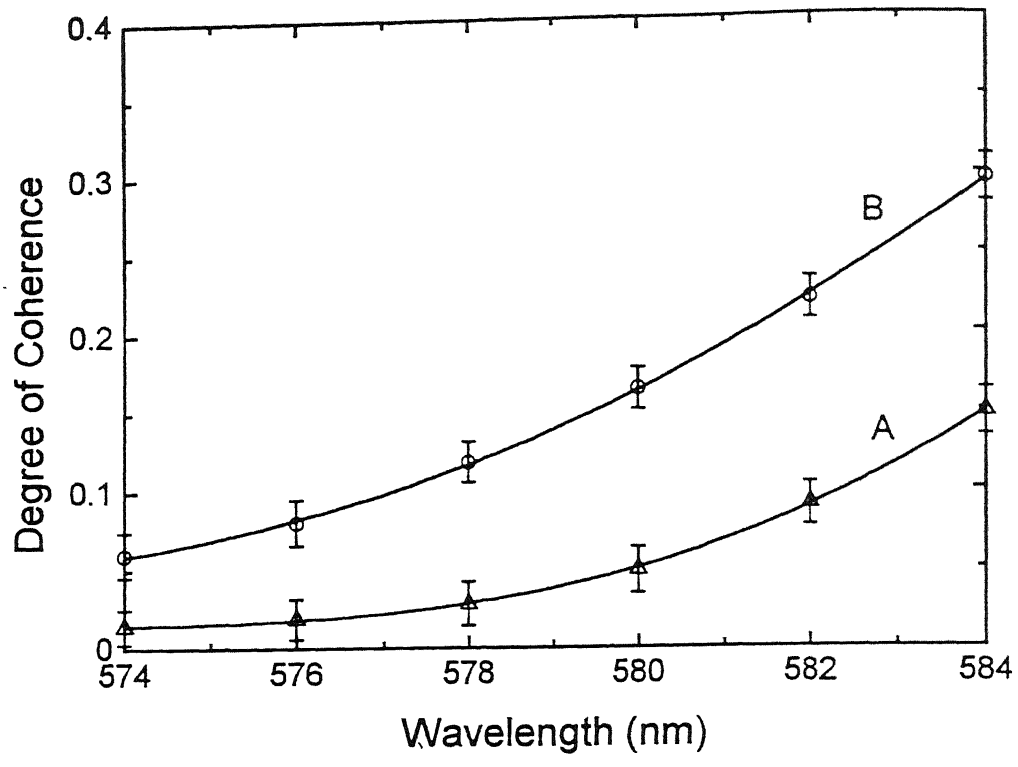

Fig. 6.8 Curves A and B - the spectral degree of coherence obtained experimentally at S_1 and S_2 respectively for the spectral profile extending from 574 to 584 nm.

quasi-homogeneous source in the direction specified by a unit vector s which is given by

$$S^{(\infty)}(r\mathbf{s},\omega) = K\frac{\omega^2}{c^2}S^{(0)}(\omega)\tilde{\mu}^{(0)}\left(\frac{\omega}{c}\mathbf{s}_{\perp},\omega\right) \tag{6.3}$$

where K is a normalization constant. A look at Eq. (6.3) reveals that the far-zone spectrum is dependent on the Fourier transform of the spectral degree of coherence of the secondary source. In earlier experiments conducted to verify Wolf's theoretical predictions, secondary sources were generated which violated either the scaling law [2] or the quasi-homogeneity condition[4]. Indebetouw [3] synthesized a secondary source using some dispersive elements and a pupil mask function which violated Wolf's scaling law [2]. In some practical situations mentioned in the

introduction, a monochromator may have to be used to synthesize a secondary source and optical fields of different states of coherence may be incident at the entrance slit of a monochromator. For the theoretical estimation of the spectrum which is expected to be observed in the far-zone of a secondary source. Fourier transform of the actual SDC of the secondary source should be taken. Otherwise the spectral shifts calculated theoretically and that observed experimentally are bound to differ this may lead to confusion and erroneous calculations. In the present study it is shown experimentally that the SDC of the field at the exit slit of a monochromator differs from its state of coherence at the entrance slit of the monochromator. The change occurs due to the influence of the auxiliary optics in the monochromator.

§6.4 Conclusion

In the present research the effect of monochromator on the coherence properties of the radiation, when a monochromator is used to produce a secondary source at the exit slit of a monochromator, is studied. Experiments are conducted with different states of coherence of the incident field at the monochromator. The experimental results show that the degree of coherence of the field at the exit slit of a monochromator is modified considerably by the optics of the monochromator. Therefore, if one uses a monochromator to synthesizes a secondary source whose far-zone spectral properties are to be studied, the coherence properties of the incident field and that of the secondary source produced after the incident field has propagated through the monochromator should be studied carefully because the far-field spectrum is very much dependent on the coherence properties of the source. On the other hand, if one uses a monochromator to analyze the spectra of optical field at the exit slit, one should no concern regarding the changes of spatial coherence of the field.

References

[1] D.F.V. James and E. Wolf, *Opt. Commun.* **81** (1991) 150.

[2] E. Wolf, *Phys. Rev. Lett.* **56** (1986) 1370.

[3] G. Indebetouw, *J. Mod. Opt.* **36** (1989) 251.

[4] J.T. Foley, *Opt. Commun.* **75** (1990) 347.